LOCKHEED MISSILES & SPACE COMPANY

HUNTSVILLE RESEARCH & ENGINEERING CENTER

HUNTSVILLE RESEARCH PARK

4800 BRADFORD DRIVE, HUNTSVILLE, ALABAMA

WEIGHT-SAVING THROUGH USE OF BERYLLIUM-ALUMINUM ALLOYS FOR SATURN-TYPE VEHICLE STRUCTURES

December 1965

Contract NAS8-11298

PREPARED BY: _____
H. H. Armstrong
Project Engineer

APPROVED BY: _____
R. E. Bieber
Mgr., Structures & Mechanics

_____
for   J. S. Farrior
Resident Manager

ABSTRACT

$2 4 9 7 9$

A comparison of material properties of conventional light weight metals indicates beryllium-aluminum alloys offer potential weight savings of 50 to 70 percent for compression-loaded primary structures. The premise that beryllium-alluminum alloys with a modulus of elasticity equal to steel, yet weighing one-fourth as much as steel, could save 50% of the weight of a Saturn-type-upper-stage structure is investigated and confirmed. Additionally, hardware costs, costs per pound, and net cost savings per launch are considered. It is shown that the case for 50% weight savings through beryllium-aluminum alloys can be accomplished at a cost of only $240 per pound of weight saved, a very competitive figure in view of the high cost of payloads (up to $10,000 per pound.)

Cylindrical interstages, 22 feet in diameter, loaded by a uniformly distributed axial load typical of a Saturn V upper-stage were optimized structurally for minimum weight. Digital computer programs were used to optimize automatically the stiffened constructions, consistent with manufacturing restraints deemed advisable. The materials investigated included unalloyed beryllium, beryllium-aluminum alloys, and alloys of titanium, aluminum and magnesium. Constructions considered included integral stiffeners conventional flanged open sections, and corrugation-type closed sections.

FOREWORD

INTRODUCTION

In the structural design of large space vehicles, weight and structural stiffness are of paramount importance. The availability of commercially-produced beryllium-aluminum (Be-A*l*) alloys offers the structural designer an opportunity to capitalize on a comparatively new development in light-weight structural materials. Weight reductions as well as increased rigidity can be anticipated.

The largest weight savings result when the use of new or improved materials is combined with optimum structural design methods. Evaluations based on these two techniques are covered in this study. In the design phase, the material property of most concern in rigidity and stability considerations is the modulus of elasticity, E. The higher the E, the better the stiffness, for the same thickness. Relating E to material density is one measure of stiffness efficiency.
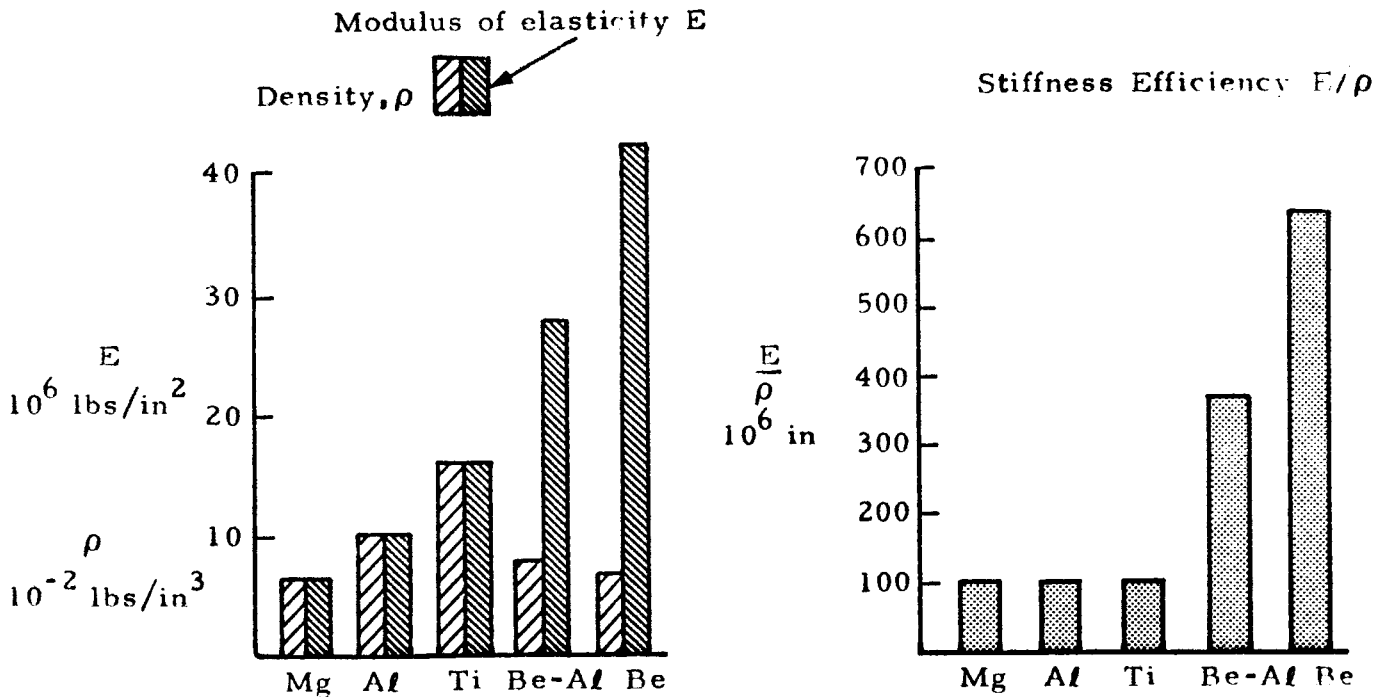
The modulus to density ratio of 100×10^6 which is normal for most structural metals is seen to quadruple or more in the cases of beryllium-aluminum alloys (Be-38% Aℓ) and unalloyed Be. Relating this indicated advantage to upper-stage Saturn structures is a major goal of the study.

The particular emphasis on beryllium-aluminum alloys is due to the fact that they retain to a large extent the desirable properties of unalloyed beryllium, notably the high modulus and low density, while achieving significantly improved ductility, fabricability, machinability and impact resistance. The alloys do not require the tedious and costly chemical etching treatments following working operations which are required by unalloyed beryllium. Their improved handling characteristics plus the lower temperature requirements for processing compared to beryllium, should result in significantly lower installed costs compared to beryllium.

Substantial improvements in structural optimization and analysis methods have occurred in recent years. The general instability analysis of shell structures has been undergoing extensive study i.e., B. O. Almroth (References 1 and 2); and optimization procedures and methods developed by A. B. Burns (References 3, 4, 5) have resulted in design-oriented mechanized solutions which consider practical design and manufacturing restraints. That eccentricities of stiffeners with respect to the midsurface od the skin would drastically affect the shell critical load was predicted as early as 1947 by van der Neut (Reference 6), and more recently by Baruch and Singer (Reference 7). The addition of eccentricity effects into any preliminary design optimization is considered mandatory to avoid distorted weight reporting.

The latest structural methods have been employed to optimize various constructions of the most attractive lightweight metals. Digital computer programs are used to optimize the three general classes of stiffened construction:

- Integral Stiffening - A Lockheed developed program (Reference 3)

- Closed Section Stiffeners - A Lockheed developed program (Reference 4)

- Open Section Flanged Stiffeners - Program developed under this study (Reference 5)

Additionally, the cost-producibility of such structures are compared through a cost effectiveness study which delineates cost per pound of weight saved as well as total mission cost savings on the basis of weight saved.

CONCLUSIONS

The conclusions reached in the study are:

1. Structures of Be-Aℓ alloys optimize at approximately 50% of the weight of optimized aluminum structures for application to current Saturn upper-stage structures.

2. Structures more heavily loaded show smaller weight savings (30%), but these are still very significant in view of the cost per pound of orbital and escape payload weight.

3. The cost study shows the cost per pound of weight saved to be reasonable, indicating that immediate consideration of beryllium-aluminum alloys for primary structures is warranted.

4. The use of digital computer programs for preliminary structural design yields useful stress, weight and configuration detail results of a depth not heretofore available.

RECOMMENDATIONS

This study has shown significant weight and cost advantages are available to designers using the light-weight materials optimized through improve structural methods employing digital computer techniques. There are areas where expanded work is necessary and problem areas where improvements can be made. Additionally, experimental verification of the conclusions is necessary prior to hardware incorporation. It is recommended that additional work in the following areas be performed:

- **Combined Loading**

  Add the effect of external and internal pressure to the existing computer programs to analyze the effects of expected Saturn combined loadings.

- **Plasticity Effects**

  Include plasticity effects in the computer programs where stress levels exceed the proportional limit.

- **Pre-Buckling Considerations**

  Determine possible weight advantages by permitting the skin to buckle between stringers.

- **Panel Test Program**

  Test Be-Aℓ panel stability to demonstrate light-weight design behavior under failure conditions.

- **Wood-Polymer Composite Materials**

  Evaluate wood-polymer composite construction as an economical short interstage.

- **Higher Strength Be-Aℓ Alloys**

  Evaluate further improvements by using higher strength Be-Aℓ in the as-rolled temper (currently limited to annealed).

- **Honeycomb Optimizations**

  Modify a square-cell honeycomb program to optimize hexagonal honeycomb sandwich construction.

- **Design Evaluations**

  Modify existing computer programs to evaluate specific design changes.

- **Design Detail Problem Areas**

  Investigate end rings, load introduction methods and cutout effects.

- **Be-Aℓ Producility**

  Develop manufacturing-producibility capability for beryllium-aluminum.

- **Be-Aℓ Data Book**

  Publish a Beryllium-Aluminum Design Data Handbook.

ACKNOWLEDGEMENTS

CONTENTS

CONTENTS (Continued)

LIST OF ILLUSTRATIONS

Contents (Continued)

CONTENTS (Continued)

CONTENTS (Concluded)

LIST OF APPENDIXES

NOTATION

C	geometric constant
d_y	ring spacing (centerline to centerline)
E_w, E_x, E_y	Young's modulus for cylinder wall, stringer and ring material, respectively
F	allowable stress
L	cylinder length
N_x	applied axial load per unit of circumference
R	cylinder radius
t	cylinder wall thickness
$\bar{t}$	equivalent thickness of a stiffened cylinder having uniform material properties, for purposes of weight calculation
$\bar{\bar{t}}$	equivalent thickness of a stiffened cylinder having non-uniform material properties, for purposes of non-dimensionalization of weight. Equal to W_i / ρ_w
W_i	weight of cylinder per unit of surface area
ϵ	strain
ν_w, ν_x, ν_y	Poisson's ratio for cylinder wall, stringer and ring material, respectively
ρ_w, ρ_x, ρ_y	material density for cylinder wall, stringers and rings, respectively
σ	uniform axial compressive stress
ϕ	empirical correction factor

Subscripts

cr	critical
e	effective
s	stringer
r	ring
w	cylinder wall

NOTATION (Continued)

Subscripts

x or 1	axial coordinate
y or 2	circumferential coordinate
cl	classical
c	compression
y	yield

Other Notations may occur on specific figures.

CONTENTS (Concluded)

LIST OF APPENDIXES

NOTATION

C	geometric constant
d_y	ring spacing (centerline to centerline)
E_w, E_x, E_y	Young's modulus for cylinder wall, stringer and ring material, respectively
F	allowable stress
L	cylinder length
N_x	applied axial load per unit of circumference
R	cylinder radius
t	cylinder wall thickness
$\bar{t}$	equivalent thickness of a stiffened cylinder having uniform material properties, for purposes of weight calculation
$\bar{\bar{t}}$	equivalent thickness of a stiffened cylinder having non-uniform material properties, for purposes of non-dimensionalization of weight. Equal to W_i / ρ_w
W_i	weight of cylinder per unit of surface area
ϵ	strain
ν_w, ν_x, ν_y	Poisson's ratio for cylinder wall, stringer and ring material, respectively
ρ_w, ρ_x, ρ_y	material density for cylinder wall, stringers and rings, respectively
σ	uniform axial compressive stress
ϕ	empirical correction factor

Subscripts

cr	critical
e	effective
s	stringer
r	ring
w	cylinder wall

NOTATION (Continued)

Subscripts

x or 1   axial coordinate

y or 2   circumferential coordinate

cl   classical

c   compression

y   yield

Other Notations may occur on specific figures.

TECHNICAL DISCUSSION INTRODUCTION

The light-weight materials chosen for structural optimization of upper-stage Saturn structures are:

- Aluminum $\qquad$ 7075-T6
- Beryllium-Aluminum $\qquad$ Be-38 Al
- Beryllium $\qquad$ Be
- Magnesium Lithium $\qquad$ LA-141
- Magnesium Thorium $\qquad$ HK31A-H24
- Titanium $\qquad$ 6 Al-4V

The properties used are shown on the next page.

The Optimization Methods and Configurations are discussed on page 3 and the results of the Optimum Weight Studies on page 8.

The Cost Effectiveness Study and material cost are covered beginning on page 17 and a summary bar graph is shown on page 22.

The International System of Units (SI) conversion factors are shown on page 24 with the report references on the next page.

The following appendixes are included:

MATERIALS

The material properties for the materials used in this study are given in the following table:

Material	F_{cy} Compressive* Yield Stress (ksi)	ρ Density (lb/in^3)	E *Modulus of Elasticity (10^6 lbs/in^2)	Poisson's Ratio
Aluminum 7075-T6	71	0.101	10.3	0.33
Beryllium-38% Aluminum BE-Al	32	0.075	27.5	0.14
Beryllium, Be	45	0.066	42.0	0.09
Magnesium-Lithium LA 141	15	0.049	5.9	0.33
Magnesium-Thorium HK 31A-H24	19	0.065	6.5	0.35
Titanium 6Al-4V	126	0.160	16.0	0.28

*MIL-HBK 5 Data or estimated equivalent.

The materials chosen were considered standard light-weight materials with well-documented allowables. The Beryllium-38% Aluminum alloy properties are shown in Reference 8 and in Appendix D. Other titanium or aluminum alloys could have been selected, with no resulting weight penalty, as modulus rather than yield stress was the critical Al and Ti material parameter for the loading and geometry investigated.

Mg-Li (LA-141) was added late in the study as a result of NASA interest. Applications of this, the lightest of all structural alloys, is limited to about the 150°F temperature range. Corrosion protection, also, is a significant problem area.

OPTIMIZATION METHODS AND CONFIGURATIONS

Summary

Digital computer programs were modified to optimize automatically the minimum weight stiffened cylinder configurations, consistent with manufacturing restraints deemed advisable.

The three configurations considered were:

a. Integrally-stiffened rectangular stringers and circumferential rings

b. Corrugated-core semi-sandwich (trapezoidal corrugation with a single face sheet) stiffened circumferentially with angle section rings

c. Conventional flanged stiffeners and rings: Zees, Channels, "J" sections.

In the latter case, (c), the capability exists for optimizing cylinders with different materials in the cylinder wall, rings, and stringers.   In all cases, the effects of stiffener eccentricity are considered.

In addition to manufacturing producibility restraints (slenderness ratios, commercially available sheets, etc.), two additional restraints are included:

● The analysis must be capable of yielding optimum design data when the wall thickness is pre-determined.

● Stresses remain elastic; provisions for a maximum stress limitation are incorporated.

The effect of the latter restraint is to ensure that stresses do not exceed the proportional limit of the material; however, maximum stresses above this level may be specified and the error so incurred will depend upon the amount of plastic strain at the maximum stress.

Having recognized these restraints, equations are written for:

● Local instability of the cylinder wall and stringers.

● General instability involving the composite structure. Two variations are considered:

    a. panel instability involving the cylinder wall-stringer composite between rings, and

    b. overall instability involving the cylinder wall-stringer-ring composite.

Ideally, the lowest structural weight results when the various equations are solved so that instability in every mode occurs simultaneously at the critical design load. However, the effect of the restraints imposed is often to upset this idealization. In this case, the problem is to find that set of parameters which comes closest to this ideal, yet satisfies the restraints imposed. This procedure often involves numerous calculations and is therefore programmed for the IBM 7094 and/or Univac 1107 computers.

The equations used represent the case of simply supported cylinders ends; that is, at the ends of the cylinder, the radial and circumferential displacements are zero, and the force and moment resultants in the axial direction are also zero. Additionally, end ring weights are not included as they are usually designed by local conditions, such as load introduction, separation, etc.

Rectangular Rings and Stringers

The rectangular ring and stringer configuration (Figure 1) is particularly applicable to welded cylindrical structures constructed of curved panels and is useful for tank design where joints are critical. This construction may be manufactured by mechanical milling, chem-milling, or combinations of both.

Original formulation of the computer programs for the structural optimization of cylinders stiffened with rectangular rings and stringers, (Reference 3) was carried out under the Lockheed Independent Development Program. This company-sponsored work was furnished at no cost to NASA; adaptation to Fortran IV was required for operational status at the MSFC Computational Lab.

The structural optimization accounts for several practical restraints on the structure; for example, optimum designs may be determined when the cylinder-wall thickness is fixed by burst-pressure considerations, and when the height of rings and/or stringers is limited by commerically available plate stock.

Almroth's method (References 1 and 2) for predicting the general mode of instability is used in the analysis. In this method, the critical buckling load is equal to the minimum postbuckling load plus a percentage of the difference between the classical buckling load and the minimum postbuckling load depending upon the cylinder geometry. A description of this method is contained in Appendix B.

Four degrees of restraint are considered in this analysis (Reference Figure 1). These are listed below together with the nondimensionalized parameters which will be used to describe them:

- Wall thickness fixed by internal pressure, R/t

- Overall cross-sectional height fixed, $(b_x/R)_{max}$, $(b_y/R)_{max}$

- Slenderness ratio of rings and stringers fixed, $(b_x/t_1)_{max}$, $(b_y/t_2)_{max}$

- Maximum stress not to exceed proportional limit, $(\sigma/E)_{max}$

The first restraint stems from the requirement for a predetermined wall thickness to sustain internal burst pressure if the structure is a tank structure. The second restraint represents the limitation on maximum plate thickness commercially available with uniform mechanical properties through the thickness for integrally machining the rings and stringers. The third restraint is an arbitrary restraint intended to minimize deviations in straightness in the rings and stringers as they are machined, and also to limit damage to the rings and stringers which may be incurred during handling and transporting the cylinder. The fourth restraint is included to ensure an elastic analysis.

Cylinders Stiffened with Corrugations and Rings

The structural optimization of axially compressed cylinders stiffened longitudinally with trapezoidal corrugations and circumferentially with rings having a 90-deg angle cross section is an efficient economical construction for large vehicles, see Figure 2 . The formulation of the structural optimization analysis is contained in Reference 4 ; only general criteria will be discussed here.

The effects of corrugation/ring eccentricity are included in the analysis and the change in efficiency as the reinforcement is moved from one side of the cylinder wall to the other may be investigated. In this analysis, as in previous similar analyses, practical restraints on the configuration are recognized; for example, the minimum widths for corrugation-cylinder wall attachment and for ring-cylinder wall attachment, and the maximum permissible ring height. It is known that practical values of these restraints may influence the choice of cylinder reinforcement. Limitations in the work relate principally to uncertainties in assessing the torsional stiffness of the corrugation; in addition, more test data are needed to permit upgrading the empirical relation used in connection with predictions for the general mode of instability.

Six degrees of restraint are considered. These are listed below together with the nondimensionalized parameters used to describe them:

- Wall thickness fixed, R/t_f

- Minimum width of corrugation/cylinder-wall attachment fixed, $(b_a/R)_{min}$

- Maximum height of ring fixed, $(b_y/R)_{max}$

- Maximum slenderness ratio of ring fixed, $(b_y/t_2)_{max}$

- Width of ring attachment flange fixed, a_y/R
- Maximum stress not to exceed proportional limit $(\sigma/E)_{max}$

The first restraint may be applicable to tank or cabin structures subject to internal burst pressure, assuming maximum burst pressure does not occur simultaneously with maximum axial load. (The methods do not consider the simultaneous application of these loads.) The second restraint represents the practical requirements for a minimum width b_a either for welding or bonding. The third restraint is included to account for clearance limitations which may exist, while the fourth is an arbitrary restraint intended to minimize deviations in straightness in the rings, and to limit damage to the rings during manufacturing and handling of the cylinder. The fifth restraint recognizes the requirement for a specified width of ring attachment flange for attaching the ring to the cylinder wall. The last restraint is included to ensure an elastic analysis.

The analysis also includes the option for optimizing a corrugation whose side and top dimensions are dissimilar. The parameter used to accomplish this is the constant C (see Figure 2), which, when multiplied by the width of the top of the corrugation b_c, results in the dimension of the sides of the corrugation, Cb_c. Note that the dimensions b_c, Cb_c, and b_a are measured from the intersections of lines drawn through the midplanes of the corrugation elements. The option is intended primarily as a device for final design to find, by small variations in the lengths of elements, the most efficient proportions which utilize standard gages in both cylinder wall and corrugation.

Cylinders Reinforced with Conventional Flanged Stiffeners and Rings

The basis for the structural optimization of axially compressed cylinders reinforced with J, Z, or channel section stringers and optional J, Z, or channel section rings is presented in Reference 5 and discussed below.

The cross-sectional geometry for axially compressed, J-stiffened cylinders is shown in Figure 3. By eliminating one of the elements of width c_s, the stiffeners become either Zees or channels. This operation is easily handled in the optimization analysis, as will be demonstrated in Appendix A. Thus, the following analysis has been developed to handle any one of these three stiffener shapes; further, the analysis is capable of utilizing one stiffener shape for the stringers and a second stiffener shape for the rings, if desired. The rings and stringers may be located on either side of the cylinder wall; the analysis appropriately evaluates the eccentricity effects.

Additional options written into the program include a capability for specifying ring and stringer flange thicknesses which are a multiple of the web thickness. This option appears in the analysis in the form of the ratios t_{1c}/t_{1b}, t_{1a}/t_{1b}, t_{2c}/t_{2b}, t_{2a}/t_{2b}. It is included to enhance those designs utilizing extruded rings and/or stringers by increasing the bending stiffness of the section in the most efficient manner. A final option permits specifying

6

separate material properties for the rings (E_y, ν_y, ρ_y), stringers (E_x, ν_x, ρ_x) and cylinder wall (E_w, ν_w, ρ_w). This option permits cost-efficiency investigations of mixed-material designs; for example, Be-Al rings in an otherwise aluminum design.

The following restraints are recognized. The parameters used to describe the restraints in the analysis are also noted:

- Wall thickness known, R/t

- Maximum height of ring and stringer fixed, $(b_y/R)_{max}$, $(b_x/R)_{max}$

- Width of ring and stringer attach flange fixed, a_y/R, a_x/R

- Ring and stringer candidate gages specified, $(t_{1b}/R)_1 \rightarrow (t_{1b}/R)_3$, $(t_{2b}/R)_1 \rightarrow (t_{2b}/R)_3$

- Maximum strain not to exceed proportional limit in stringers and cylinder wall, $(\sigma/E_x)_{max}$, $(\sigma/E_w)_{max}$.

The first restraint is included to permit specifying a standard wall gage which is the minimum acceptable for either manufacturing reasons or accommodating other design conditions. The second restraint accounts for clearance limitations which may exist, while the third restraint recognizes the requirement for a specified width of flange to attach the rings and stringers to the cylinder wall. The fourth restraint limits the design to specified standard gages. A capability for considering three stiffener thicknesses is provided, where the first thickness specified is the minimum standard gage acceptable and the third thickness specified is the heaviest standard gage judged to be required. The fifth restraint is included to ensure an elastic analysis.

The equations for local and general instability and a discussion of optimization procedures are included in **Appendix A** of this report and **Reference 5.**

OPTIMUM WEIGHT STUDIES

Introduction

Using the three digital computer programs and the light-weight materials previously described, structural optimizations were carried out for a Saturn Upper-Stage of 260-inch diameter. The 1300 lb/in. loading shown is typical for a Saturn V structure just forward of the S-IVB stage. Other loadings of 1600, 2000, and 5000 lbs/in. were also investigated.

In general, curves are plotted showing the effect of ring spacing on the structural weight (mass); basic skin thickness variations are also shown. Both a short ($\ell = 36$ inch) and long ($\ell = 260$ inch) cylinder were investigated.

The curves are presented on a dual scale of U.S. Customary Units and the International System of Units. The conversion factors are given on page 24.

The effects of stiffener eccentricity were considered in all cases. As previously stated, end rings are not considered in this study. Figure 4 shows a typical interstage with rectangular stiffeners.

Summary

Short Cylinder, 1300 lb/in. Loading

A 36-inch long interstage was investigated for 1300 lb/in. loading, with no rings (stringers only) and one or two intermediate rings (ring spacing of 18 or 12 inches). In some cases the 12-inch ring spacing was too non-optimum for the results to be meaningful; these were deleted.

Several manufacturing constraints were included:

a. Maximum stringer and ring heights = 1.5 in.

b. Maximum slenderness ratio, $b/t = 15.0$

c. Zee and "J" stringer and ring attach-flange width = 0.70 in.

d. Trapezoidal corrugation attach face width = 0.40 in.

e. A maximum stress limitation equal to the compressive yield allowable was set.

Three basic skin thicknesses (0.030, 0.045, 0.060) were used for the initial computer runs. Additional optimizations were made to determine the optimum thickness based on the initial results.

A comparison of the minimum weight designs for the three configurations is shown in Figure 5 . The lower three curves are the Be construction. The next three above are Be-38% Aℓ, etc. The points are jointed for clarity and do not, of course, indicate other ring spacings are permissable.

While the minimum weight configuration in each material was the corrugation stiffened cylinders with no rings, the competitiveness of the Z stiffened cylinders is particularly interesting.

With the most efficient aluminum design exceeding 200 lbs and the Be-38% Aℓ configuration weighing less than 100 lbs, the premise that 50% weight-saving is available using Beryllium-Aluminum alloy structures is verified for Saturn applications.

The intermediate ring configurations varied in their efficiency and were, no doubt, influenced by the constraints imposed.

The optimum weight configurations for each material and construction are shown in Figures 6 through 17. Weight, stress level and the ring and stringer dimensions are given for each configuration.

The closeness of the longitudinal stiffening is a characteristic of all the designs shown. In the non-optimum configurations investigated, the minimum weight designs always evolved from closely-spaced stringers.

RECTANGULAR RINGS AND STRINGERS
(Integrally Stiffened)

Short Cylinders

Basic optimization studies were made with the following parameters:

Length = 36 inches, Radius = 130 inches (L/R = 0.277)

The Saturn V load of 1300 lbs/in. was applied.

Ring spacing = 12, 18, 36 in.

Restraints were: ring and stringer heights limited to 1.5 inches and slenderness ratios limited to 15.0.

Cylinder skin thicknesses of 0.030, 0.045, and 0.060 inches were first investigated.

Charts showing the effect of ring and stringer eccentricity upon structural efficiency are presented in Figures 18 through 26. Figures 18 through 20 show the optimized structural weights of the external rectangular rings and stringers for cylinder wall thicknesses of 0.030, 0.045, and 0.060 inches, respectively. Figures 21 through 23 show the corresponding weights for internal rings and stringers. Comparing these sets of curves, the external rings and stringers are seen to be the most efficient for all five materials and three thicknesses. While the one intermediate ring configuration is seen to be the lightest for external stiffening, the stringers only solution is lightest for the internal stiffening.

Figures 24-26 compare the internal and external ring/stringer configurations of Aℓ and Be-38% Aℓ for the three thicknesses. The percent weight difference between the two configurations decreases as the skin thickness increases; however, these heavier gages are non-optimum configurations. The effect of stringers external and rings internal, and vice-versa, and the effect of ignoring eccentricity is intermediate weight values between the extremes shown (Reference 3).

Figure 27 shows the structural weights of the three basic skin thicknesses for the external ring/stringer Aℓ and Be-38% Aℓ configurations. The 0.030 skin is the most efficient, but the Aℓ 0.045 construction is very competitive at the 18-inch ring spacing, and stringers-only configurations.

Based on the indicated trend of Figure 27 additional computer runs were made to determine the optimum skin thickness. Values of 0.020 and 0.010 were used for both materials. The skin thickness of 0.030 inch was optimum for the Aℓ construction while 0.020 was most efficient for Be-38Aℓ. Figure 28 shows the Be-38% Aℓ weights for the series of basic skin thicknesses.

The indicated optimum weight for each of the six materials investigated is summarized in Figure 29. The Aℓ structure is approximately twice as heavy as the corresponding Be-38 Aℓ structure.

In order to compare these optimizations to actual hardware, the weight of a production Saturn V interstage just forward of the S-IVB stage was calculated. Ignoring splices, cutouts, end rings, etc., the flight hardware weight of the aluminum honeycomb interstage is 240 pounds, based on:

One-inch thick aluminum honeycomb

0.030 outer and 0.020 inner face sheets

3.25 lb/ft^3 aluminum core

0.006-inch thick resin (0.095 lb/ft^2 per face)

While the honeycomb does not compete in this case, it is recognized that other criteria may have influenced the design.

Additional optimization studies were performed for the integral rectangular ring/stringer configurations using increased axial compression lineloads of 1600, 2000 and 5000 lb/in. Again, basic cylinder skin thicknesses of 0.030, 0.045, and 0.060 inches were used, with additional thicknesses selected as required to determine the optimum design. Figure 30 - 32 show the optimum weights and thicknesses for the 1600, 2000 and 5000 lb/in. lineloads, respectively, for the six materials considered.

The Be-38% Al structures were approximately one-half the weight of the Al structure for the 1600 and 2000 lb/in. loadings. The thicker skin gages of 0.030 and 0.045 were the optimum thicknesses for the 2000 lb/in. configurations.

As expected, the heavier lineload of 5000 lb/in. showed aluminum more efficient than the magnesium alloy structures. However, the Beryllium-Aluminum structure still showed a 25% weight advantage over the optimum aluminum configuration. No weights are shown for the intermediate rings for Be-Al or Be as the shortness of the cylinder precluded an optimum design with rings.

In Figure 33, the minimum weight rectangular ring/stringer configurations for each material are plotted versus lineload. The aluminum becomes more efficient than the Mg-Th and Mg-Li structures for the higher loadings. The titanium should also be more competitive than is indicated at the higher lineloads. Investigation showed that the restriction on the maximum ring/stringer height of 1.5 inch handicapped the titanium structures. If this restraint is relaxed to allow taller members, more competitive results are realized.

The material curves were constructed as dashed lines between the 2000 lb/in. and 5000 lb/in. loading values. These curves should be used only as an indicated trend based on the four values available. Further investigation is needed to obtain minimum weight structures for this range.

The structural weights for the three basic cylinder skin thicknesses for aluminum and beryllium-38 aluminum are plotted versus lineload in Figure 34. Based on the indicated trend, the 0.045 Be-38% Aℓ structures appear to be more efficient for loadings larger than 2000 lb/in. While the Be-38% Aℓ structural weights converge toward a common value at the 5000 lb/in. loading, this result may not be real. Reviewing Figure 32, the configurations other than the stringers-only structure resulted in non-optimum structures for this loading (no weights are available). Further study is needed for load values greater than 2000 lb/in. to define optimum weights.

The 0.060 aluminum cylinder skin thickness is seen to cross over and become more efficient at higher loadings. The 0.045 structure compared to the 0.060 configuration results in an approximately 8% heavier structure for the 5000 lb/in. lineload.

Long Cylinders (L/R = 2.0)

A long cylinder rectangular ring/stringer configuration of length equal 260 (L/R = 2.0) was also investigated during the structural optimization study. The same restrictions, materials and loadings used for the short cylinder were applied. Additional ring spacing of 65 inches was added to the 12, 18 and 36 inch spacings previously investigated. The basic cylinder skin thicknesses of 0.030, 0.045, and 0.060 were used for the initial computer runs with additional thicknesses selected as required to achieve optimum designs.

The minimum weight designs and optimum thicknesses for the 1300 lb/in. loading are shown in Figure 35. A basic skin thickness of 0.045 inches produced the minimum weight designs for the aluminum configurations. For the Be-Aℓ configurations, the basic skin thickness of 0.020 and 0.030 resulted in essentially equal weight configurations, while 0.0225 was the optimum thickness. As with the shorter cylinders, L/R = 0.277, the minimum weight aluminum configurations were approximately twice as heavy as the corresponding Be-Aℓ structures. External ring and stringer configurations produced optimum structures for each material.

As expected, the optimum weight structures resulted from different basic skin thickness as the material and ring spacing parameters changed. Figure 36 gives the structural weights for the series of basic skin thicknesses that were investigated to obtain the optimum thickness for the aluminum and Be-38% Aℓ constructions.

For the 1600 lb/in. axial compressive loading, Figure 37, the 18-inch ring spacing configuration was the most efficient for the beryllium, Be-38% Aℓ and Magnesium-Lithium materials, while the 65-inch spacing was optimum for the other three materials.

The graphs of the structural weights for the 2000 and 5000 lb/in. loadings are Figures 38 and 39, respectively. The aluminum construction becomes more efficient than the Mg-Th for a 36-inch ring spacing at the 5000 lb/in. loading. Also, the Be and Be-38% Aℓ structural weight appears to be unaffected by the variation in ring spacing.

A study was performed to determine why the titanium was not more competitive at the 5000 lb/in. loading. The effect of increasing the maximum allowable ring and stringer height from 1.5 inches to 3.0 inches resulted in reduced weights of 15 to 30% for the 0.060 titanium structure subjected to the 5000 lb/in. loading. The effects of this restraint on the weight and ring/stringer cross-sections are shown in Figure 40 and Table I . The ring thicknesses reduced from approximately 1.0 inch to 0.20 inches, while the ring height doubled in most cases.

Figure 41 presents a summary plot of the minimum weight rectangular ring/stringer configurations for each material versus axial load. The Be-38% Aℓ structure remains approximately 50% lighter than the Aℓ structure for most loadings.

The material curves were constructed as dashed lines between the 2000 lb/in. and 5000 lb/in. loading values. Because only the four values were available, these graphs serve as trend indicators only. Further investigation is needed to obtain minimum weight structures for the intermediate range.

Effects of Slenderness Ratio Restraints

Studies were made of the effect of increasing the maximum allowable ring and stringer slenderness ratios from 15 to 30. The external rectangular ring and stringer, aluminum and Be-Aℓ, configurations with skin thicknesses of 0.030, 0.045 and 0.060 were used.

The result of imposing a restraint of 15.0 on the slenderness ratios is a weight penalty of approximately 4%. The (b/t) max = 30 restriction gave slightly thinner and taller stringers, spaced closer together, while the rings showed little change. Table II (page 71) shows typical results.

TRAPEZOIDAL CORRUGATION

The stiffening orientation used in the optimization study was external corrugations and internal rings. While this was not as efficient as external rings/internal corrugations, a more practical structure results (Reference 3).

The restraints used in this study were (Figure 2):

(1) Minimum width of corrugation/cylinder-wall attachment, $b_a = 0.4$

(2) Maximum height of ring, $b_y = 1.5$

(3) Maximum slenderness ratio of ring, $b_y/t_2 = 15.0$

(4) Width of ring attachment flange, $a_y = 0.7$

(5) Maximum stress not to exceed the compressive yield allowable.

The basic cylinder configuration was:

Diameter = 260 inches

Length = 36 inches (L/R = 0.277)

Axial Lineload = 1300 lb/in.

Ring spacing = 0, 18 and 36 inches

These parameters are typical for a Saturn V interstage.

Computer runs were made using a series of skin thicknesses, ranging from 0.015 to 0.040 inches, for the four materials investigated. These materials were:

Aluminum
Beryllium
Beryllium-38% Aluminum
Magnesium-Thorium

Figure 42 shows the optimum weight designs for each material. In all cases the "corrugation only" configurations were the most efficient, i.e., no rings. The optimum cylinder-wall skin thickness varied with material.

Again, the Be-38 Aℓ structure is seen to be approximately 50% lighter than the corresponding aluminum configuration.

The minimum weight detail configurations for each material are shown in Figures 7 , 10, 13 and 16. The dimension "cb_c" is the slant height of the corrugation.

CONVENTIONAL FLANGED (ZEE AND "J") RING/STRINGER CONFIGURATIONS

An optimization study was performed for an axially compressed cylinder reinforced with external stringers and internal rings of Zee or "J" section. The Zee can also be configured as a channel.

The materials considered were:

Aluminum
Beryllium
Beryllium-38% Aluminum
Magnesium-Thorium

A structure composed of Aluminum walls with Be-38% Aℓ rings and stringers was also investigated.

The basic cylinder parameters were:

Diameter = 260 in.

Length = 36 in. (L/R = 0.277)

Lineload = 1300 lb/in.

Ring spacing = 0, 18, 36 inches

The restraints used in the analysis were (Reference Figure 3):

(1)   Maximum height of ring and stringer, b_{max} = 1.5

(2)   Width of ring and stringer attach flange, $a_x = a_y = 0.70$

(3)   Ring and stringer candidate thicknesses limited to standard gages.

(4)   Maximum strain not to exceed the compressive yield allowable in stringers and cylinder wall.

A series of basic skin thicknesses and a range of ring/stringer gages were considered for each construction.

The optimum weights, and type of construction for each material are shown in Figure 43. The optimum thickness, most efficient configuration and J or Zee construction varied from material to material. The Be-38% Aℓ structure was 50% lighter than the corresponding aluminum structure, while the Aℓ wall/Be-38% Aℓ ring and stringer configuration fell mid-way between the two.

The minimum weight configurations for each material are shown in Figures 8, 11, 14 and 17.

REDUCED COMPRESSIVE YIELD STRESS FOR
BERYLLIUM-38% ALUMINUM

The weight-saving study showed that the Be-38% Al structures generally optimized at the highest allowable stress assigned, usually the compressive yield value. Since the Be-38% Al stress-strain curve has a rounded knee, the compressive yield stress region requires a plasticity reduction factor. As this was not available in the existing computer programs, a study was made of the effects of reducing the compressive yield stress for Be-38% Al. Three values were used: F_{cy} = 24 ksi, 28 ksi and 32 ksi. As seen in Figure 44, the configurations using F_{cy} = 32 ksi resulted in the minimum weight designs. The F_{cy} = 28 ksi restriction caused no significant weight increase, but the F_{cy} = 24 ksi configurations resulted in a 17% weight penalty for small ring spacing. For a large ring spacing, 65 in., the weights for all three compressive yield configurations were approximately the same (but were not optimum).

Additional study is needed in this area to include the plasticity reduction factor in the optimization analysis and evaluate this effect on structural weight.

COST EFFECTIVENESS

The recognition that valuable weight-saving possibilities exist leads to the logical assessment of cost. Relating cost and weight parameters to an overall system cost to evaluate the net gain/loss per launch is a convenient method of presenting cost effectiveness.

Material Cost

The material costs estimated by the Beryllium Corporation were based on the following:

- a sponsored material development program originating 24 months prior to delivery

- a yearly market of 10,000 pounds.

On this basis, the estimated cost of 36 x 96 inch sheet sizes in 0.020 inch thick beryllium-38% aluminum alloy would be $257 per pound. In thicker gages, Be-38% Al alloy of 0.070 inch thickness would cost $110 per pound.

For unalloyed beryllium, 0.020 sheets would cost $338 per pound; $136 per pound for 0.070 in thick.

ESTIMATED COSTS OF ALLOYED AND UNALLOYED
BERYLLIUM IN SHEET SIZES 36" x 96"

Thickness (inches)	Alloyed Beryllium Be-38% Al Lockalloy		Unalloyed Beryllium Be	
	Dollars per lb	Dollars per sq. in.	Dollars per lb	Dollars per sq. in.
0.020	257	0.385	338	0.446
0.070	110	0.58	136	0.63

The above table summarizes the cost information. For thicknesses below 0.020, the cost per square inch should remain constant, increasing the cost per pound.

Technological advances can be expected to reduce the price of the Be-38% Aℓ alloys in the future even below the tabulated values. For example, improved methods of making the raw material and fabricating wrought products can be expected if the potential usage is proven by consumer groups so that the use of either private risk capital or Government funds are shown to be feasible and economically sound. By way of illustration one could conceive of producing Be-38% Aℓ alloy by a continuous process such as the direct powder rolling process developed by The Reynolds Metals Co., provided the required volume were sufficient to justify the investment. Recently, General Astrometals have installed new electrolytic cells, developed by the Pichiney Co., to process low grade beryllium ore deposits in Utah. They claim that this new development offers the potential of reducing the cost of unalloyed beryllium by 50%. This, of course, would be expected to lower the cost of the Be-38% Aℓ alloy, whose price should always be at least 25% less than that of unalloyed beryllium.

Hardware Cost Analysis

A detailed cost-producibility study was performed on a wide variety of configurations and materials; these results are presented in Appendix C of this report, and partially summarized below.

In Appendix C, hardware costs are presented for manufacturing lots of 1, 10, 50 and 100. Here we will discuss lots of 10 only, since they are fairly representative. These costs do not include some of the standard expenses that would apply universally to each structure and the results presented, therefore, represent comparative prices.

A cost summary, Table III , is reproduced from Appendix C which shows the unit costs of each construction along with a general description. These costs are based on a 260-inch diameter interstage, 36 inches long.

Further refinements into costs per pound of weight saved and net cost savings per launch have been made in Tables IV and V and the results summarized graphically in the bar graphs of Chart I.

Weights and costs are shown for construction of aluminum, beryllium, beryllium-38% aluminum alloy, and a composite structure of aluminum skin stiffened by beryllium-38% aluminum alloy stringers. The costs shown are for individual units purchased in lots of ten. The weight values are those from the optimization study; the cost values from Appendix C. Two cost adjustments were made. In the composite construction, aluminum skin with Be-Aℓ stringers, the cost figures included a center ring. In the Be-Aℓ stringer and skin, the cost study was on a slightly non-optimum configuration; so material costs were excessive. These two changes resulted in slightly lower finished prices.

Bar graph A shows the total structural weights of the Z stiffened structures. The comparison point chosen for reference was aluminum, and graph B showing the weight saved for each material compared to aluminum. The percentage weights saved compared to aluminum are:

Be	64% lighter
Be-38 Aℓ	53% lighter
Composite	31% lighter

The total cost of the structures is shown in graph C and the cost per pound of weight saved in graph D. The $240 per pound cost for each pound saved for Be-Aℓ alloy structures is considered to be very competitive in the light of payload costs for space programs. The price an agency is willing to pay for a pound of upper stage weight saved may vary from as low as $500 per pound up to $10,000 per pound, or more.

To give an indication of cost saving potential through the use of the more efficient materials, an arbitrary $1000 per pound of upper-stage weight was selected, as a unit comparison figure.

In Table V the weight saved is multiplied by the unit selected and this figure reduced by the increased hardware cost compared to aluminum. The net cost saving figure represents the unit net cost saving per launch in terms of additional payload capability (Bar graph E). For Be-Aℓ structures the saving is $84,000 per launch based on the $1000 per pound payload. The composite structure saves about half this much and the beryllium construction $11,000 more. Considerations of Beryllium-Aluminum superiority in ductility, impact resistance, and ease of modification through field repairs make the Be-38Aℓ cost effectiveness results particularly attractive.

Since the structure studied is only 36 inches long, it is evident that consideration of longer interstages, plus payload costs in excess of $1000 per pound, could result in cost savings per launch of a million dollars or more. The logical conclusion is that the advantages of weight savings through more efficient materials can more than offset increased original costs in upper-stage applications.

TABLE III

COST SUMMARY

260 in. Diameter Cylinders, 36 in. Long

Configuration	Description	Stringers	Rings	Cost Each (lots of 10) dollars
I	Rectangular rings and stringers, integrally milled 2219 Aluminum, $t_{wall} = .030$	0.808 high .054 thick, spaced 1.30	One only, 0.77 high 0.246 thick	13,231
IIA	Single-face sheet, trapezoidal core 7075 Aluminum, $t_{wall} = 0.040$	$\theta = 80$ deg, 0.85 high $t_c = 0.0185$	No ring	4,680
IIB	Single-face sheet, trapezoidal core, Be-38 Al Alloy, $t_{wall} = .030$	$\theta = 74$ deg. 0.68 high $t_c = .012$	No ring	51,100
IIIA	Conventional flanged stringers & rings, Aluminum skin, $t = .025$ Be-38 Al stringers	Be-38 Al "J" stringer $t_{1b} = 0.025$ height $b_x = .74$, spacing = 1.43	No ring	41,235
IIIB	Conventional flanged stringers & rings Aluminum skin, $t = .025$ Be-38 Al stringers	Be-38Al "J" stringers $t_{1b} = .025$ height $b_x = .74$, spacing = 1.43	Be-38 Al "J" ring $t_{2b} = .025$ height $b_x = 1.14$	43,601
IV	Conventional flanged stringers & rings Aluminum skin, $t = .030$ Be-38 Al stringers	Be-38 Al "Z" stringers $t_{1b} = .025$ height $b_x = .82$ spacing = 1.51	Be-38 Al "Z" ring $t_{2b} = .025$ height $b_x = 1.14$	40,336

20

TABLE III

COST SUMMARY (Continued)

Configuration	Description	Stringers	Rings	Cost Each (lots of 10) dollars
V A	Conventional flanged Be-38 Aℓ Alloy stringers & rings Be-38 Aℓ skin t = .020	"Z" Be-Aℓ t = .020 height = .75 spacing = 1.6	"Z" Be-Aℓ t = .020 height - 1.02	44,800
V B	Conventional flanged Be-38 Aℓ Alloy stringers & rings Be-38 Aℓ skin t = .025	"Z" Be-Aℓ t = .025 height = .75 spacing = 1.6	"Z" Be-Aℓ t = .025 height - 1.02	46,450
V C	Conventional flanged Be-38 Aℓ Alloy stringers & rings Be-38 Aℓ skin t = .030	"Z" Be-Aℓ t = .030 height = .75 spacing = 1.6	"Z" Be-Aℓ t = .030 height = 1.02	48,300
VI	Aluminum skin, t = .030 Conventional flanged Alum stringers & rings	"Z" Alum t = .025 height = 1.0 spacing = 1.35	"Z" Alum t = .040 height = 1.6	13,200
VII	Be skin t = .020 Conventional flanged Be stringers and rings	Be "Z" t = .015 height = .78 spacing = 1.31	Be "Z" t = .015 height - 1.5	52,140

CHART I - Cost Effectiveness Study 260" Diameter Stiffened
Cylinders, 36" Long (from Tables IV and V)

TABLE IV

COST PER POUND OF WEIGHT SAVED: Z STIFFENED CYLINDERS
260 INCH DIA. x 36 INCHES LONG

Material	Weight (lbs)	Weight Saved Compared to Alum. (lbs)	Cost Each (lots of 10) (dollars)	Increased Cost Compared to Aluminum (dollars)	Cost per Pound of Weight Saved (dollars/lb)
Alum.	209.3	0	13,200	0	0
Be-Aℓ	98.6	110.7	40,000*	26,800	242
Be	74.7	134.6	52,140	38,940	286
Composite: Alum skin, Be-Aℓ stringers	144.0	65.3	38,500**	25,300	388

*Adjusted for less material
**Adjusted for no ring

TABLE V

NET COST SAVINGS PER LAUNCH FOR ORBITAL PAYLOAD UNIT WEIGHT
(Based on $1,000 Per Pound Payload Cost)

① Material	② Weight Saved (lbs)	③ Gross Cost Saving ($1000 x ②)	④ Increased Hardware Cost** (dollars)	⑤ Net Cost Saving/Launch (③ - ④)
Be	134.6	134,000	38,940	95,060
Be-Aℓ	110.7	110,700	26,800	83,900 ***
Composite*	65.3	65,300	25,300	40,000
Aluminum	0	0	0	0

*Aluminum skin, Be-Aℓ Stringers
**See Table IV
***See Page 19

CONVERSION OF U.S. CUSTOMARY UNITS TO SI UNITS

The International System of Units (SI) conversion factors for the SI units used herein are given in the following table:

Physical Quantity	U.S. Customary Unit	Conversion Factor (*)	SI Unit
Length	in	2.54	centimeters
Force	lb	4.448	newtons
Force/inch	lb/in	1.751	newtons/cm
Mass	lbM	0.4536	kilogram

*Multiply value given in U.S. Customary Unit by conversion factor to obtain equivalent value in SI unit.

REFERENCES

1. Almroth, B. O., Buckling of Orthotropic Cylinders under Axial Compression, LMSC Report 6-90-63-65, Palo Alto, California, June 1963.

2. Almroth, B. O., Postbuckling Behavior of Orthotropic Cylinders under Axial Compression, AIAA JOURNAL, Vol. 2, October 1964.

3. Lockheed Missiles & Space Company, Evaluation of the Effects of Ring/Stringer Eccentricity upon the Structural Optimization of Axially Compressed Cylinders Stiffened with Rings and/or Stringers of Rectangular Cross-Section, by A. Bruce Burns, LMSC Report 6-65-65-11, Palo Alto, California, April 1965.

4. Burns, A. B., Structural Optimization of Axially Compressed Cylinders Stiffened with Corrugations and Rings, Including the Effects of Corrugation/Ring Eccentricity, LMSC Report 6-65-65-12, Palo Alto, California, May 1965.

5. Burns, A. B., Structural Optimization of Axially Compressed Cylinders Reinforced with Conventional Flanged Stiffeners, LMSC Report M-99-65-1, September 1965.

6. van der Neut, A., The General Instability of Stiffened Shells under Axial Compression, Nationaal Luchtvaartlaboratorium Report S 314, Reports and Transactions, XIII, 1947.

7. Baruch, M. and J. Singer, Effect of Eccentricity of Stiffeners on the General Instability of Stiffened Cylindrical Shells under Hydrostatic Pressure, Journal Mechanical Engineering Science, Vol. 5, No. 1, 1963.

8. Fenn, R. W. Jr., et al, A Mechanical Property Evaluation of Be-38% Aℓ Alloy From -320° to 800°F, National Metal Congress, October 1965, Detroit (See Appendix D).

STRINGER

RING

b_y

d_x

b_x

t_1

c_1
RING SPACING

t_2

t
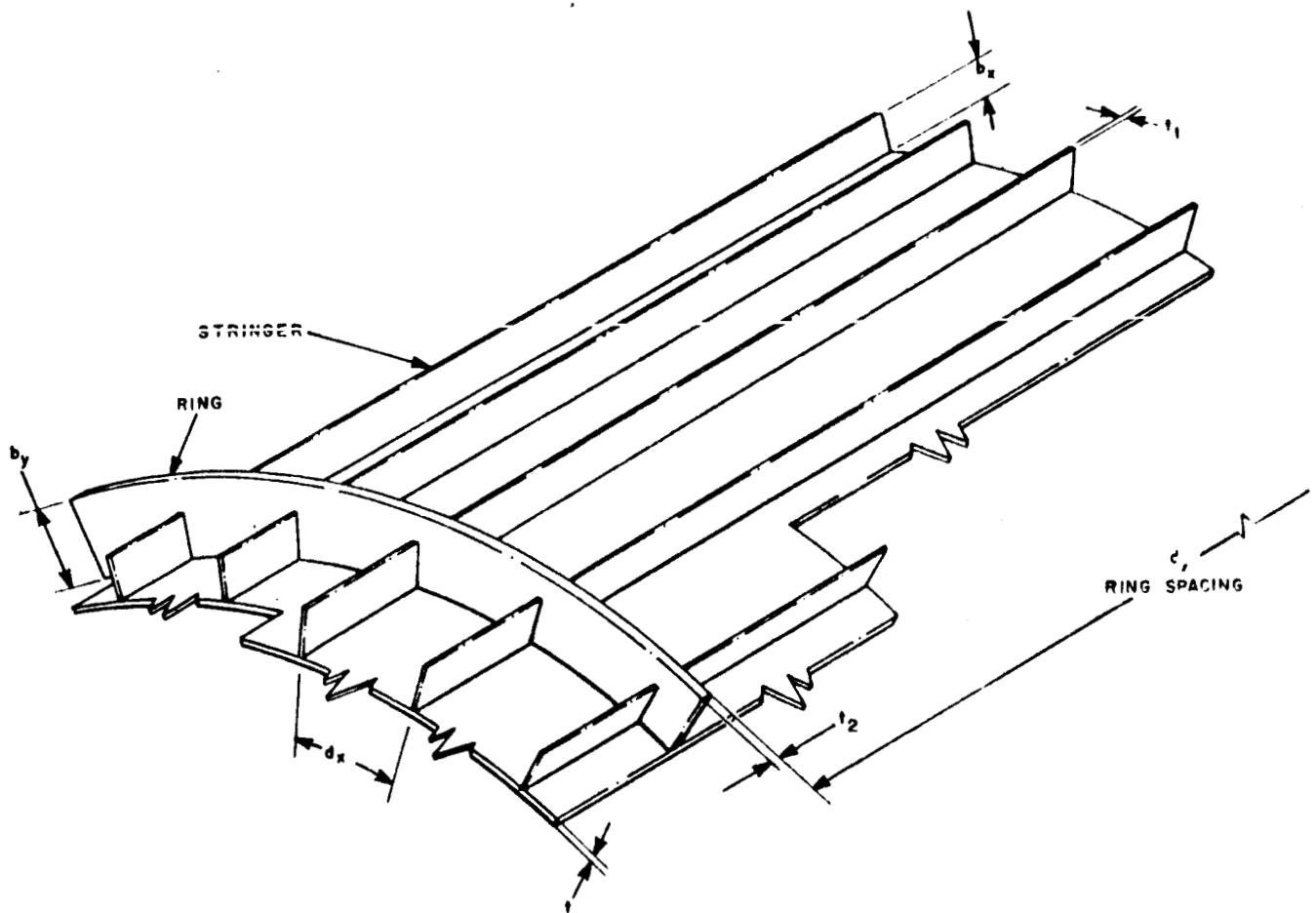
Figure 1   - Cylinder Stiffened with Rectangular
Rings and Stringers

Figure 2 - Cylinder Stiffened with Trapezoidal Corrugations
and Angle-Section Rings
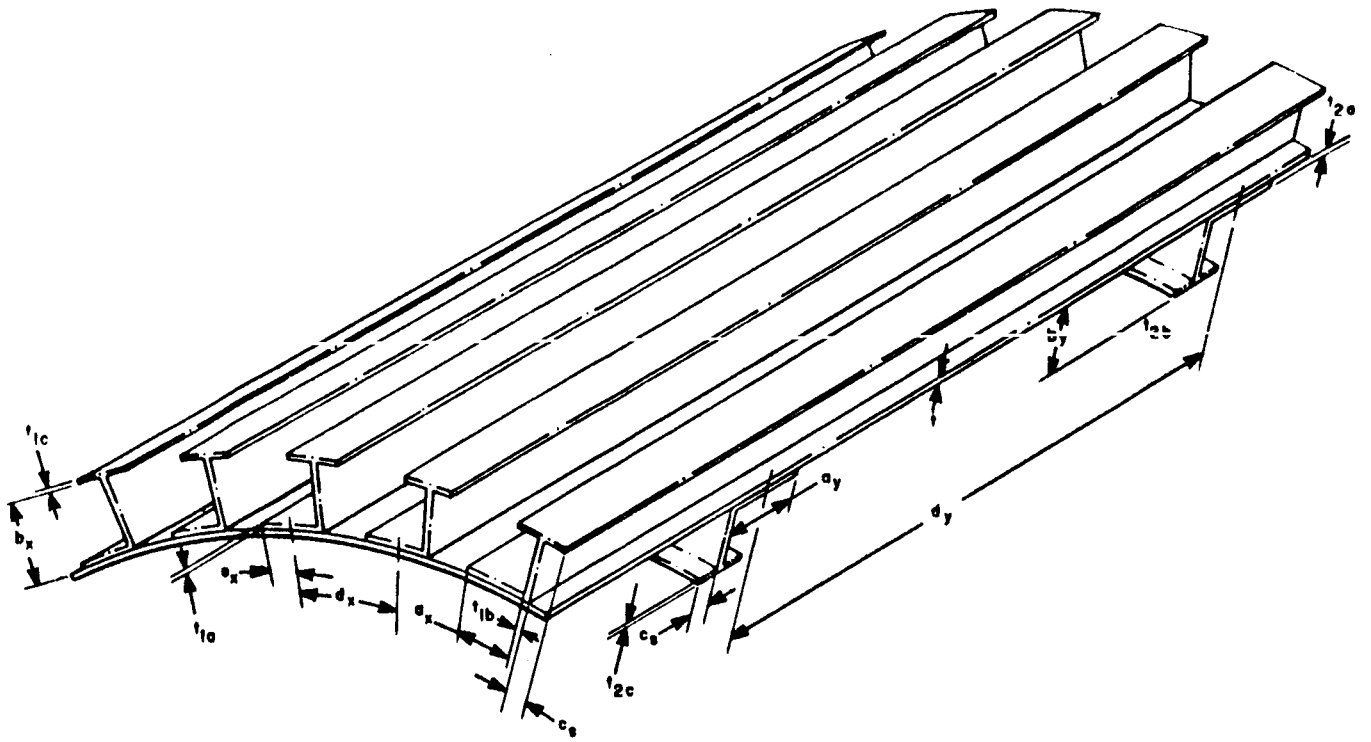
Figure 3 - Cylinder Stiffened with Conventional Flanged
Stiffeners and Rings (J, Z, Channel)
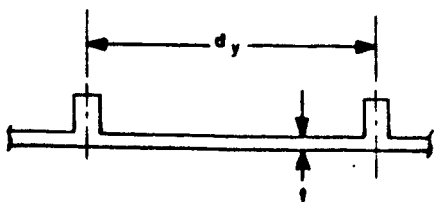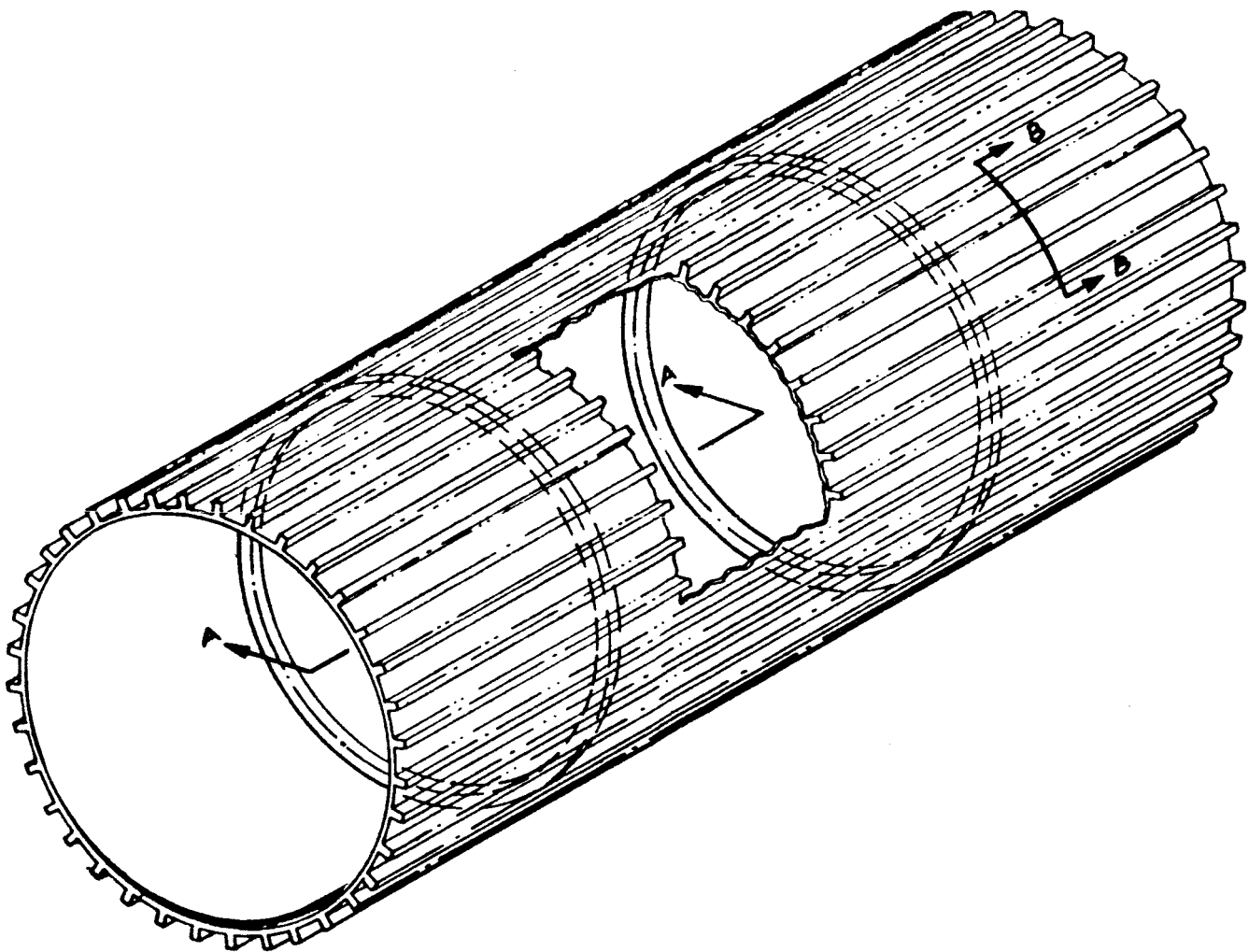
SECTION A-A
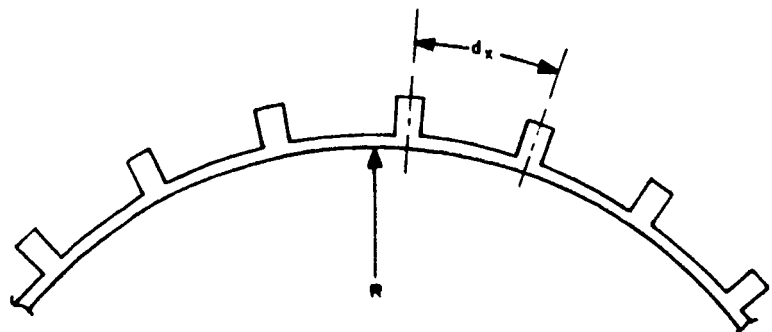
SECTION B-B

Figure 4 - Typical Interstage

Dia. = 260 in.   L = 36 in. N_x = 1300 lb/in.
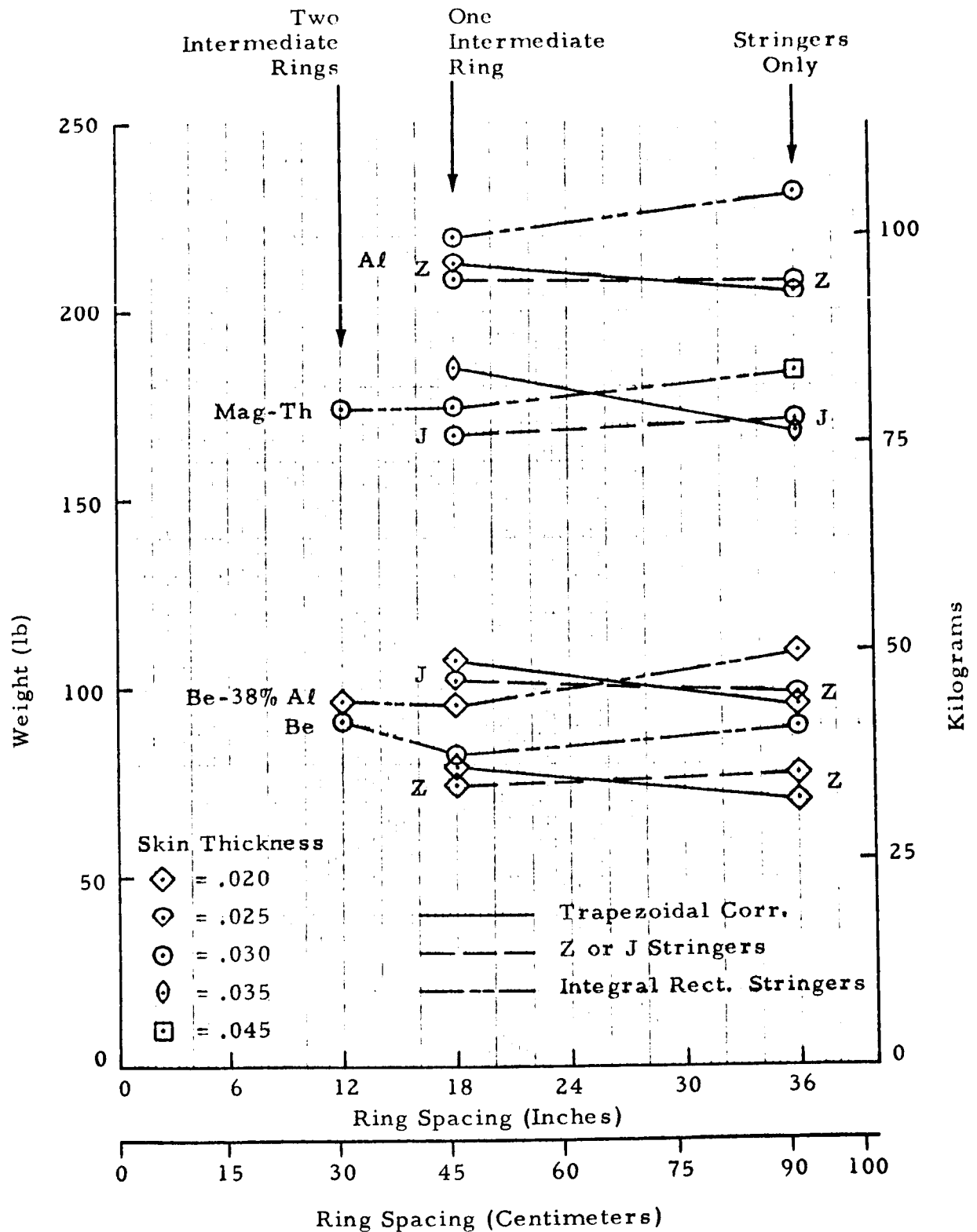
Figure 5 - Optimum Weight Summary of the Three
Constructions, L/R = 0.277
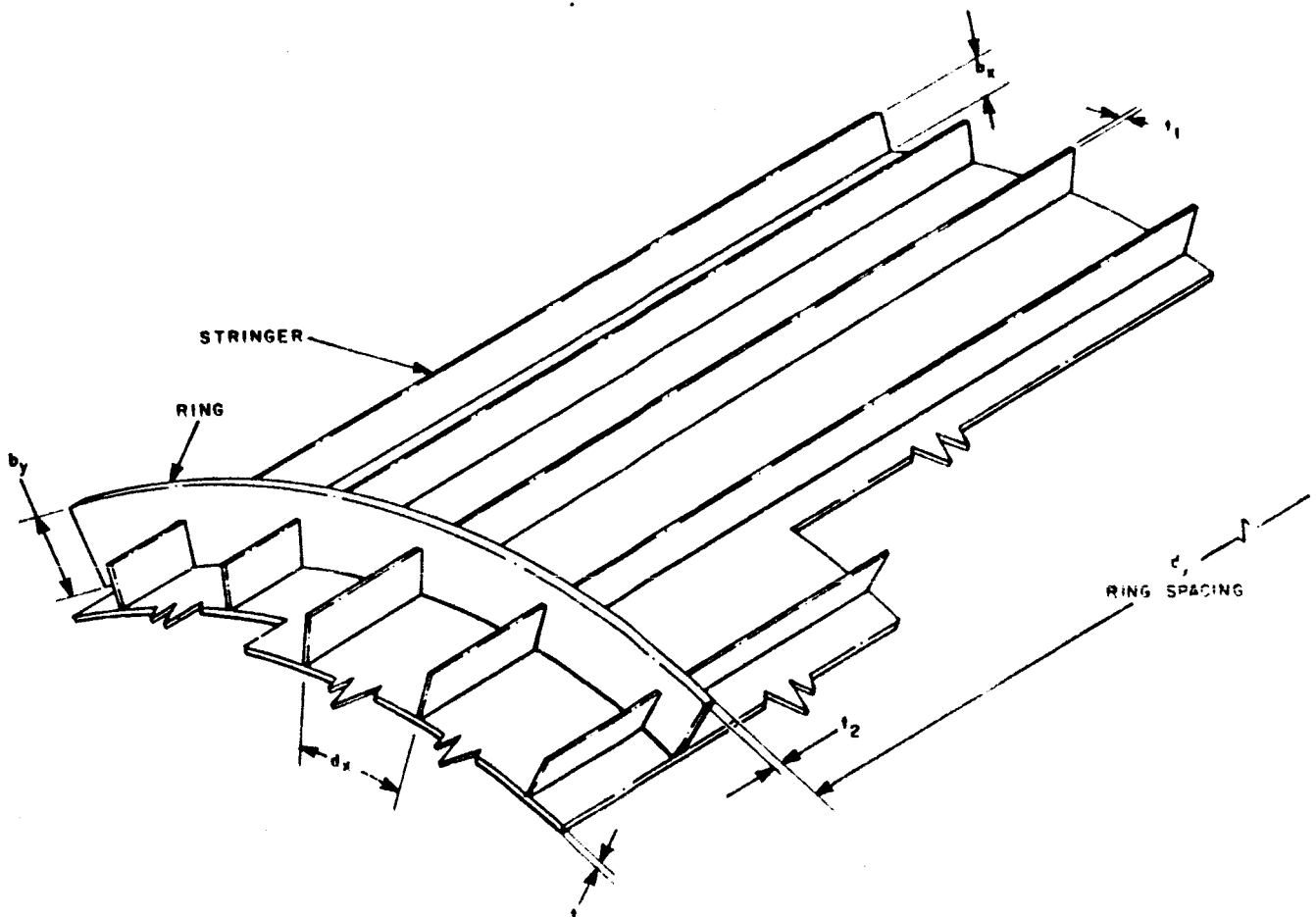
Material: BERYLLIUM-38% ALUMINUM

Axial Lineload   = 1300 lb/in.
Diameter   = 260 in.
Length   = 36 in. (L/R = 0.277)
Weight   = 95.6 lb
Skin Thickness   = t = 0.020 in.
Stress   = 32,000 lb/in.^{2}

STRINGERS: EXTERNAL   RINGS: EXTERNAL

d_x = 1.08 in. d_y = 18.0 in.

b_x = 0.582 in. b_y = 0.805 in.

t_1 = 0.039 in. t_2 = 0.054 in.

Figure 6 - Cylinder Stiffened with Integral Rectangular
Rings and Stringers - Be-38% A*l*
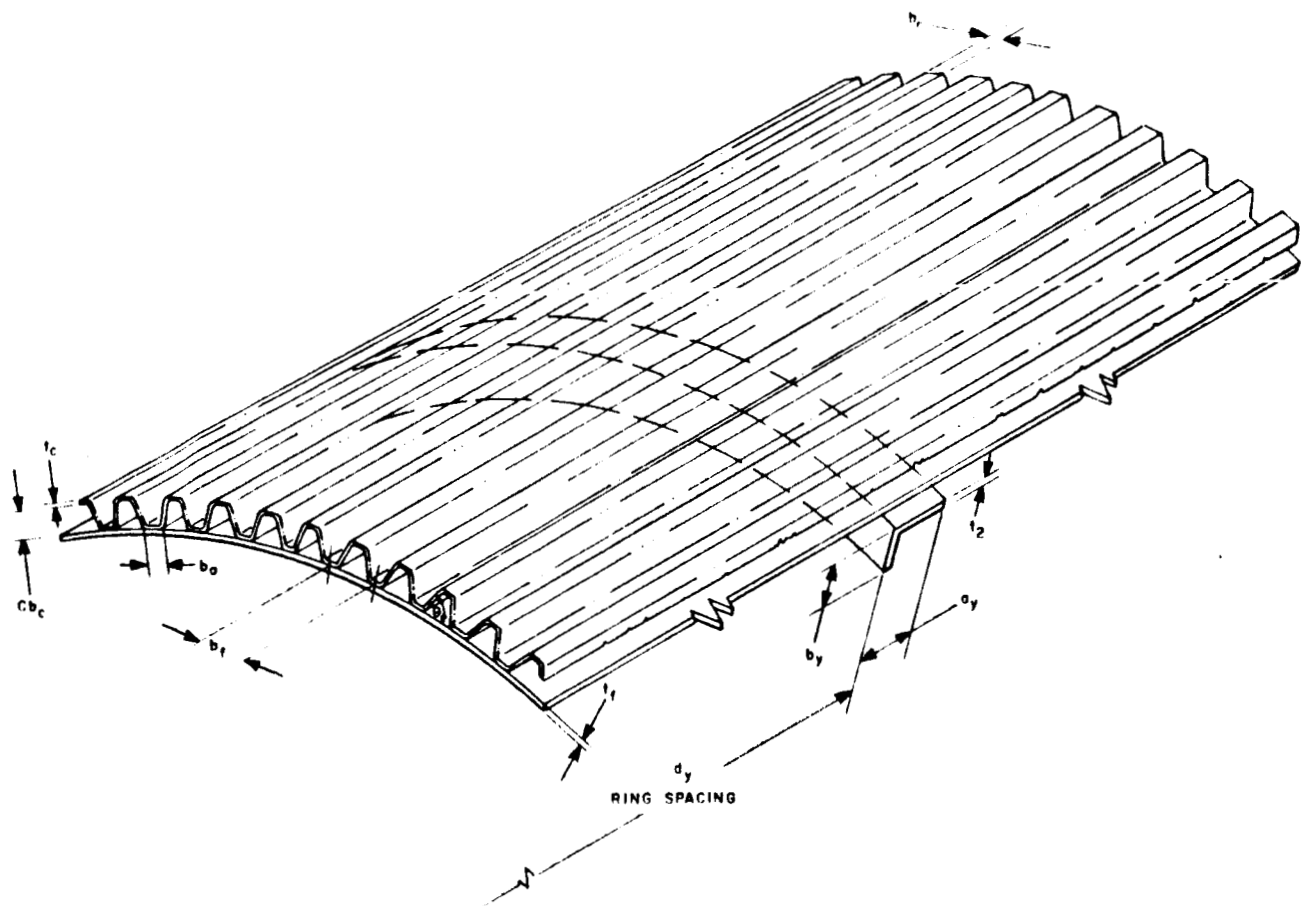
31

Material: BERYLLIUM-38% ALUMINUM

Axial Lineload   = 1300 lb/in.
Diameter   = 260 in.
Length   = 36 in. (L/R = 0.277)
Weight   = 96.5 in.
Stress   = 32,000 lb/in.^{2}
Skin Thickness   = t_f = 0.020 in.

CORRUGATED STIFFENERS: EXTERNAL   RING: NONE

θ = 78.83$^{\text{o}}$ d_y = 36 in.

b_f = 1.115 in. b_y = 0

b_c = 0.447 in. t_2 = 0

C   = 1.5 a_y = 0

Cb_c = 0.67 in.

t_c = 0.012 in.

b_a = 0.40

Figure 7 - Cylinder Stiffened with Trapezoidal Corrugation
and Angle Rings - Be-38% Al
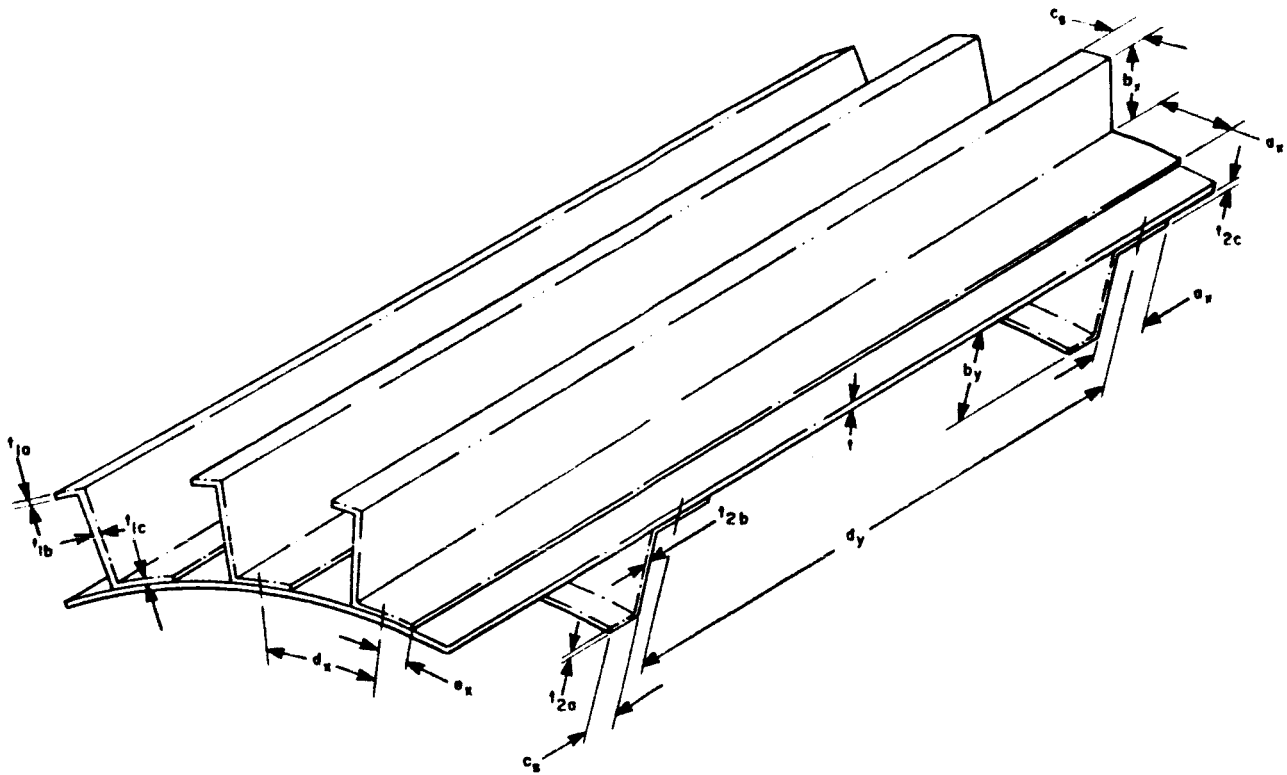
Material: BERYLLIUM-38% ALUMINUM

Axial Lineload   =   1300 lb/in.
Diameter   =   260 in.
Length   =   36 in.   (L/R = 0.277)
Weight   =   98.6 lb
Stress   =   27,500 lb/in.^{2}
Skin Thickness   =   t = 0.025 in.

Z-STRINGERS: EXTERNAL   Z-RINGS: NONE

d_x = 1.446 in. d_y = 36 in.

b_x = 0.89 in. b_y = 0

$t_{1a} = t_{1b} = t_{1c}$ = 0.015 in. $t_{2a} = t_{2b} = t_{2c}$ = 0

c_s = 0.305 in. c_s = 0

a_x = 0.70 in. a_y = 0

e_x = 0.30 in.

Figure 8 - Cylinder Stiffened with Zee Ring and
Stringers - Be-38% Aℓ
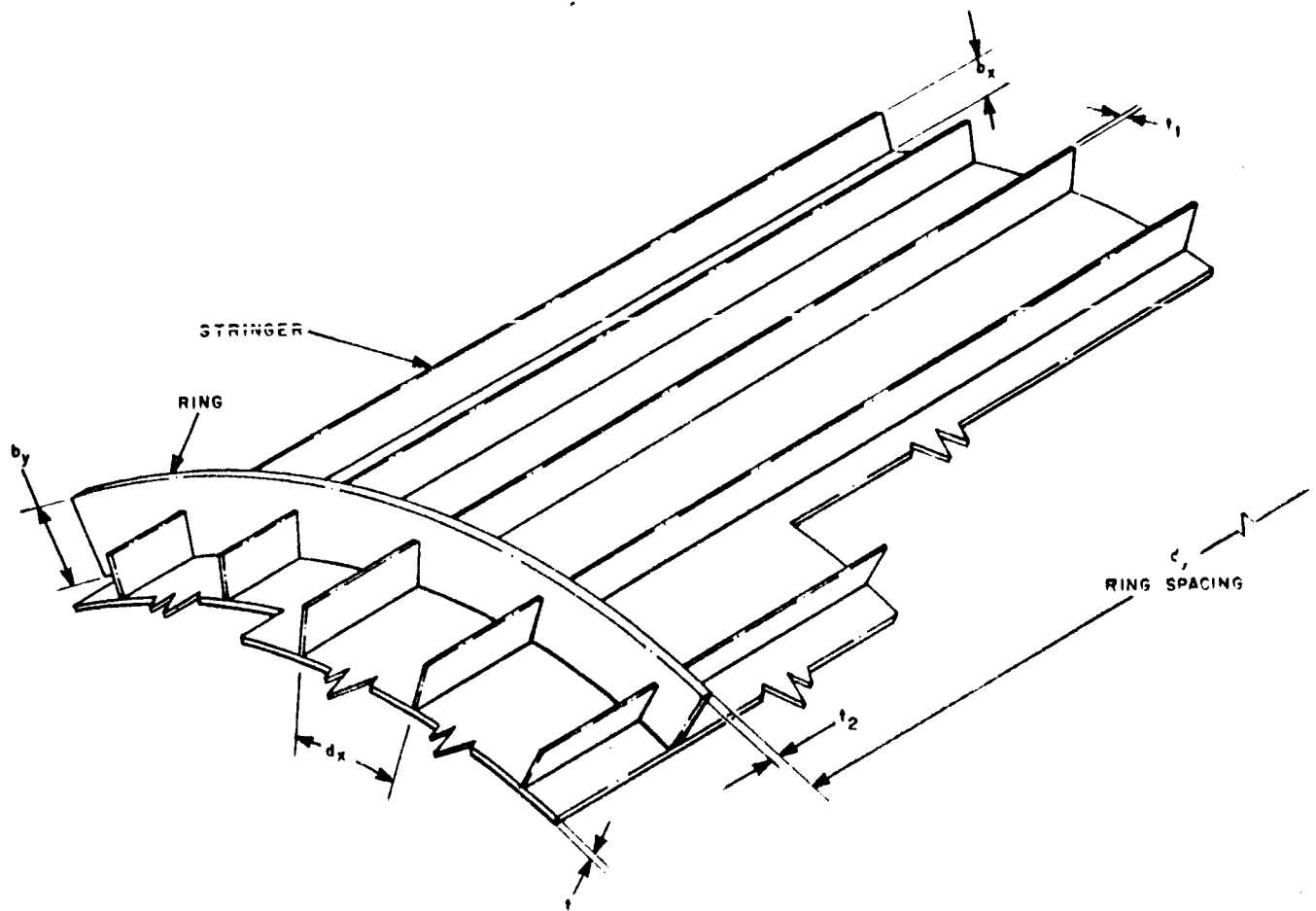
Material: ALUMINUM

Axial Lineload	=	1300 lb/in.
Diameter	=	260 in.
Length	=	36 in. (L/R = 0.277)
Weight	=	220 lb
Skin Thickness	=	$t = 0.030$ in.
Stress	=	28,150 lb/in.^{2}

STRINGERS: EXTERNAL   RINGS: EXTERNAL

d_x = 1.29 in. d_y = 18.0 in.

b_x = 0.81 in. b_y = 0.768 in.

t_1 = 0.054 in. t_2 = 0.246 in.

Figure 9 - Cylinder Stiffened with Integral Rectangular
Rings and Stringers - Aluminum

34
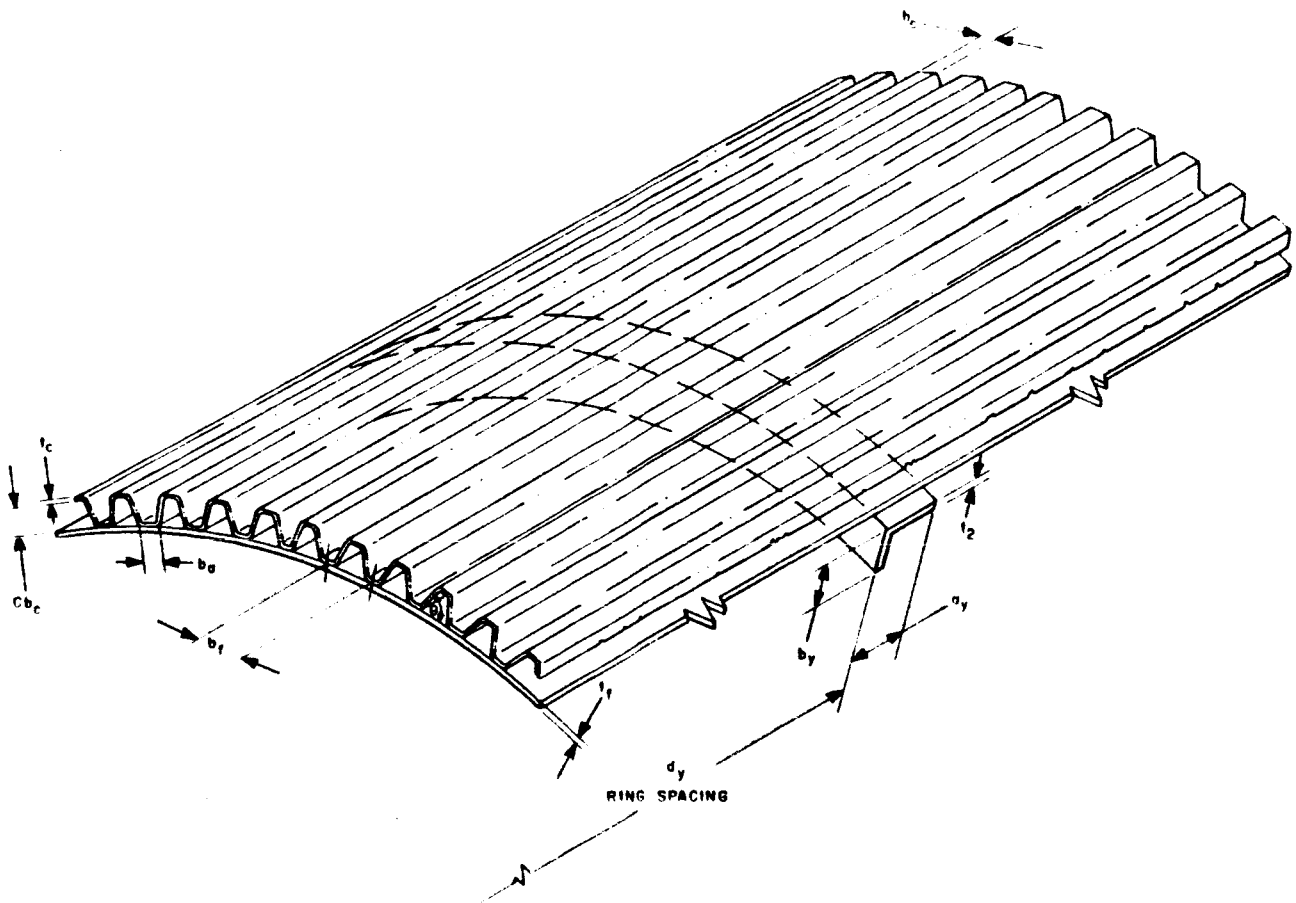
Material: ALUMINUM

Axial Lineload = 1300 lb/in.
Diameter = 260 in.
Length = 36 in. (L/R = 0.277)
Weight = 206.7 lb
Stress = 18,947 lb/in.^{2}
Skin Thickness = t_f = 0.030 in.

CORRUGATED STIFFENERS: EXTERNAL

θ = 77.97°
b_f = 1.355 in.
b_c = 0.586 in.
C = 1.5
Cb_c = 0.88 in.
t_c = 0.0195 in.
b_a = 0.40 in.

RING: NONE

d_y = 36 in.
b_y = 0
t_2 = 0
a_y = 0

Figure 10 - Cylinder Stiffened with Trapezoidal Corrugation
and Angle Rings - Aluminum
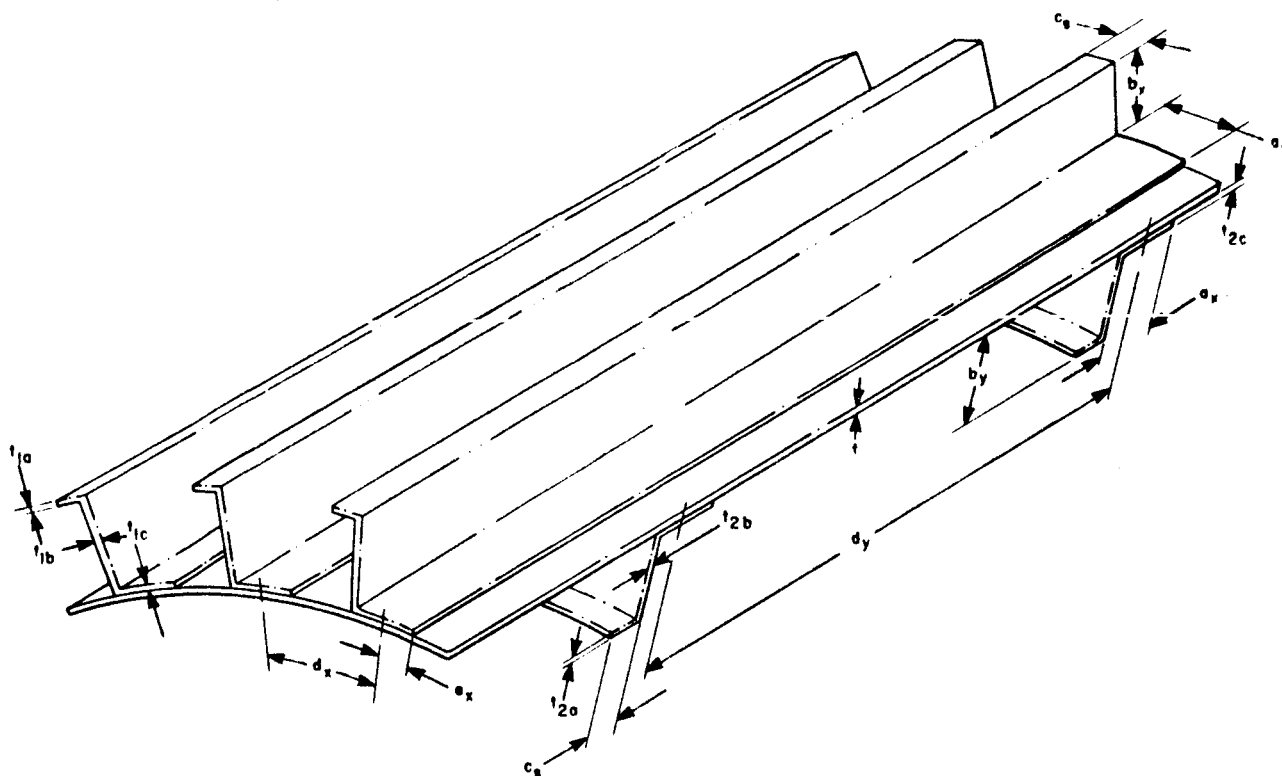
Material: ALUMINUM

Axial Lineload = 1300 lb/in.
Diameter = 260 in.
Length = 36 in. (L/R = 0.277)
Weight = 207.8 lb
Stress = 18,398 lb/in.^{2}
Skin Thickness = t = 0.030 in.

Z-STRINGERS: EXTERNAL **Z-RINGS: NONE**

d_x = 1.33 in. d_y = 36 in.

b_x = 1.09 in. b_y = 0

$t_{1a} = t_{1b} = t_{1c}$ = 0.025 in. $t_{2a} = t_{2b} = t_{2c}$ = 0

c_s = 0.368 in. c_s = 0

a_x = 0.70 in. a_y = 0

e_x = 0.30 in.

Figure 11 - Cylinder Stiffened with Zee Ring and
Stringers - Aluminum
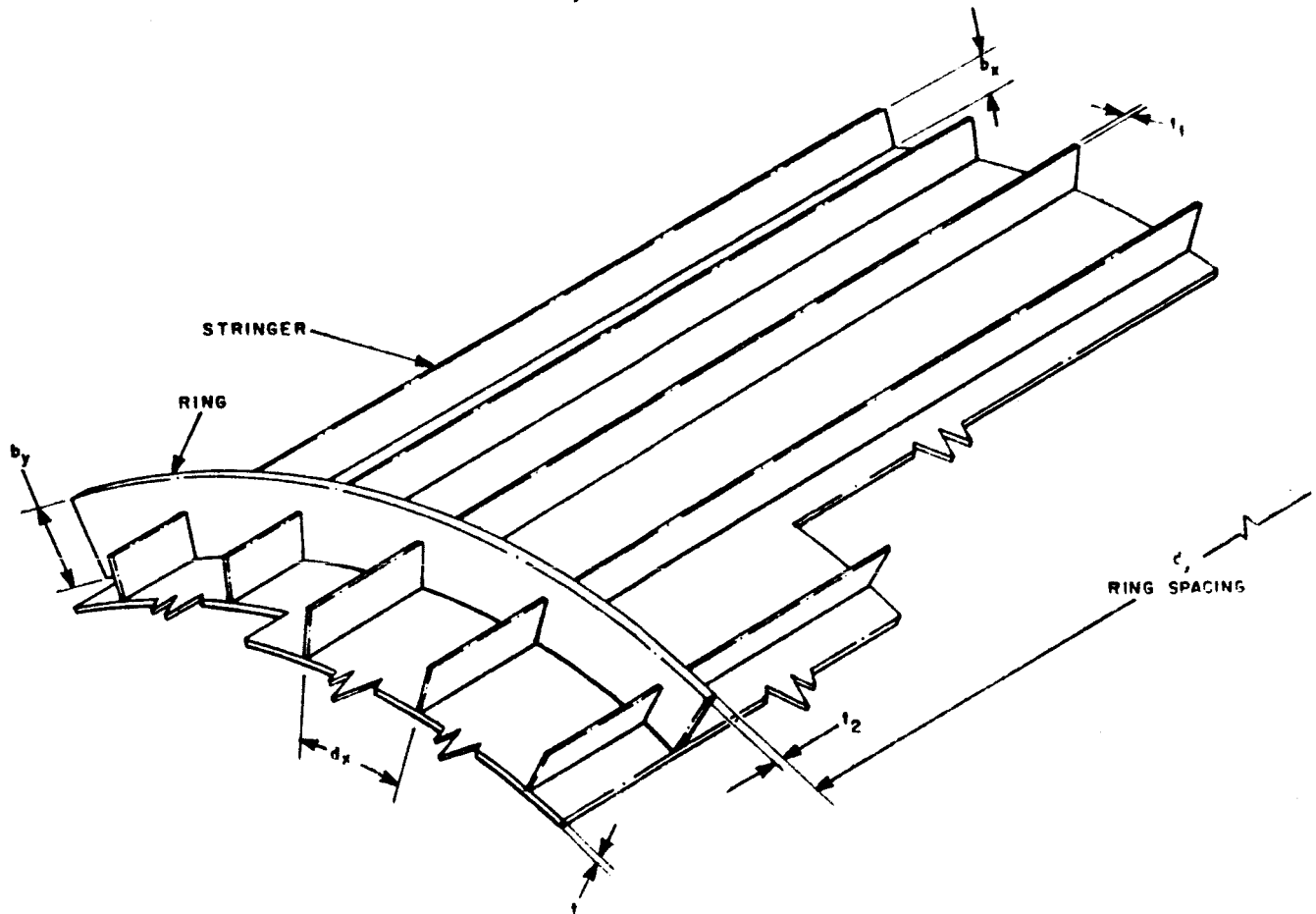
Material: BERYLLIUM

Axial Lineload = 1300 lb/in.
Diameter = 260 in.
Length = 36 in. (L/R = 0.277)
Weight = 82.4 lb
Skin Thickness = t = 0.030 in.
Stress = 41,500 lb/in.^{2}

STRINGERS: EXTERNAL   RINGS: EXTERNAL

d_x = 1.96 in. d_y = 18.0 in.

b_x = 0.539 in. b_y = 0.854 in.

t_1 = 0.036 in. t_2 = 0.057 in.

Figure 12 - Cylinder Stiffened with Integral Rectangular
Rings and Stringers - Beryllium
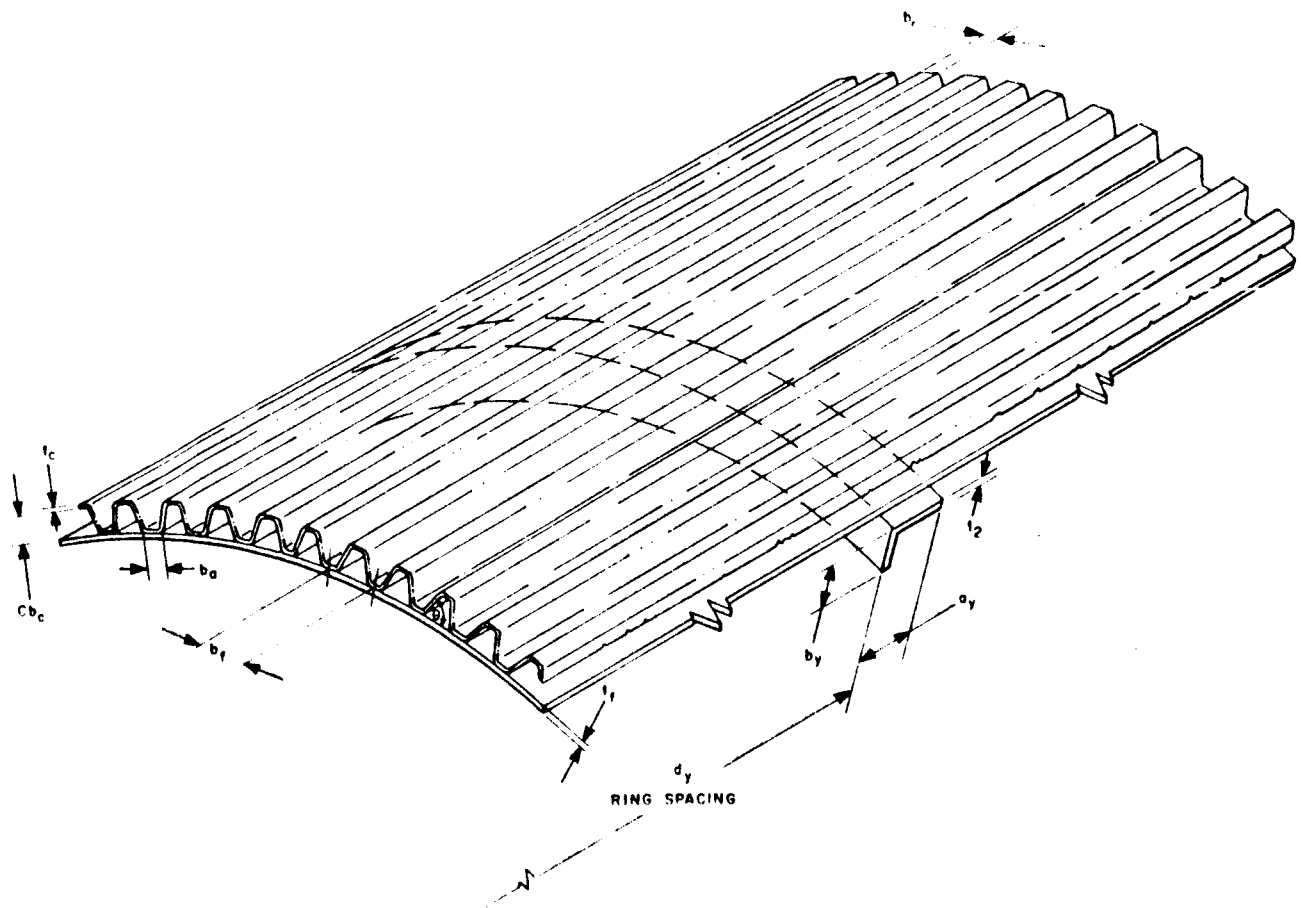
Material: BERYLLIUM

Axial Lineload = 1300 lb/in.
Diameter = 260 in.
Length = 36 in. (L/R = 0.277)
Weight = 71.2 lb
Skin Thickness = t_f = 0.020 in.
Stress = 36,102 lb/in.^{2}

CORRUGATED STIFFENERS: EXTERNAL   RING: NONE

θ = 69.95° d_y = 36 in.

b_f = 1.255 in. b_y = 0

b_c = 0.42 in. t_2 = 0

C = 1.5 a_y = 0
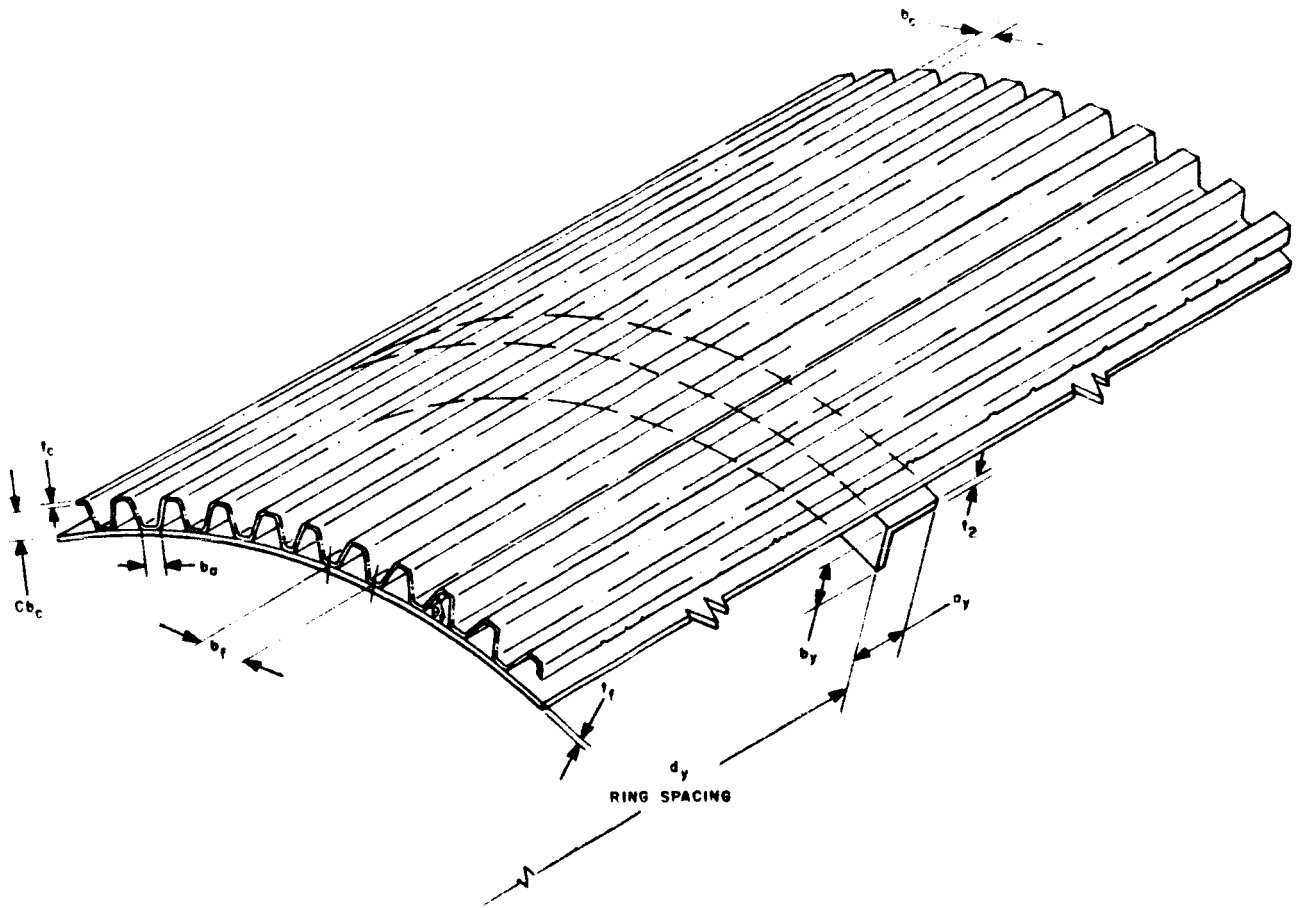
Cb_c = 0.63 in.

t_c = 0.010 in.

b_a = 0.40 in.

Figure 13 - Cylinder Stiffened with Trapezoidal Corrugation
and Angle Rings - Beryllium

38
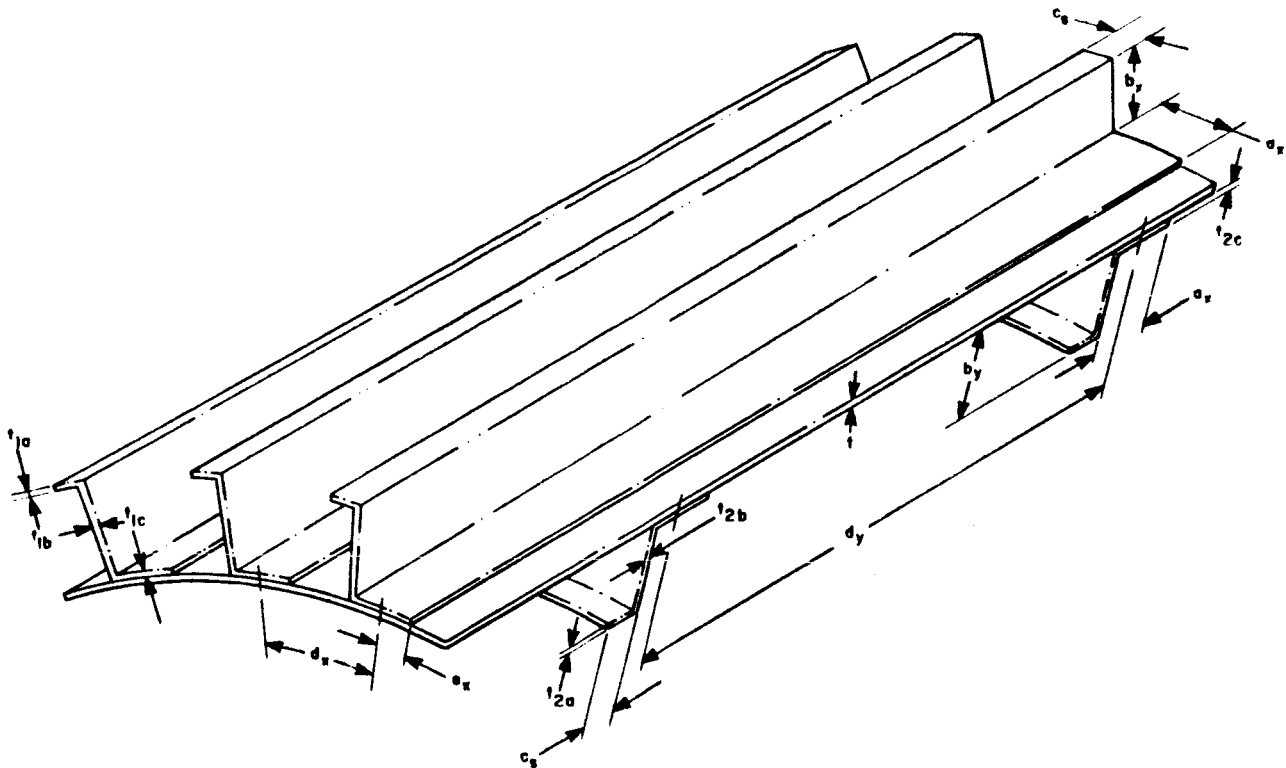
Material: BERYLLIUM

Axial Lineload = 1300 lb/in.
Diameter = 260 in.
Length = 36 in. (L/R = 0.277)
Weight = 74.7 lb
Stress = 35,800 lb/in.^{2}
Skin Thickness = t = 0.020 in.

Z-STRINGERS: EXTERNAL

d_x = 1.245 in.

b_x = 0.49 in.

$t_{1a} = t_{1b} = t_{1c}$ = 0.015 in.

c_s = 0.163 in.

a_x = 0.70 in.

e_x = 0.30 in.

Z-RINGS: INTERNAL

d_y = 18 in.

b_y = 1.48 in.

$t_{2a} = t_{2b} = t_{2c}$ = 0.015 in.

c_s = 0.512 in.

a_y = 0.70 in.

Figure 14 - Cylinder Stiffened with Zee Ring and
Stringers - Beryllium
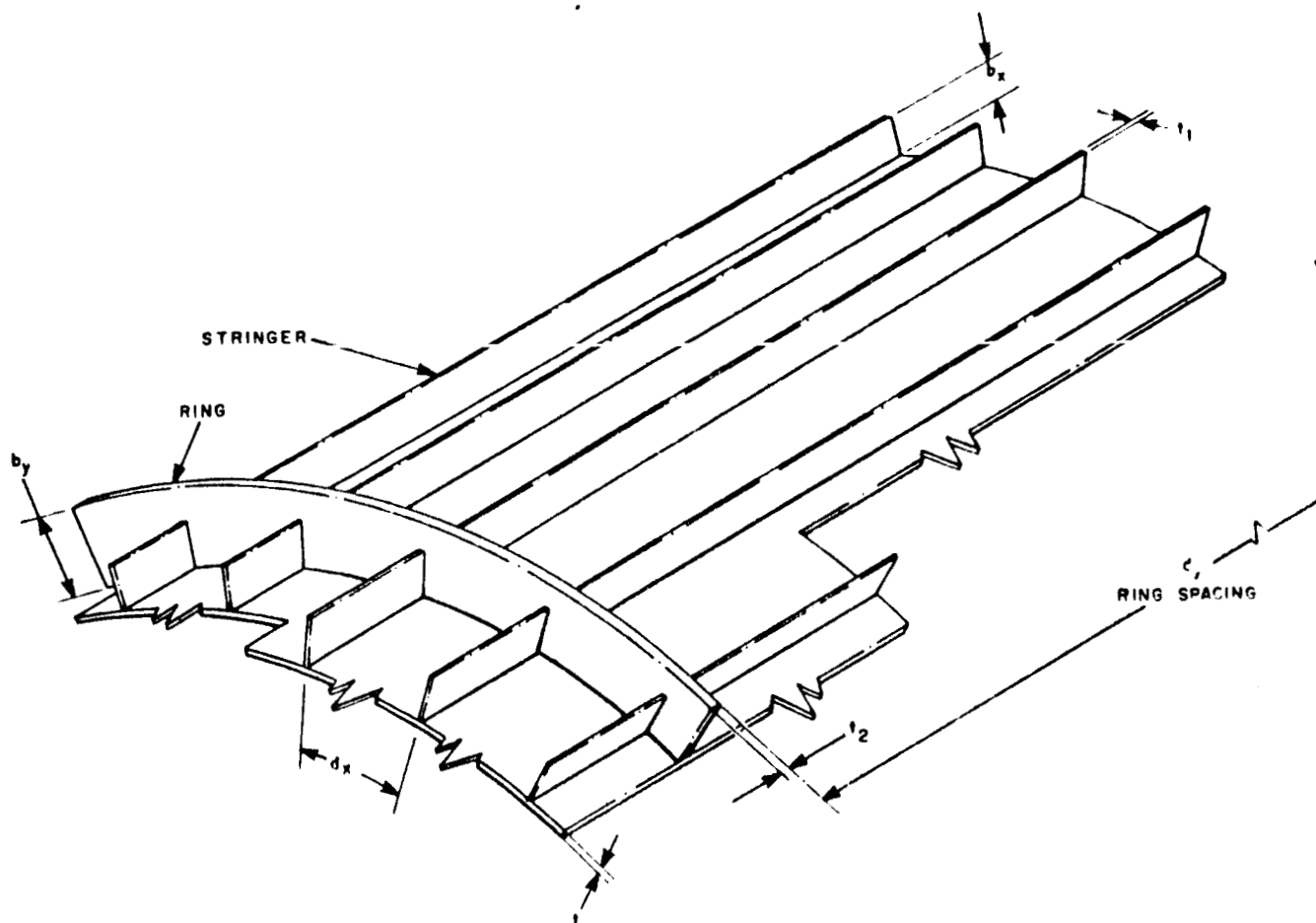
Material: MAGNESIUM-THORIUM HK31A-H24

Axial Lineload	=	1300 lb/in.
Diameter	=	260 in.
Length	=	36 in. (L/R = 0.277)
Weight	=	174 lb
Skin Thickness	=	t = 0.030 in.
Stress	=	19,000 lb/in.^{2}

STRINGERS: EXTERNAL   RINGS: EXTERNAL

d_x = 1.14 in. d_y = 12.0 in.

b_x = 0.843 in. b_y = 1.46 in.

t_1 = 0.063 in. t_2 = 0.117 in.

Figure 15 - Cylinder Stiffened with Integral Rectangular
Rings and Stringers - Magnesium-Thorium
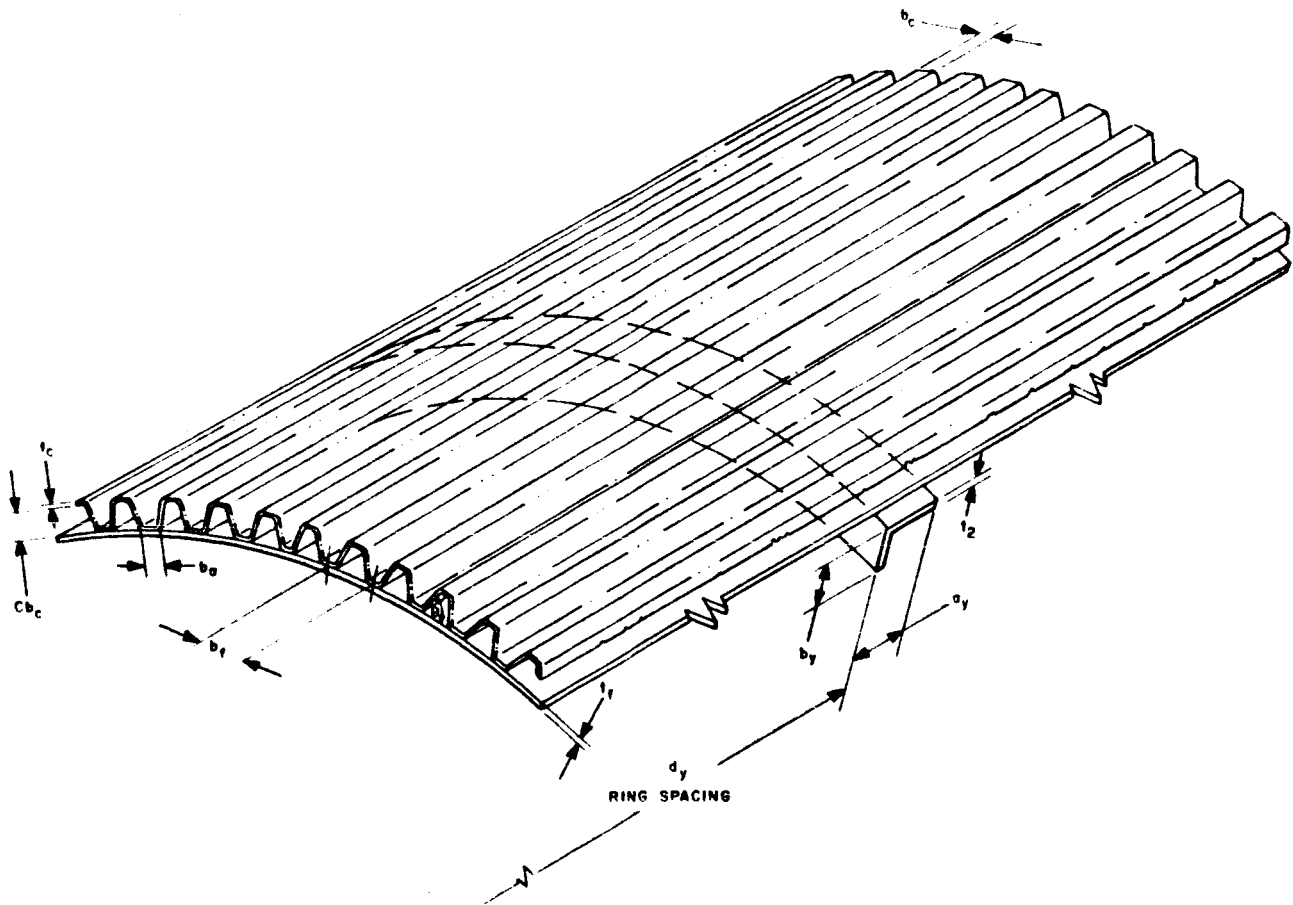
Material: MAGNESIUM-THORIUM HK31A-H24

Axial Lineload   = 1300 lb/in.
Diameter   = 260 in.
Length   = 36 in. (L/R = 0.277)
Weight   = 168.4 lb
Stress   = 14,763 lb/in.^{2}
Skin Thickness   = t_f = 0.035 in.

CORRUGATED STIFFENERS: EXTERNAL   RING: NONE

θ = 79.97$^\mathrm{o}$

b_f = 1.423 in.

b_c = 0.666 in.

C = 1.5

Cb_c = 1.0 in.

t_c = 0.0246 in.

b_a = 0.40 in.

d_y = 36 in.

b_y = 0

t_2 = 0

a_y = 0

Figure 16 - Cylinder Stiffened with Trapezoidal Corrugation
and Angle Rings - Magnesium-Thorium
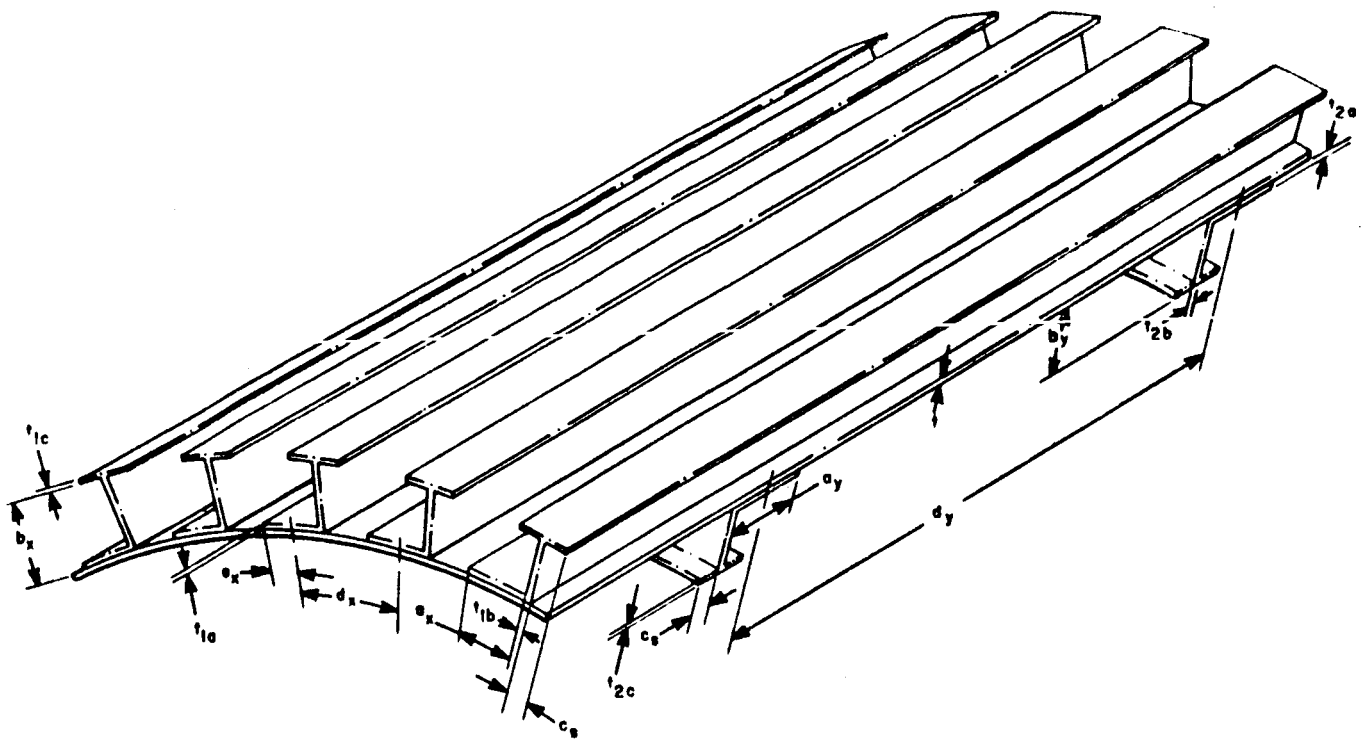
41

Material: MAGNESIUM-THORIUM HK31A-H24

Axial Lineload = 1300 lb/in.
Diameter = 260 in.
Length = 36 in. (L/R = 0.277)
Weight = 163.6 lb
Stress = 16,550 lb/in.^{2}
Skin Thickness = t = 0.030 in.

J-STRINGERS: EXTERNAL   J-RINGS: INTERNAL

d_x = 1.15 in. d_y = 18.0 in.

b_x = 0.70 in. b_y = 1.50 in.

$t_{1a} = t_{1b} = t_{1c}$ = 0.030 in. $t_{2a} = t_{2b} = t_{2c}$ = 0.040 in.

c_s = 0.226 in. c_s = 0.301 in.

a_x = 0.70 in. a_y = 0.70 in.

e_x = 0.30 in.

Figure 17 - Cylinder Stiffened with J Ring and
Stringers - Magnesium-Thorium

42

Max. Ring & Stringer Height Allowed = 1.5 in.
Dia. = 260 in.   L = 36 in. N_x = 1300 lb/in.
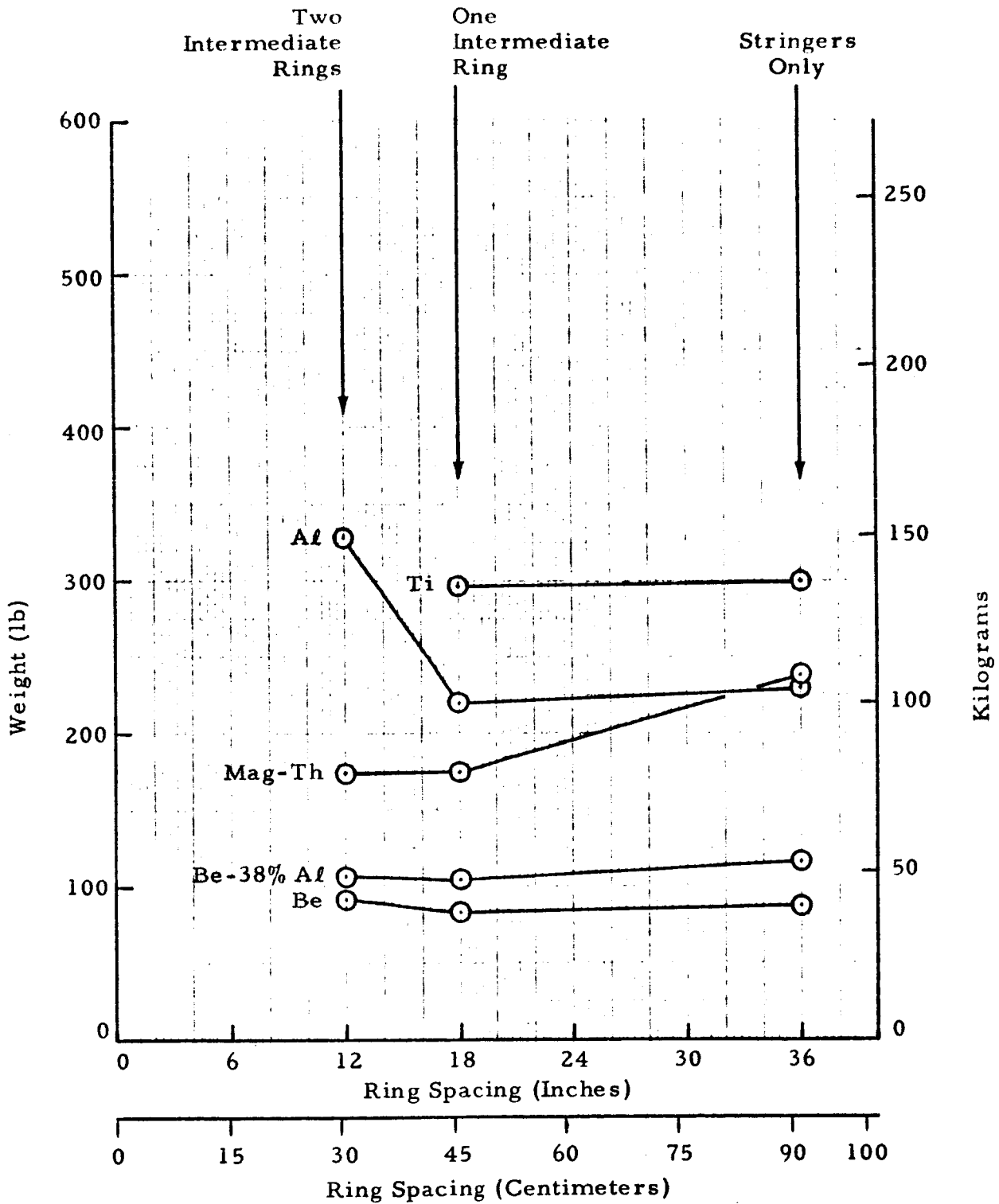
Figure 18 - Optimum Designs, t = 0.030, External Rectangular
Stiffening, L/R = 0.277

Dia. = 260 in.   L = 36 in. N_x = 1300 lb/in.
Max. Ring & Stringer Height Allowed = 1.5 in.
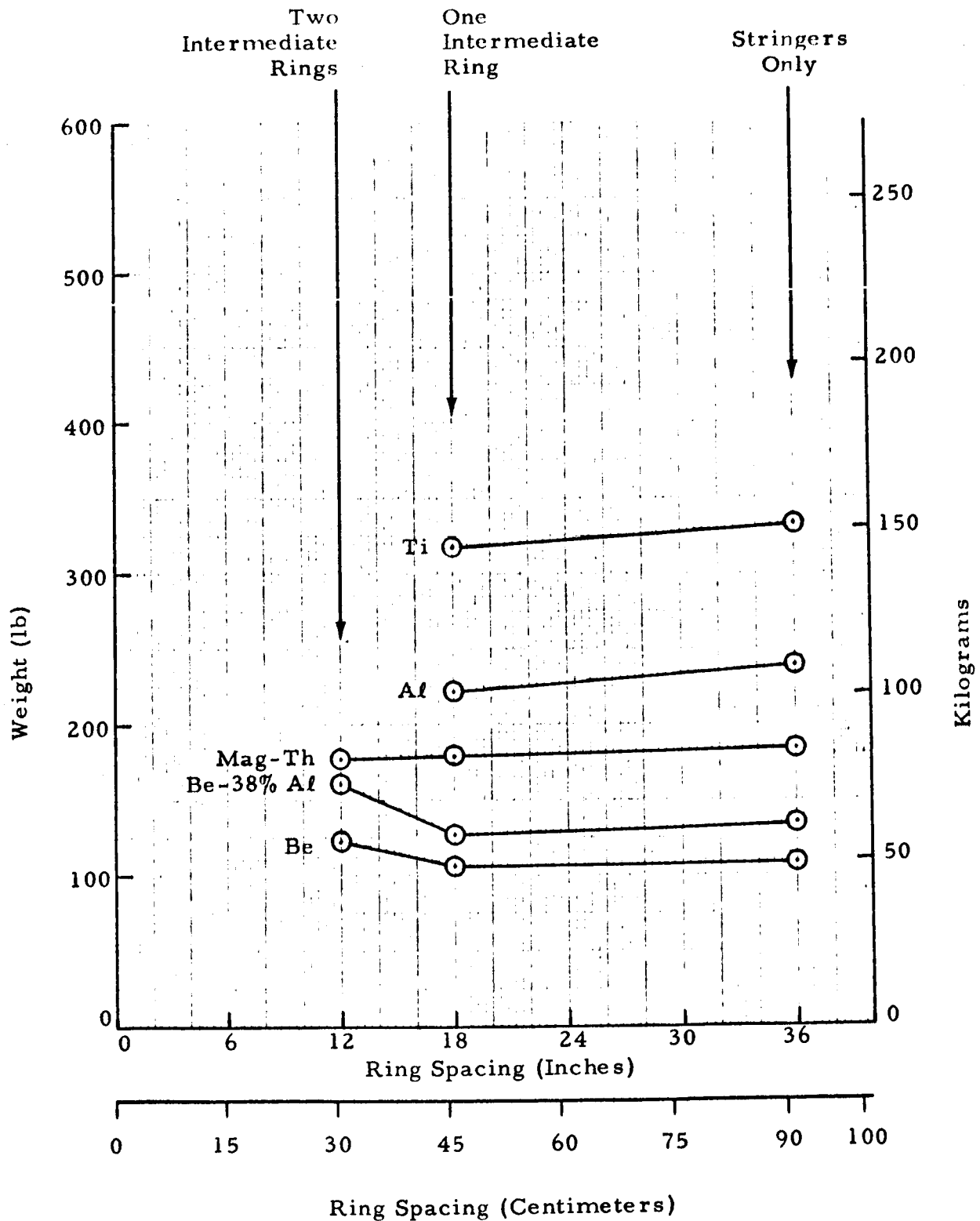
Figure 19 - Optimum Designs, t = 0.045, External Rectangular
Stiffening, L/R = 0.277
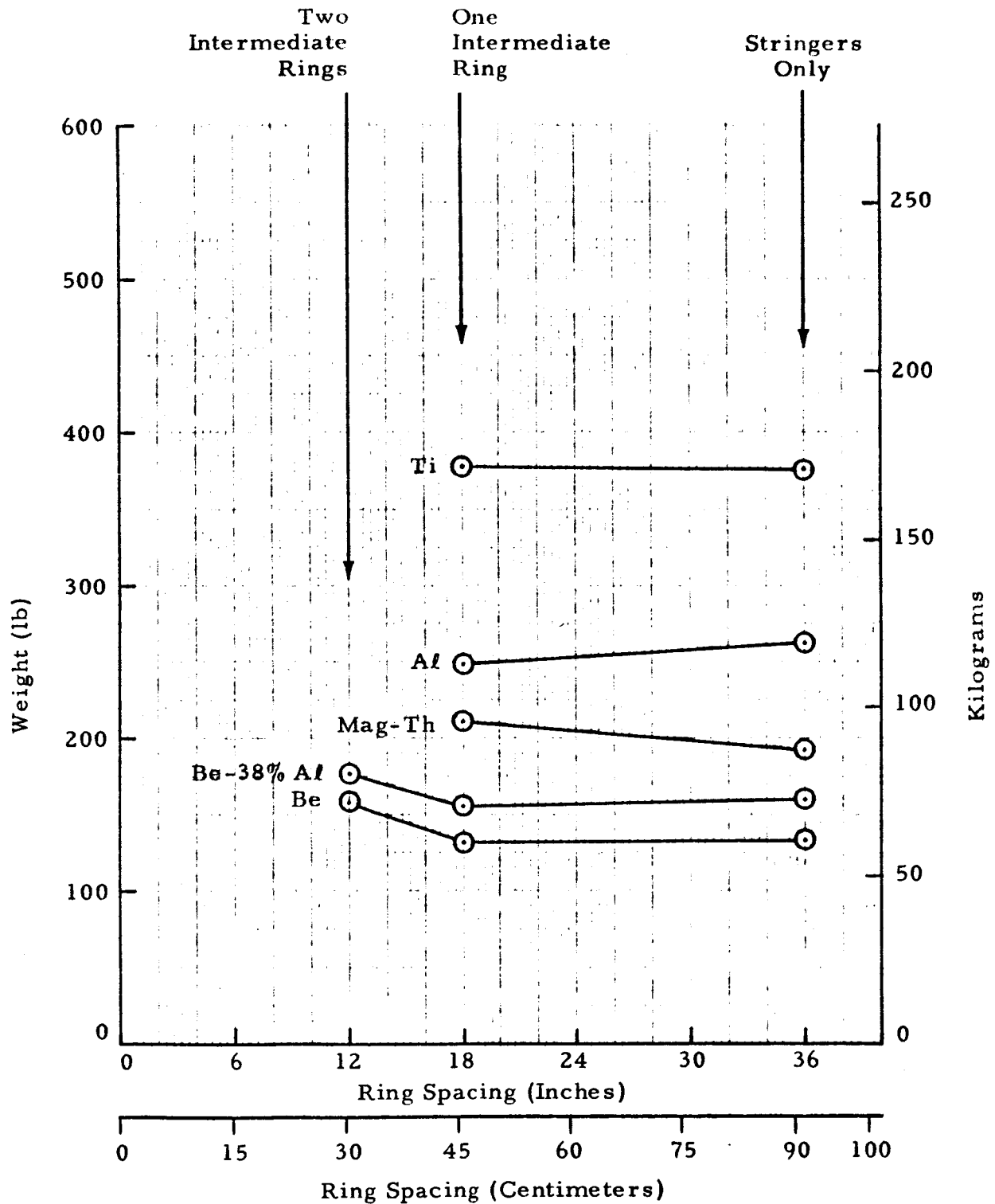
Figure 20 - Optimum Designs, t = 0.060, External Rectangular
Stiffening, L/R = 0.277

Max. Ring & Stringer Height Allowed = 1.5 in.
Dia. = 260 in.   L = 36 in. N_x = 1300 lb/in.
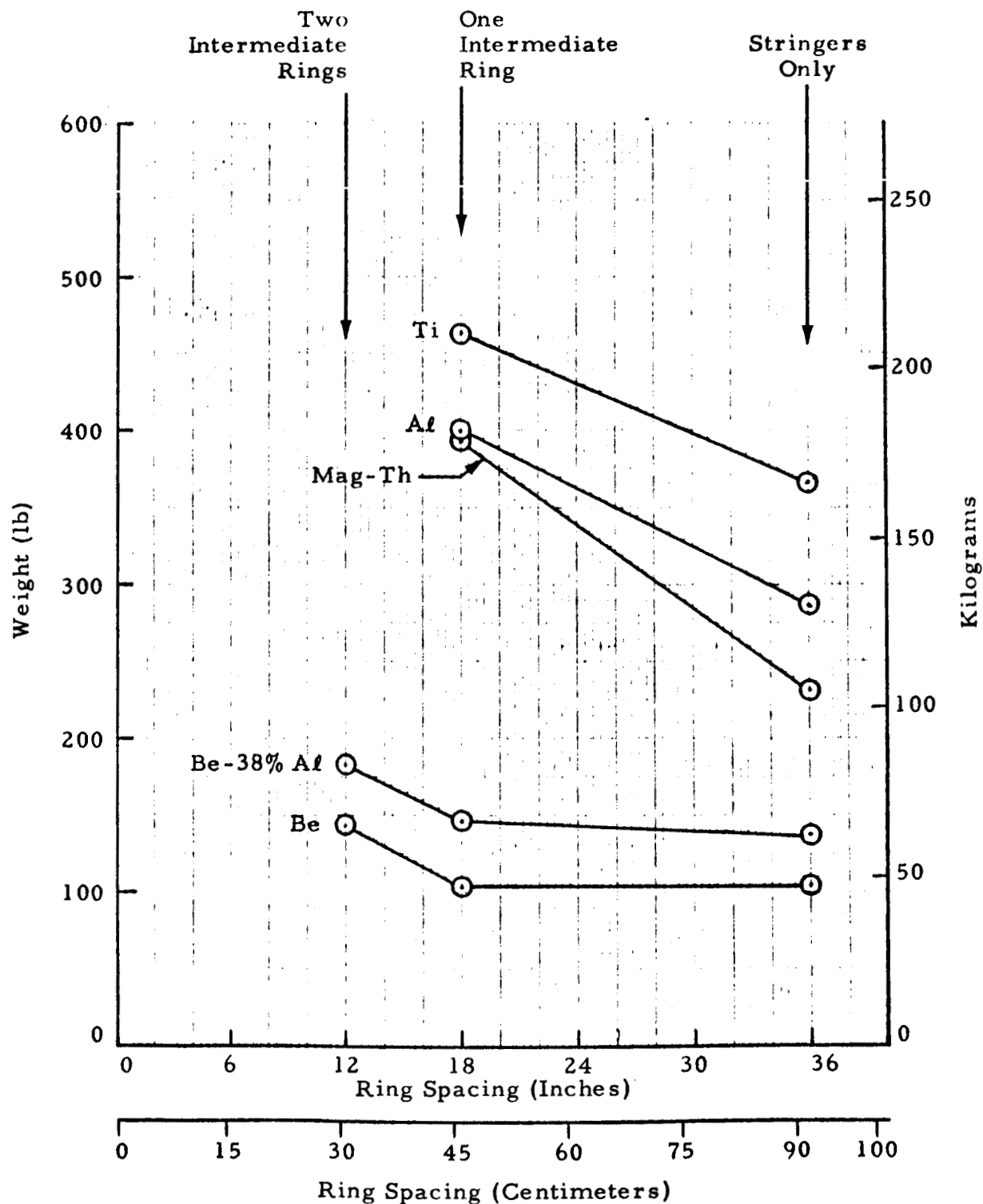
Figure 21 - Optimum Designs, t = 0.030, Internal Rectangular
Stiffening, L/R = 0.277

Max Ring & Stringer Height Allowed = 1.5 in.
Dia. = 260 in.   L = 36 in. N_x = 1300 lb/in.
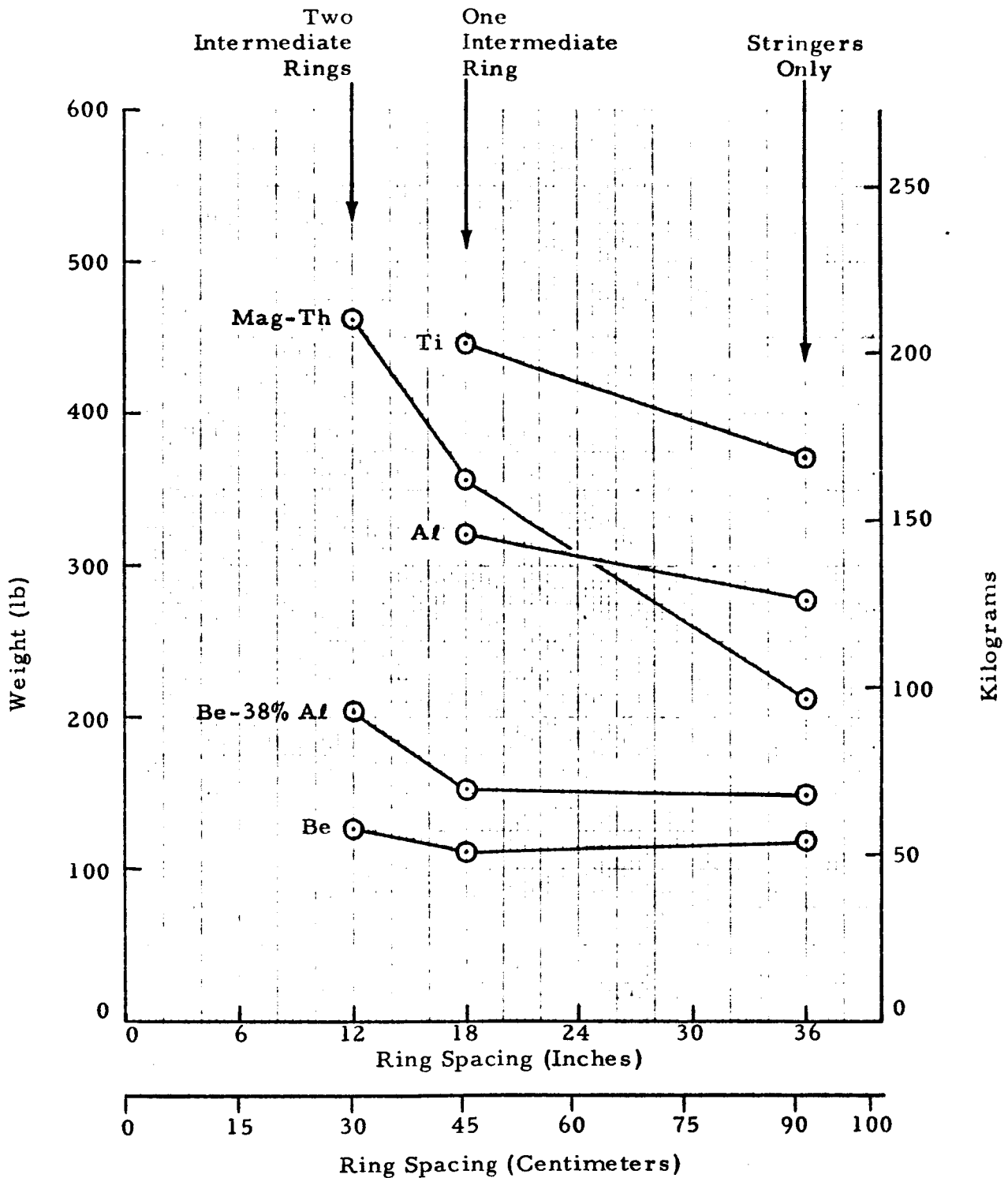
Figure 22 - Optimum Designs, t = 0.045, Internal Rectangular
Stiffening, L/R = 0.277
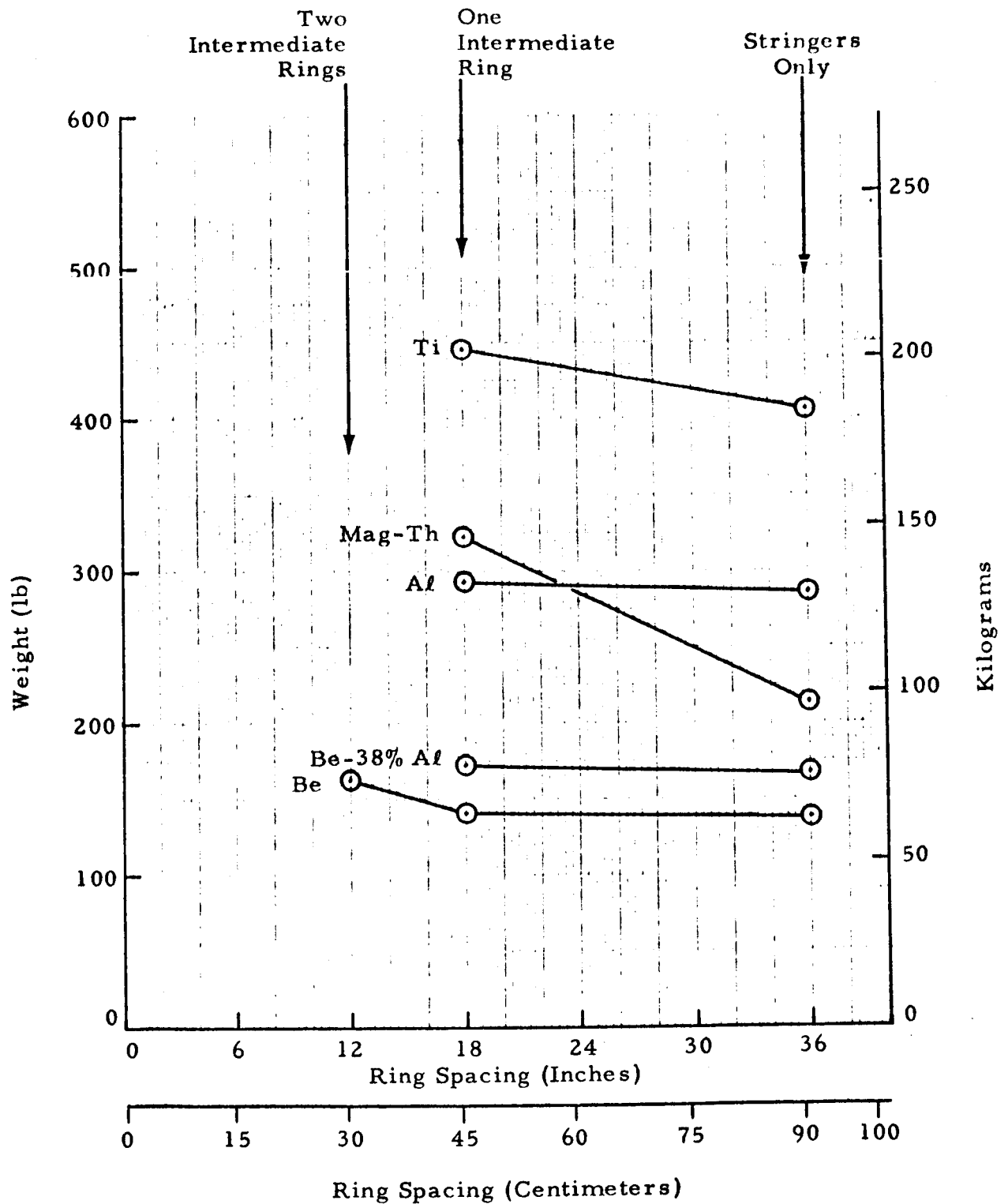
Figure 23 - Optimum Designs, t = 0.060, Internal Rectangular
Stiffening, L/R = 0.277

Rectangular Rings and Stringers
Dia. = 260 in.   L = 36 in. N_x = 1300 lb/in.
Max. Ring & Stringer Height Allowed = 1.5 in.
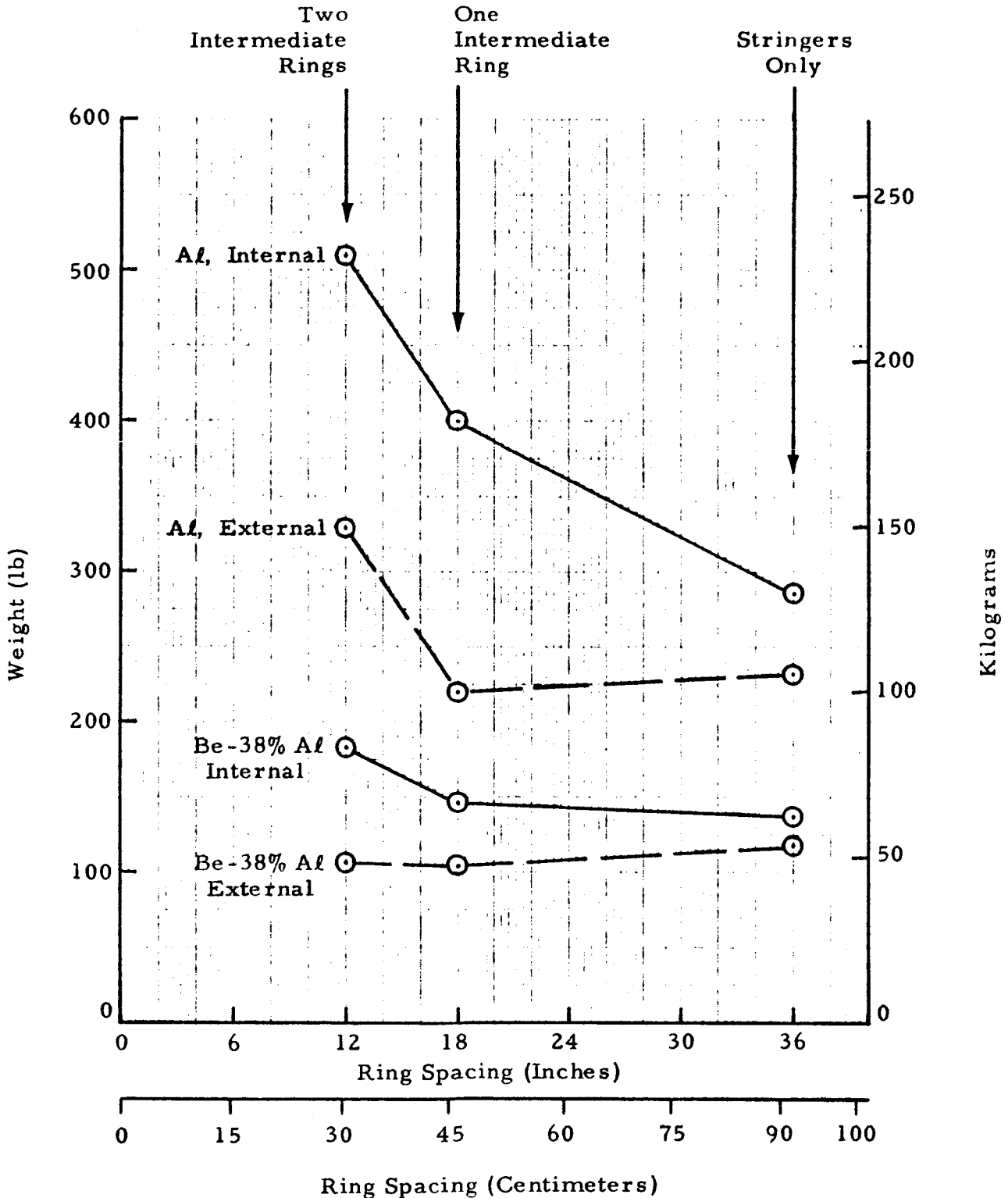
Figure 24 - Effect of Eccentricity on Cylinder Weight,
t = 0.030, L/R = 0.277

Rectangular Rings and Stringers
Dia. = 260 in.   L = 36 in. N_x = 1300 lb/in.
Max. Ring & Stringer Height Allowed = 1.5 in.
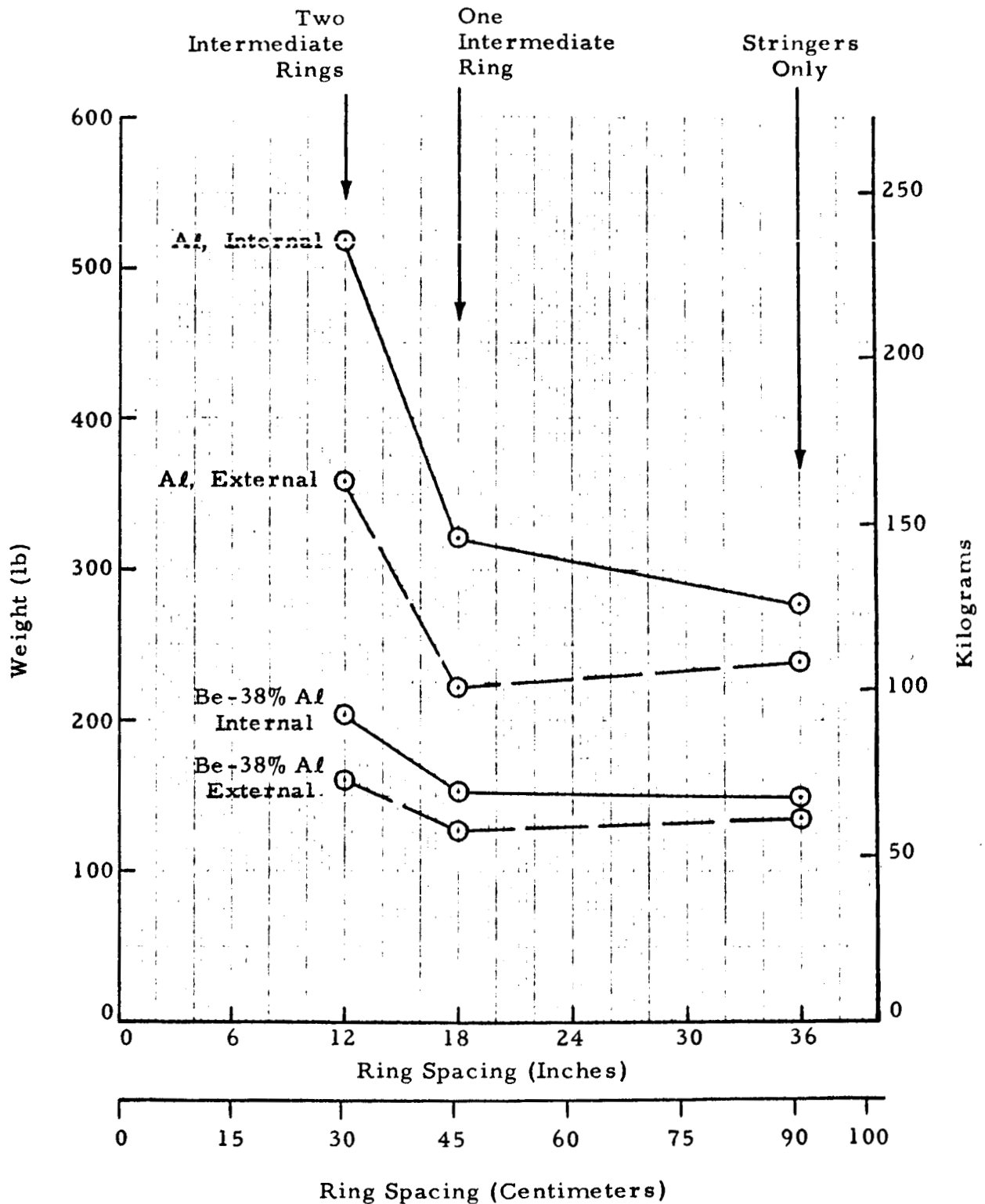
Figure 25 - Effect of Eccentricity on Cylinder Weight,
t = 0.045, L/R = 0.277

Rectangular Rings and Stringers
Dia. = 260 in.   L = 36 in. N_x = 1300 lb/in.
Max. Ring and Stringer Height Allowed = 1.5 in.
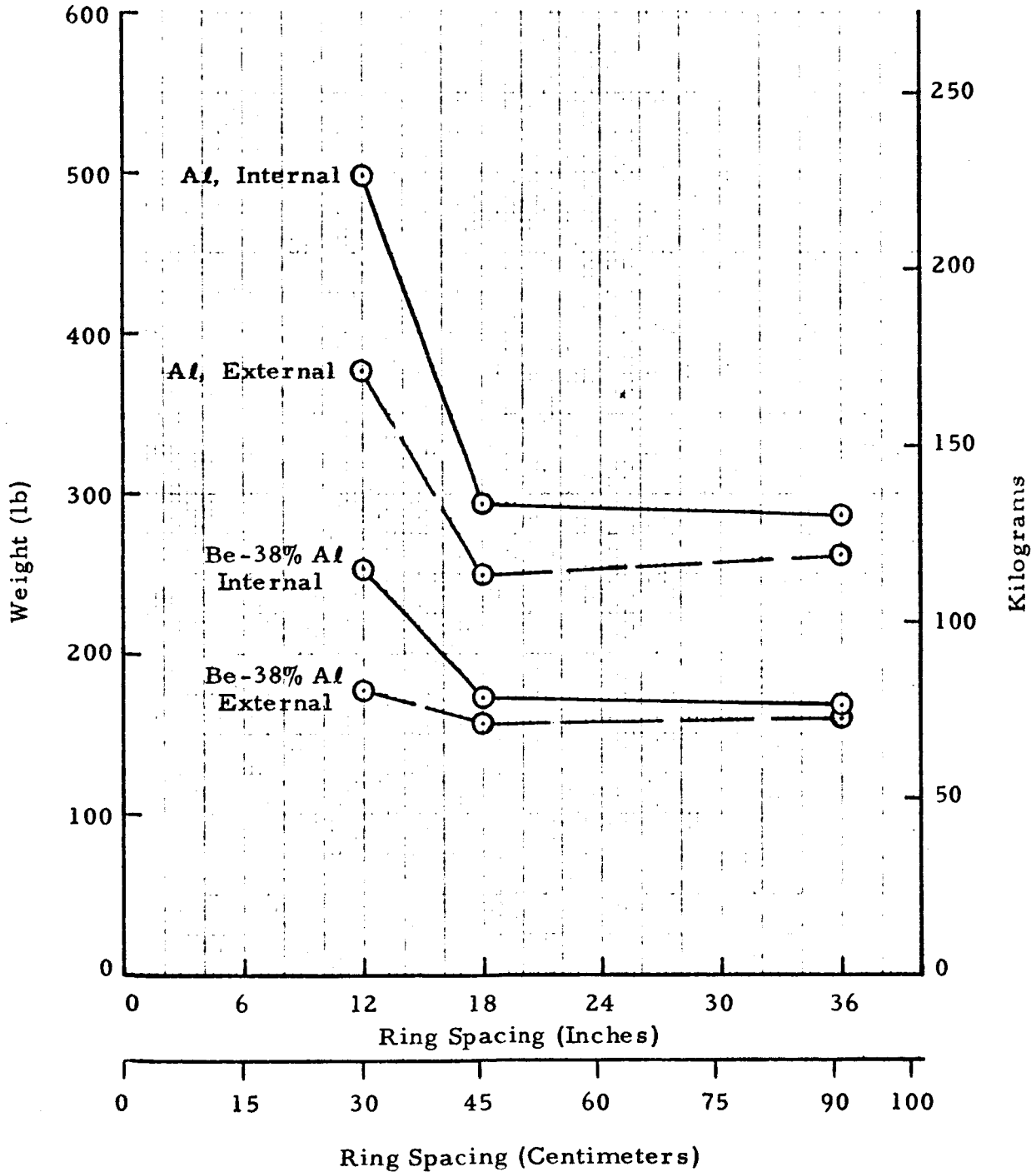
Figure 26 - Effect of Eccentricity on Cylinder Weight,
t = 0.060, L/R = 0.277

External Rectangular Rings and Stringers
Aluminum and Beryllium Aluminum
Dia. = 260 in.   L = 36 in. N_x = 1300 lb/in.
Max. Ring & Stringer Height Allowed = 1.5 in.
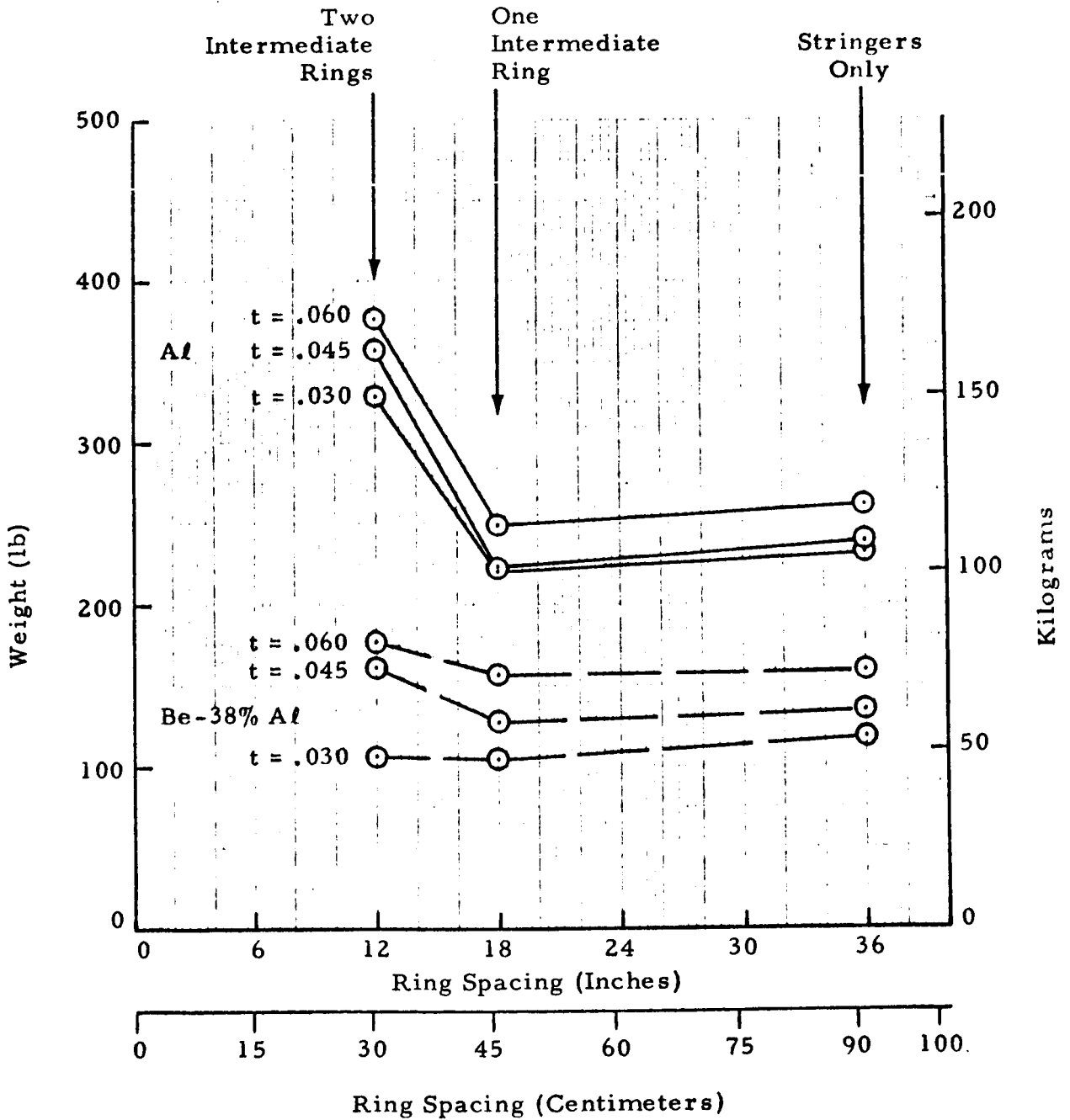
Figure 27 - Effect of Skin Thickness Variations on Weight

External Rectangular Rings and Stringers
Beryllium-38% Aluminum
Dia. = 260 in.   L = 36 in. N_x = 1300 lb/in.
Max. Ring & Stringer Height Allowed = 1.5 in.
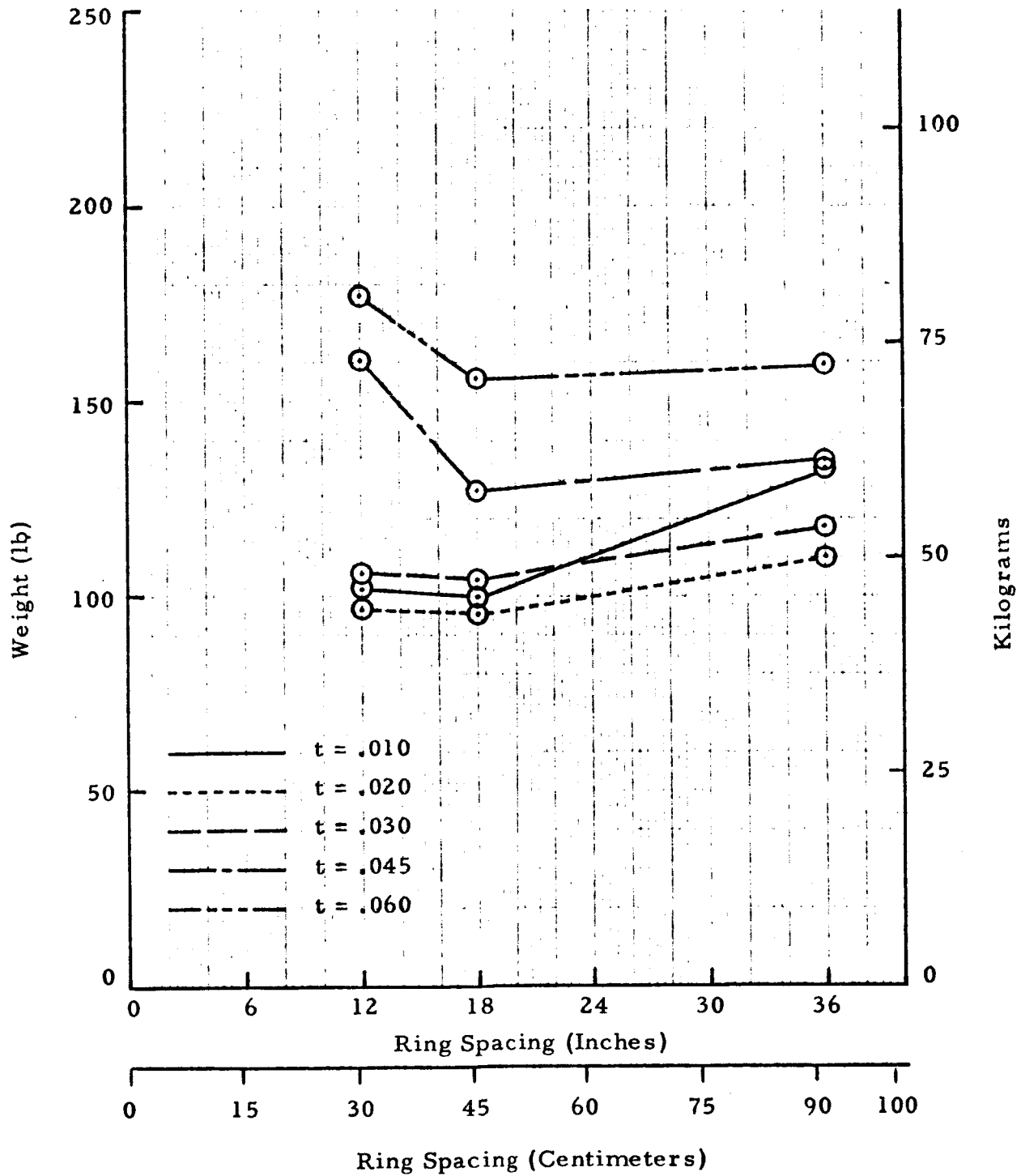
Figure 28 - Effect of Skin Thickness Variations on
Be-38% Aℓ Cylinders, L/R = 0.277

Max. Ring & Stringer Height Allowed = 1.5 in.
Dia. = 260 in.
L = 36 in.
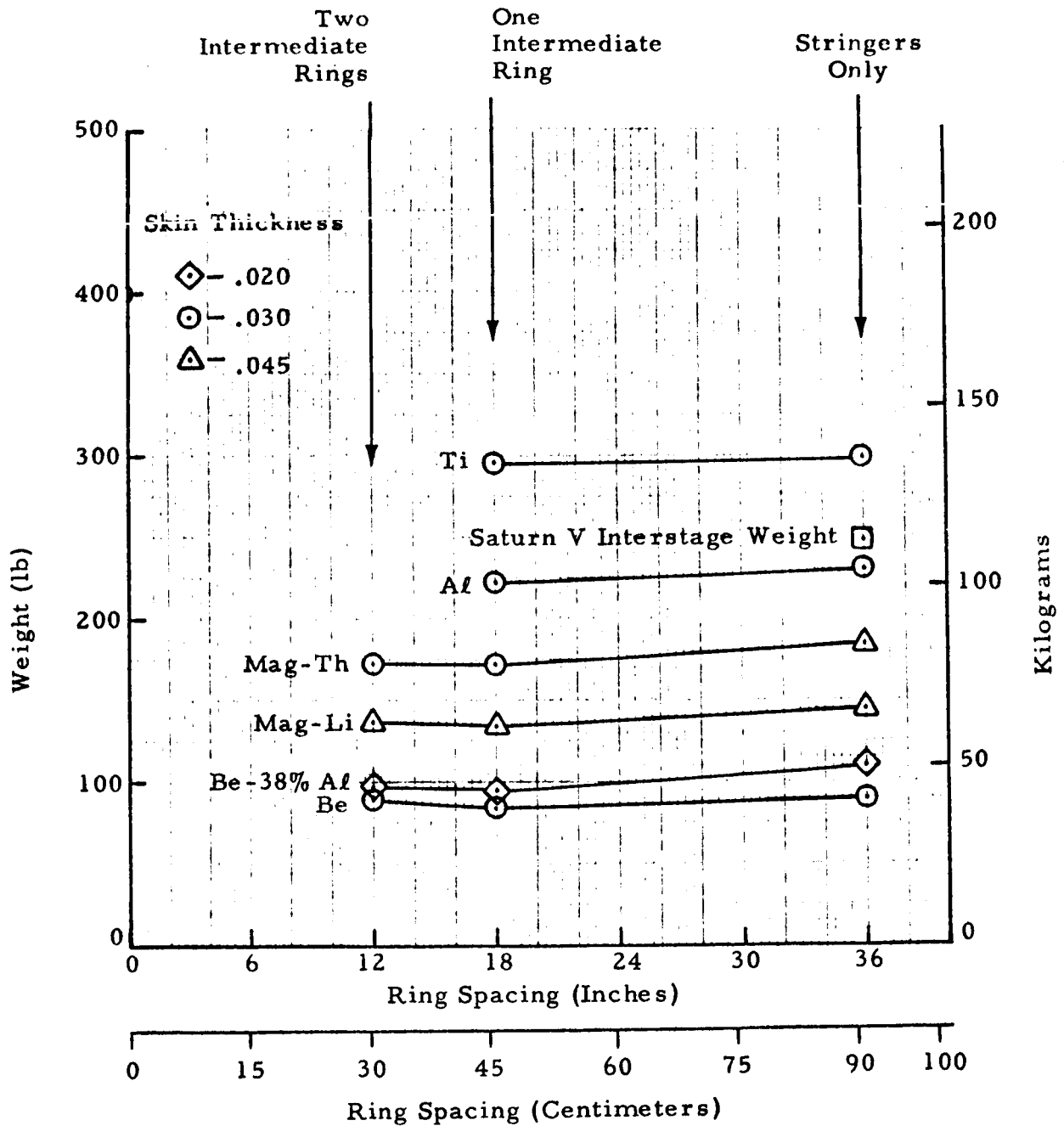
Figure 29 - Optimum Design Summary, External Rectangular
Stiffeners, 1300 lb/in. Loading, L/R = 0.277

Max. Ring & Stringer Height Allowed = 1.5 in.
Dia. = 260 in.
L = 36 in.
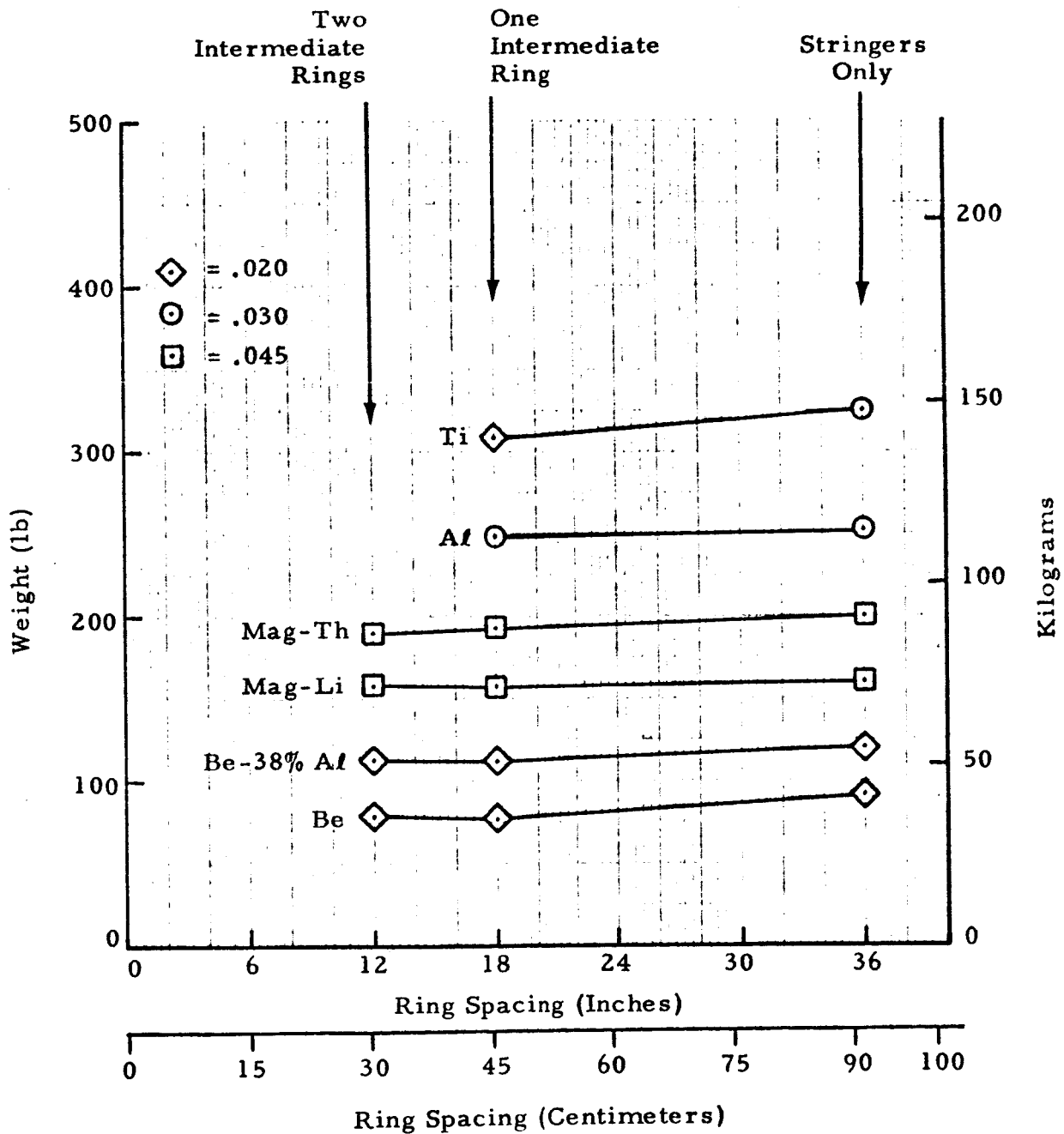
Figure 30 - Optimum Designs, External Rectangular Stiffeners,
1600 lb/in. Loading, L/R = 0.277

Max. Ring & Stringer Height Allowed = 1.5 in.
Dia. = 260 in.
L = 36 in.
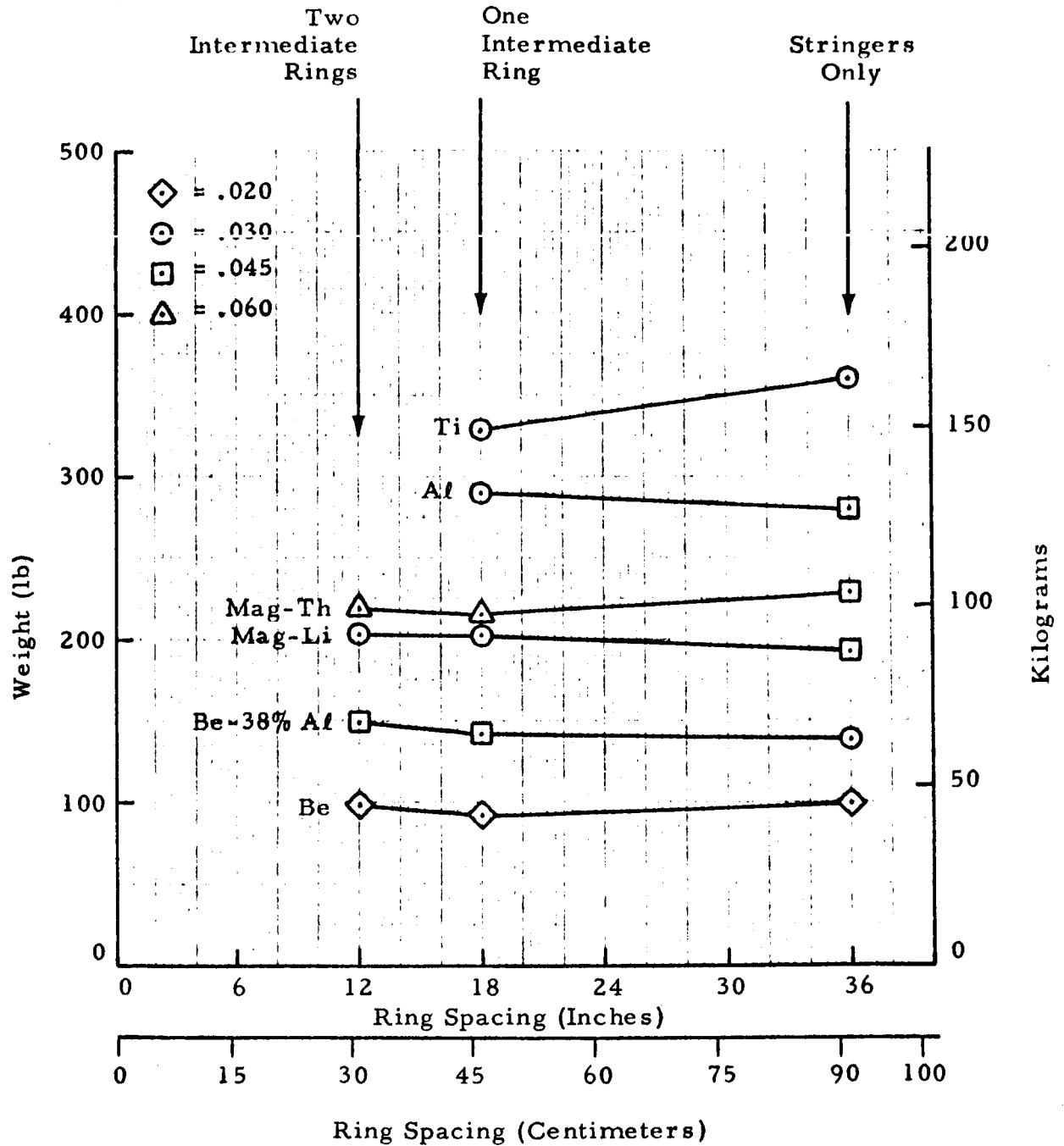
Figure 31 - Optimum Designs, External Rectangular Stiffeners,
2000 lb/in. Loading, L/R = 0.277
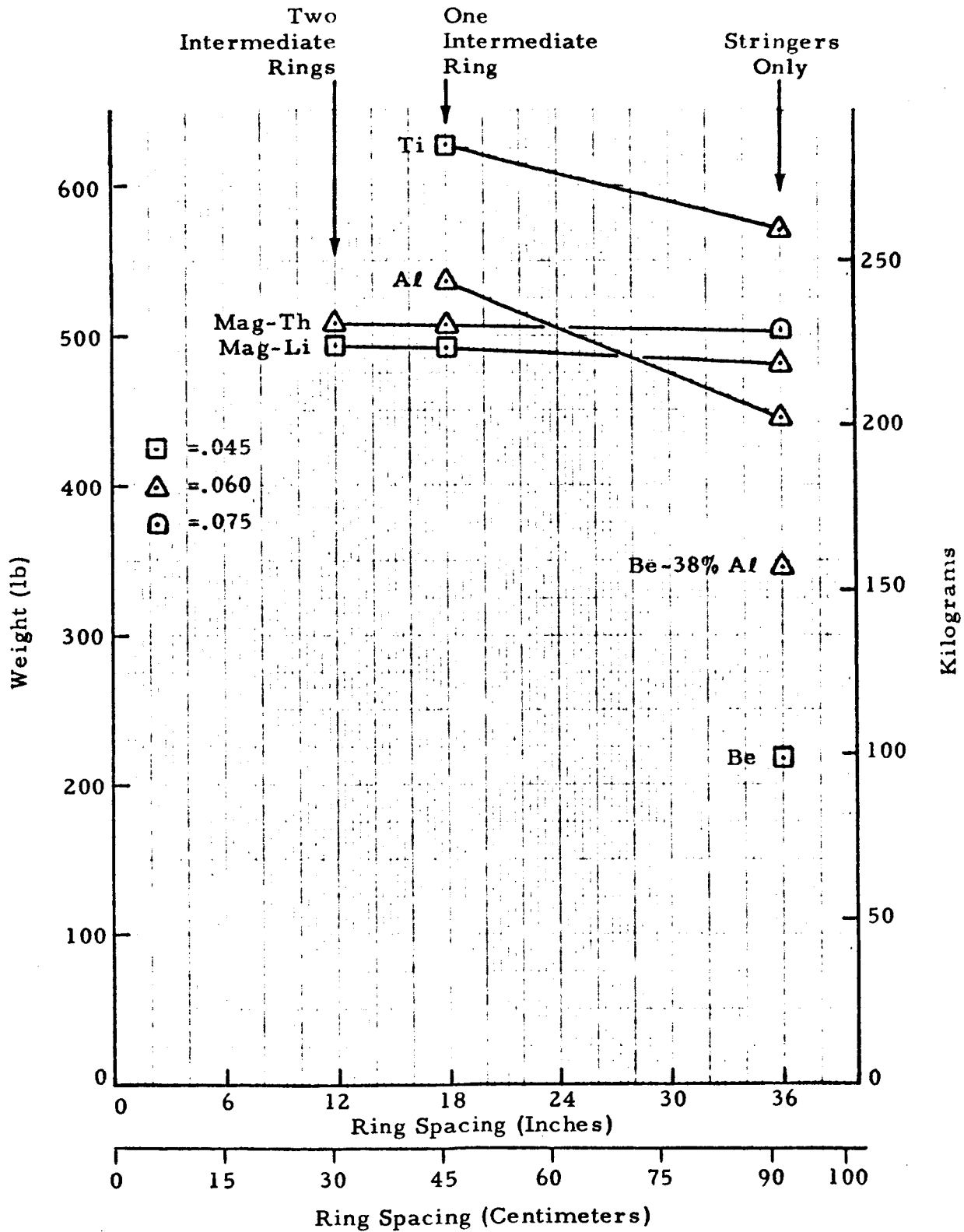
Figure 32 - Optimum Designs, External Rectangular Stiffeners,
5000 lb/in. Loading, L/R = 0.277

External Rectangular Stiffening
Variable Skin Thickness
L = 36 in.
Dia. = 260 in.
Max. Ring & Stringer Height Allowed = 1.5 in.
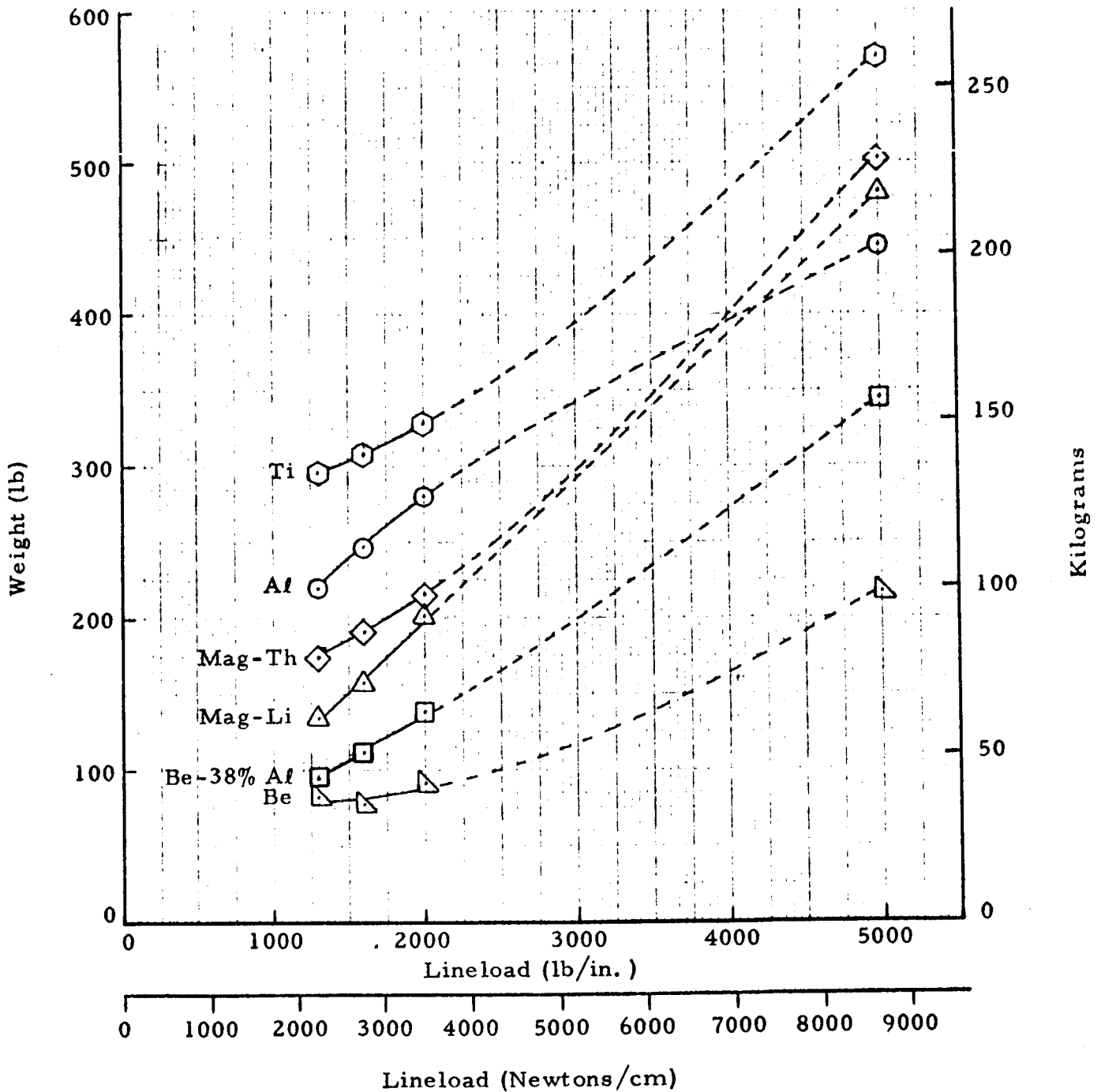
Figure 33 - Effect of Loading on Optimum Weights, L/R = 0.277

External Rectangular Stiffening
Max Ring & Stringer Height Allowed = 1.5 in.
Dia. = 260 in.
L = 36 in.
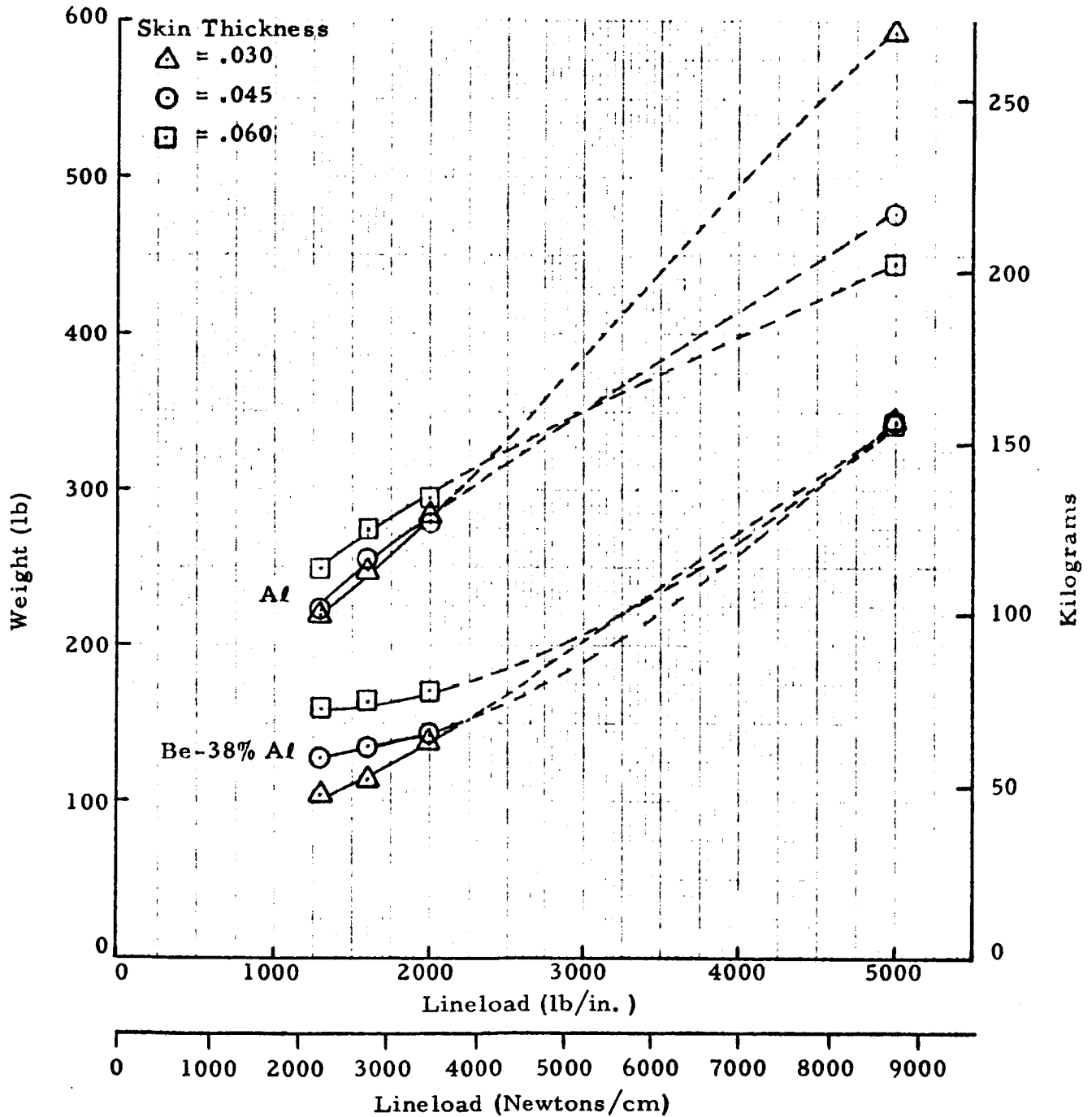
Figure 34 – Effect of Skin Thickness and Lineload
on Weight, L/R = 0.277
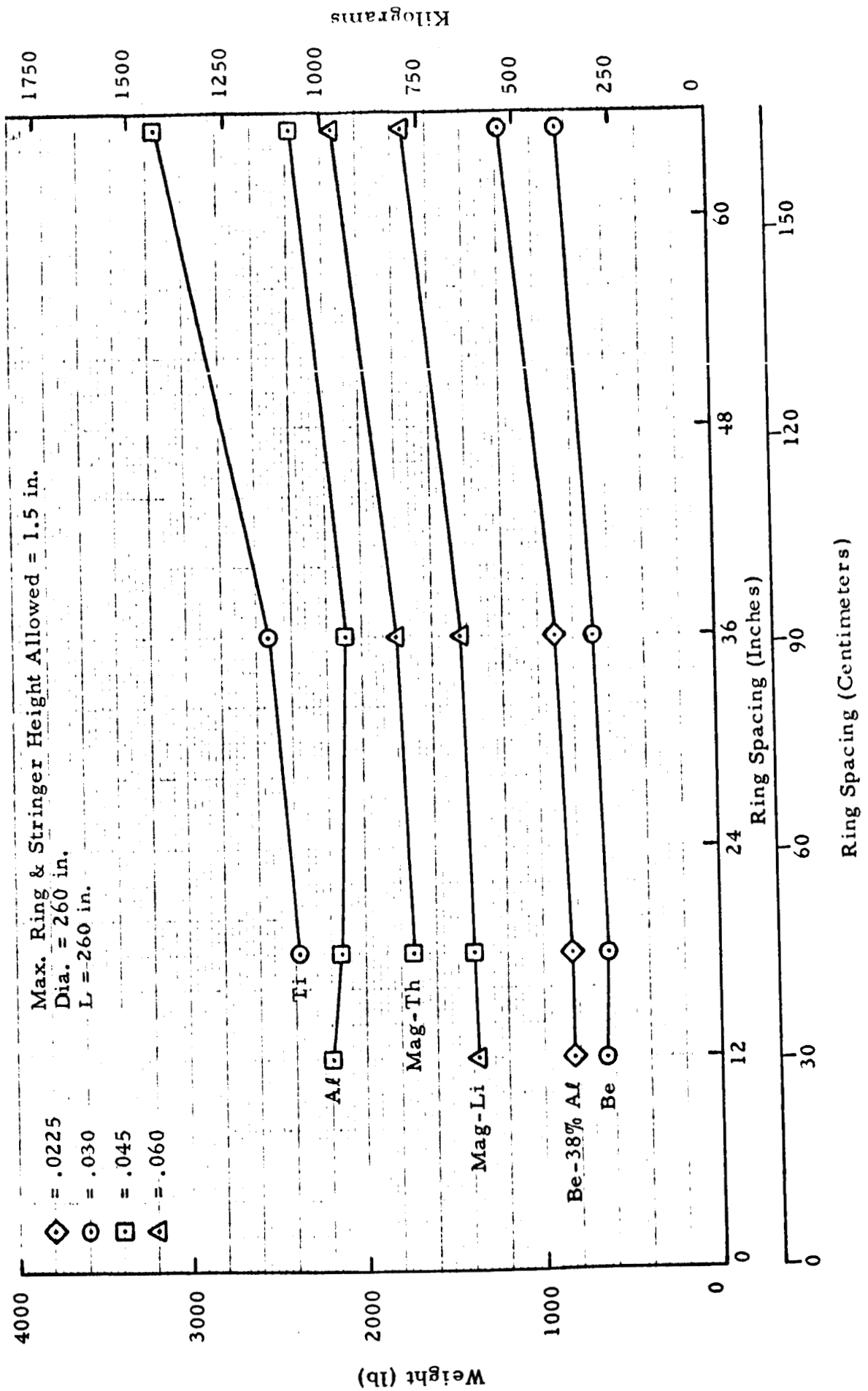
Figure 35 - Optimum Designs, External Rectangular Stiffeners, 1300 lb/in. Loading, L/R = 2.0
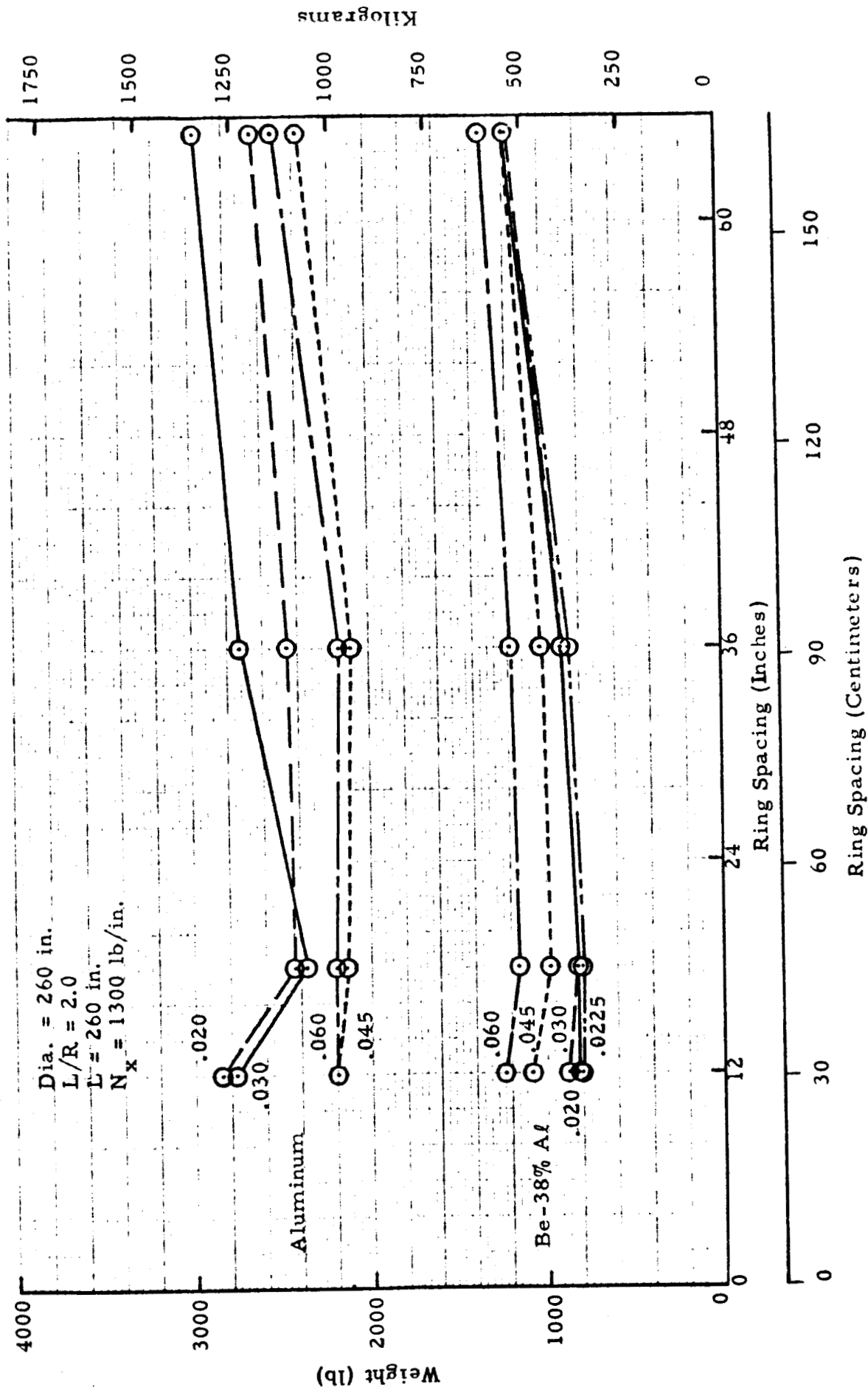
Figure 36 - Comparison of Aℓ and Be-38% Aℓ Long Cylinders of Variable Thickness
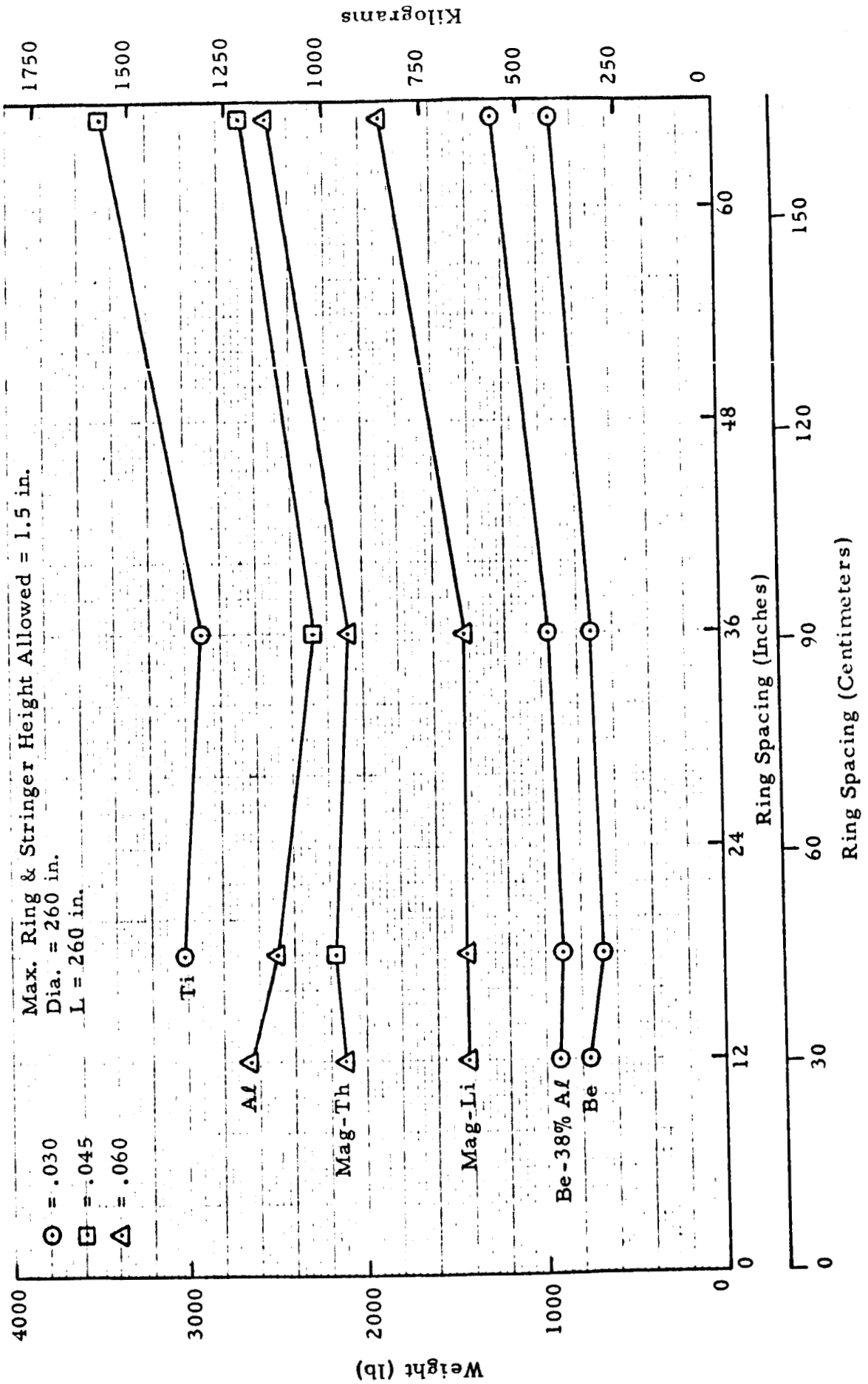
Figure 37 - Optimum Designs, External Rectangular Stiffeners, 1600 lb/in. Loading, L/R = 2.0
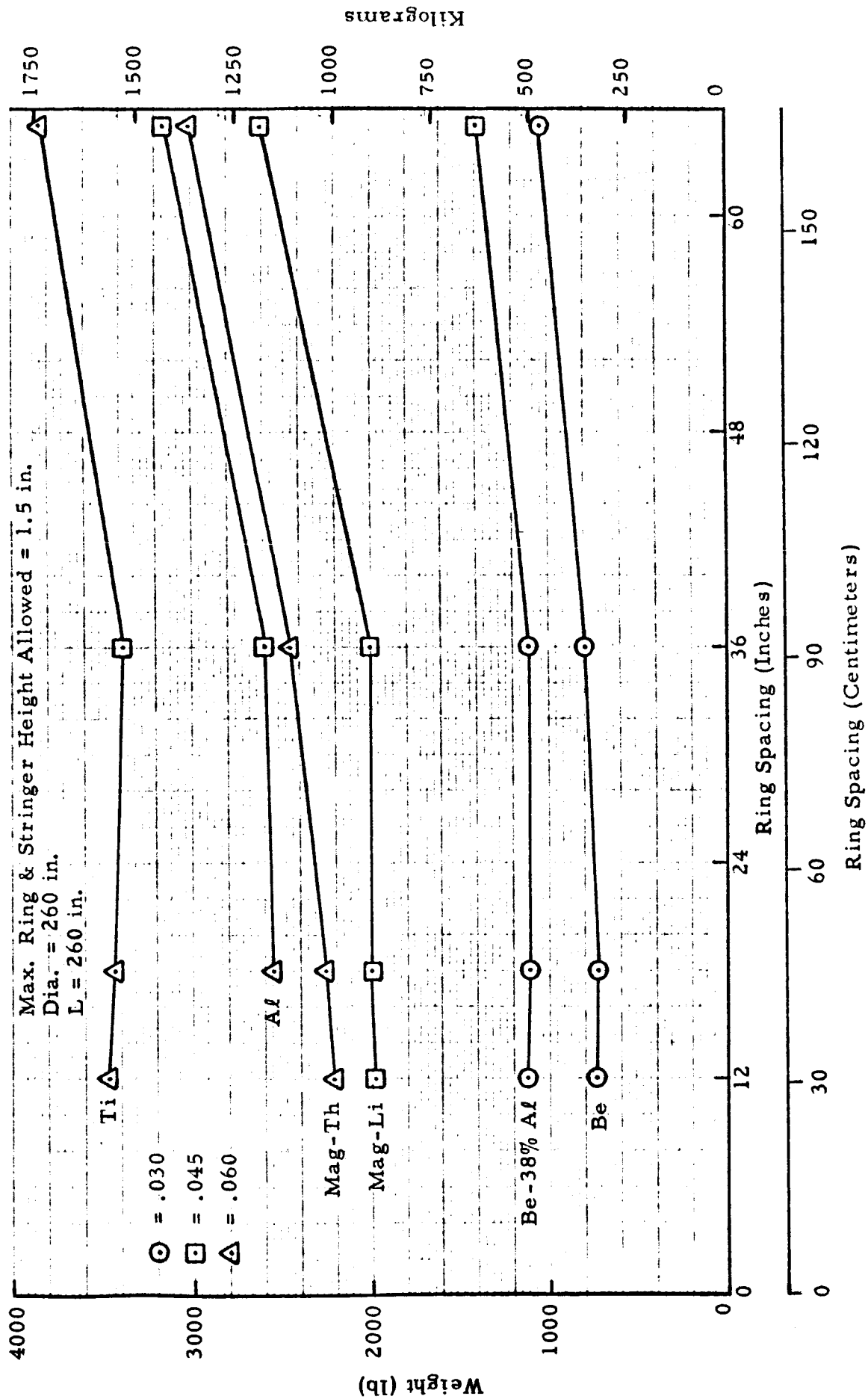
Figure 38 - Optimum Designs, External Rectangular Stiffeners, 2000 lb/in. Loading, L/R = 2.0
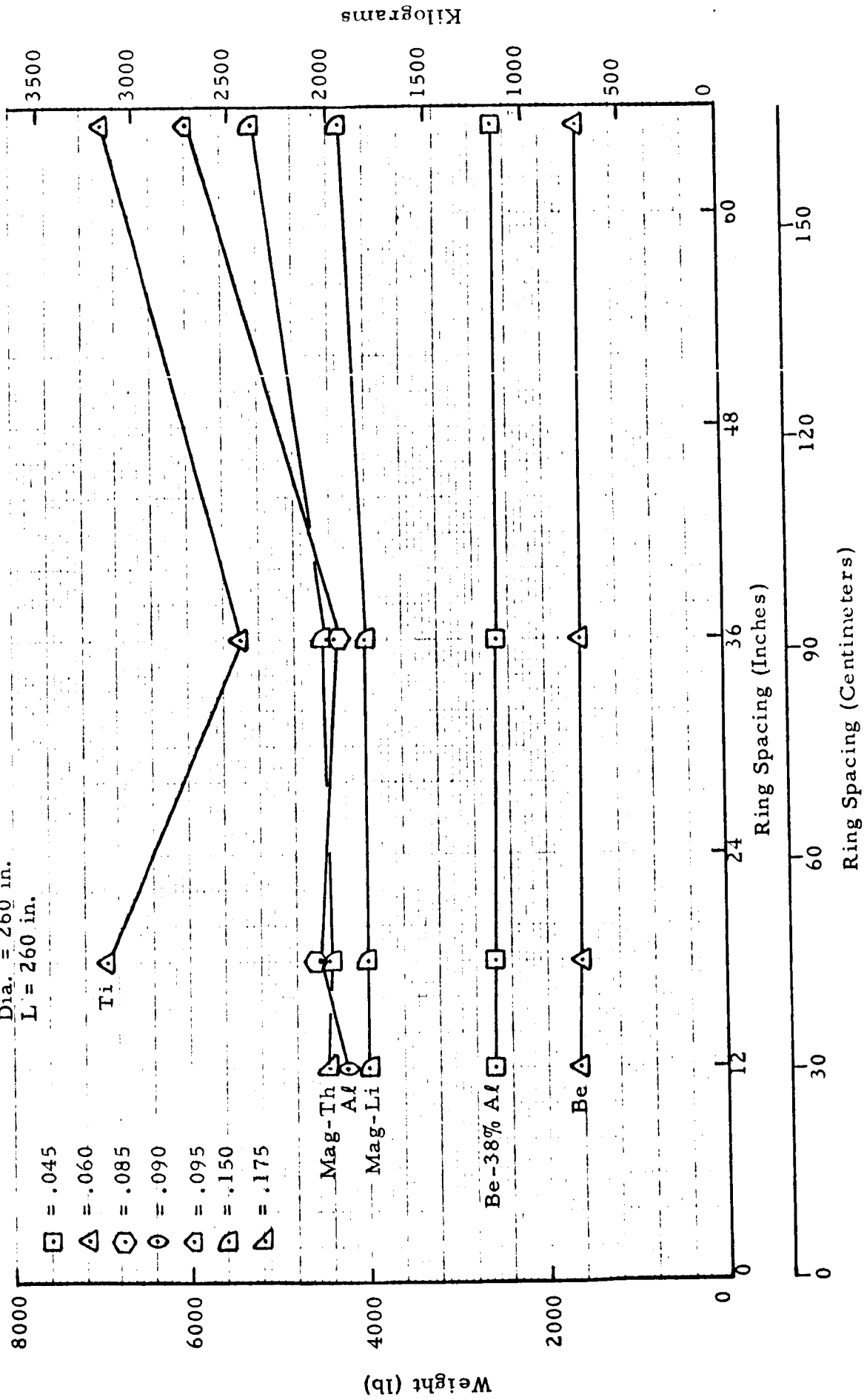
Figure 39 - Optimum Designs, External Rectangular Stiffeners, 5000 lb/in. Loading, L/R = 2.0
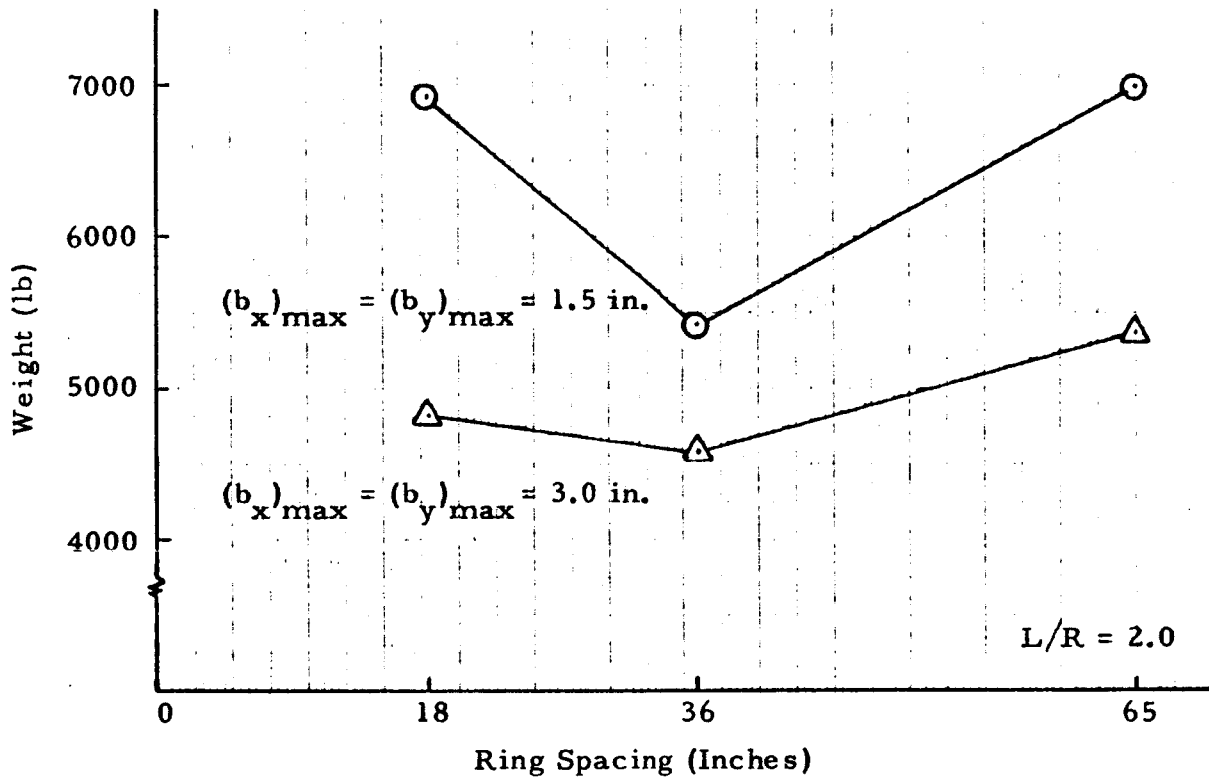
Figure 40 - Variation of Optimized Titanium Structural Weight with Stiffener Height Restrictions for 5000 lb/in. Loading

TABLE I

DETAIL CONFIGURATIONS FOR TITANIUM STRUCTURE OF VARYING HEIGHT STIFFENERS

	Max. Ring & Stringer Height = 1.5 in.						Max. Ring & Stringer Height = 3.0 in.					
d_y	b_y	t_2	b_x	t_1	d_x	Weight	b_y	t_2	b_x	t_1	d_x	Weight
18	1.50	1.269	0.959	0.081	2.01	6928	2.66	0.212	1.168	0.093	2.13	4831
36	1.28	1.082	1.339	0.102	2.23	5422	2.56	0.195	1.339	0.102	2.23	4588
65	1.24	0.895	1.500	0.240	2.79	7005	2.13	0.144	1.861	0.126	2.51	5370

Basic Skin Thickness = 0.060 in.
L/R = 2.0
N_x = 5000 lb/in.

Variable Skin Thickness
Dia. = 260 in.
L = 260 in.
Max. Ring & Stringer Height Allowed = 1.5 in.
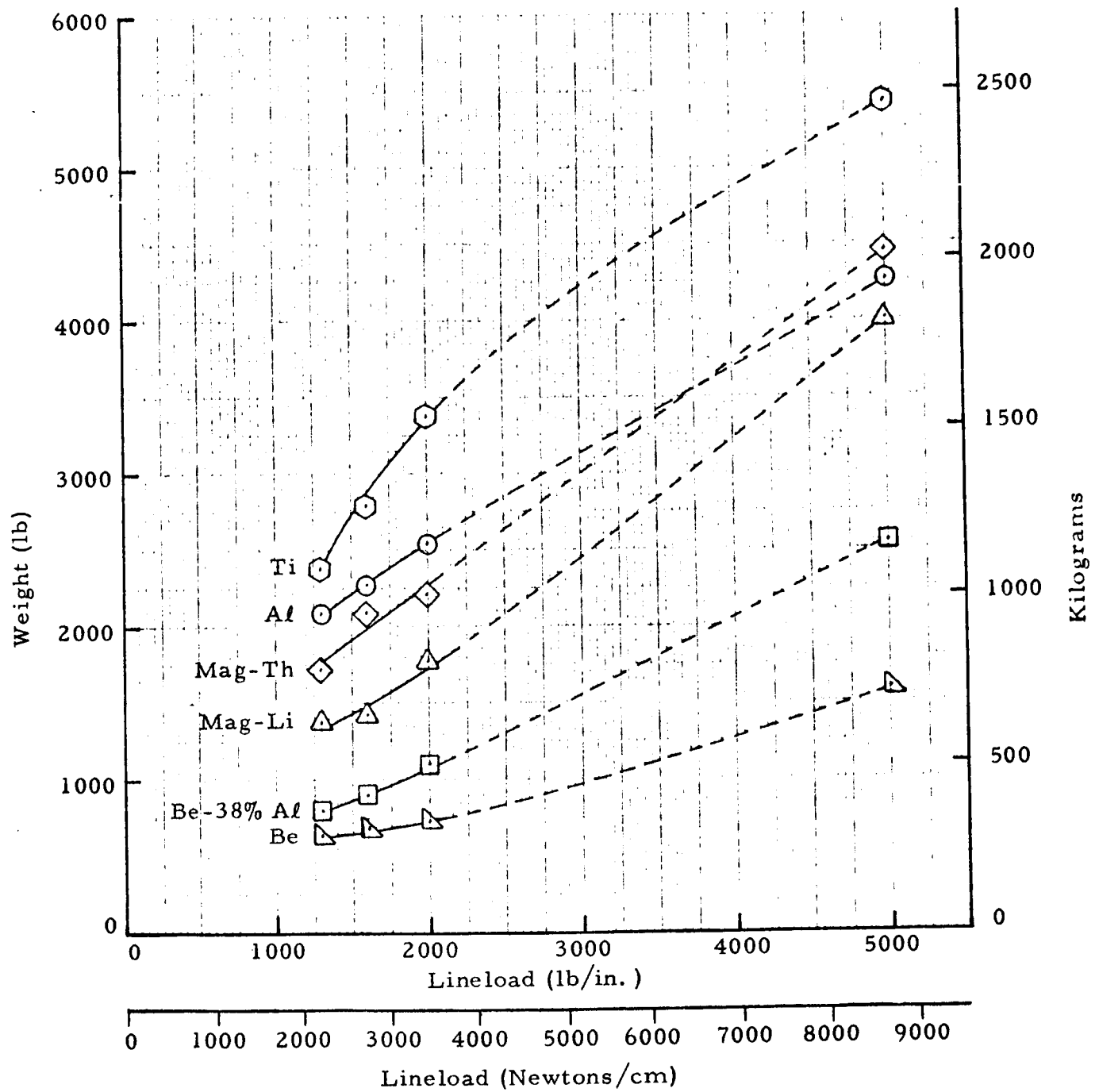
Figure 41 - Optimum Designs Versus Lineload, External
Rectangular Stiffeners, L/R = 2.0

TABLE II
EFFECT OF VARIABLE SLENDERNESS RATIO
Be-Aℓ - EXTERNAL RINGS AND STRINGERS
L/R = 2.0, t = 0.030,
1300 lb/in. Loading

	Parameters	(B/t) max = 15	(B/t) max = 30
Ring spacing	d_y	18.0	18.0
Ring height	b_y	1.42	1.41
Ring thickness	t_2	0.11	0.09
Stringer spacing	d_x	1.67	1.65
Stringer height	b_x	0.58	0.64
Stringer thickness	t_1	0.04	0.03
Stress level		32 ksi	32 ksi
Weight	Weight	826 lb	793 lb

Effect of Slenderness Ratio

Figure 42 - Optimum Designs, Trapezoidal Corrugation,
1300 lb/in. Loading, L/R = 0.277

Stringers External - Rings Internal
Dia. 260 in.   L = 36 in.
Max. Ring & Stringer Height Allowed = 1.5 in.
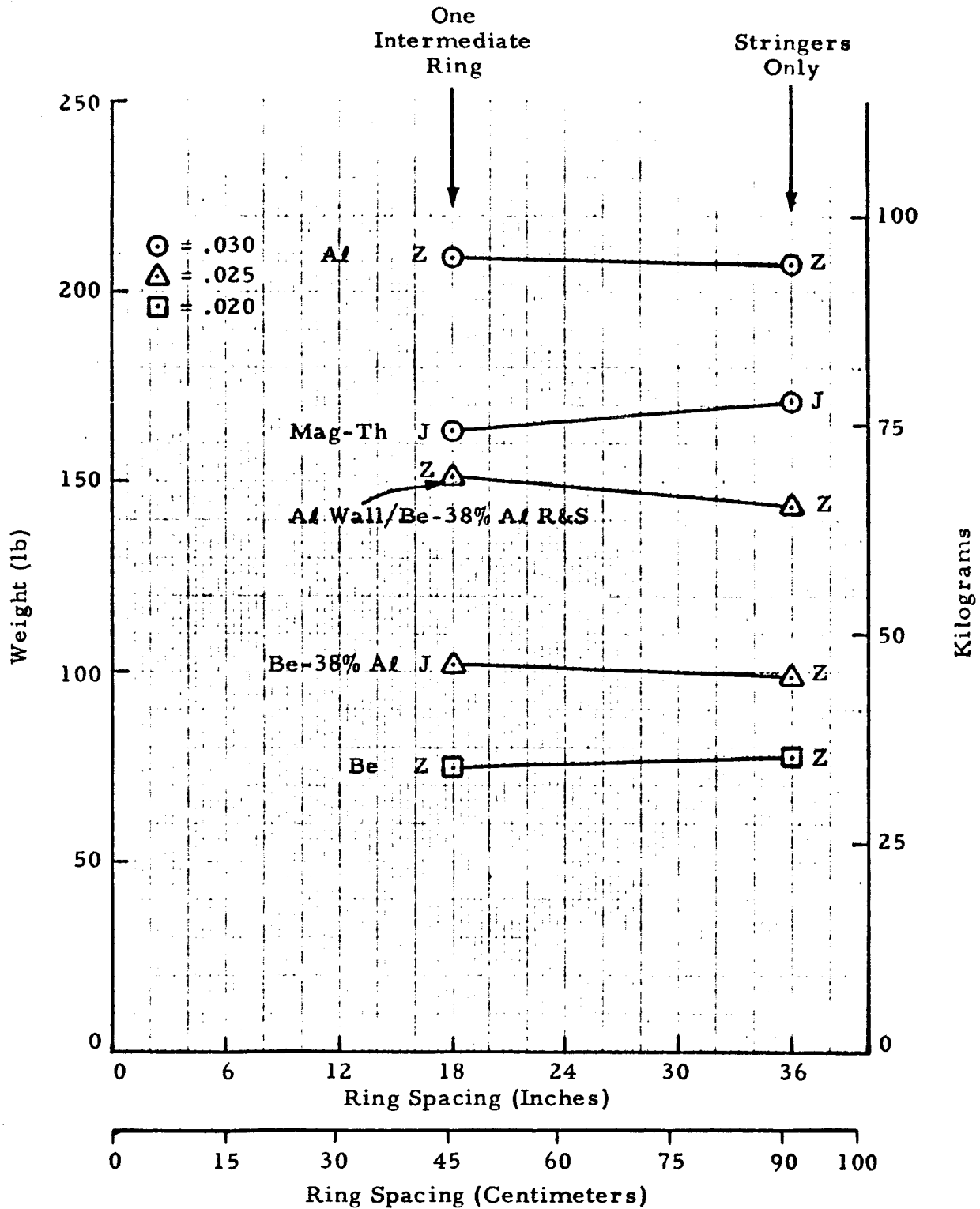
Figure 43 - Optimum Designs, J and Z Stiffeners,
1300 lb/in. Loading, L/R = 0.277
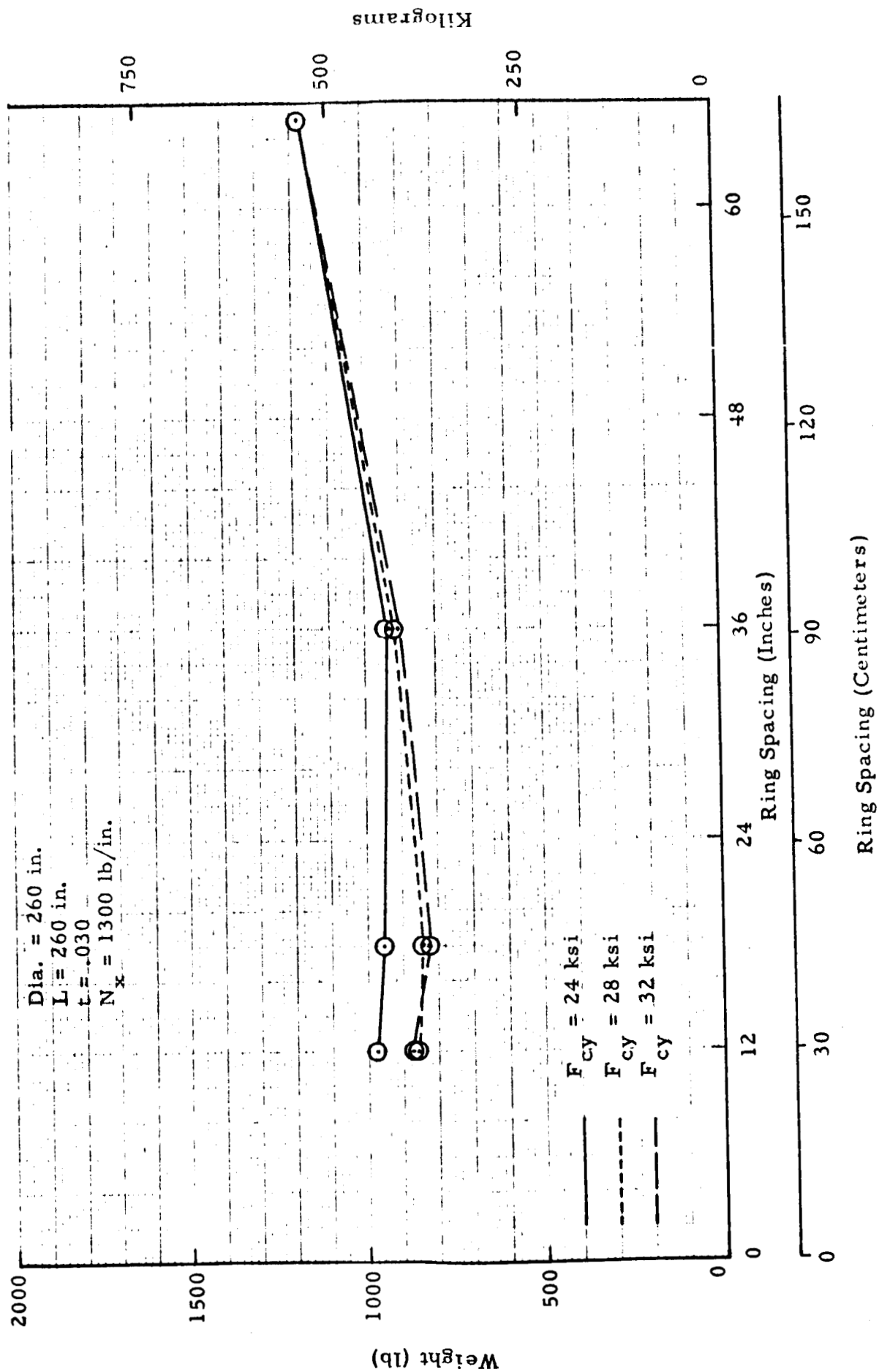
Figure 44 - Weight Comparison of Be-38% Aℓ Cylinders with Arbitrarily Reduced Compressive Yield Values, L/R = 2.0

APPENDIX A

OPTIMIZATION METHODS FOR CYLINDERS REINFORCED
WITH CONVENTIONAL, FLANGED STIFFENERS

APPENDIX A

OPTIMIZATION METHODS FOR CYLINDERS REINFORCED
WITH CONVENTIONAL, FLANGED STIFFENERS*

1.0   INTRODUCTION

The analytical basis for the structural optimization of axially com-
pressed cylinders stiffened with J (or Z) section stringers and optional
J (or Z) section rings is described. (See Figure A-1.) The methods employed
for predicting the various modes of instability are consistent with the
methods employed in previous optimization studies of this type (References
A-1, A-2 and A-3). Therefore, comparisons of optimum J(or Z) stiffened
cylinders with the detailed configurations previously studied are as realistic
as is presently possible. It should be noted that at present the empirical
factor ϕ requires additional substantiation. Therefore, comparisons of
optimum detailed configurations may be subject to adjustment in a quantitative
sense although they are now realistic in a qualitative sense.

It should be noted that, since the attach-flange widths, a_x and a_y,
are specified by the designer in the present analysis, it is possible to set
these quantities to zero and, as a result, additionally investigate integrally
stiffened cylinders. The same selection capability for outstanding flanges
remains; however, in this situation, the stiffeners are more properly defined
as integral tee sections or integral flanged sections.

---

*excerpt from Reference A-7

Figure A-1 - Cylinder Reinforced with Conventional
Flanged Stiffeners

NOTATION FOR APPENDIX A

a_n	D_{1n}/D_{0n}, Eq. (19)
A_{11}, A_{12}	coefficients of extensional rigidity for orthotropic shells
A_{22}, A_{33}	
A_s	cross-sectional area of stringer
A_r	cross-sectional area of ring
b_n	D_{2n}/D_{0n}, Eq. (20)
c	correction factor, Eq. (51)
C	geometric constant
d_y	ring spacing (centerline to centerline)
D_{0n}, D_{1n}	expressions defined by Eqs. (21), (22), and (23)
D_{2n}	
D_f	$E_w t^3/12(1 - v_w^2)$
D_x, D_y	coefficients of flexural and torsional rigidity for orthotropic shells
D_{12}, D_{33}	
e_1	distance between centroid of stringer cross section and wall middle surface
e_2	distance between centroid of ring cross section and wall middle surface
E_w, E_x, E_y	Young's modulus for cylinder wall, stringer and ring material, respectively
J_x	stringer torsion constant per unit of circumferential width of cylinder wall
J_y	ring torsion constant per unit of length of cylinder wall
K	geometric constant
L	cylinder length
L_1	length; equal to d_y for panel instability calculations, equal to L for overall instability calculations

m	number of axial half-waves
n	number of circumferential full waves
N_{cl}	classical buckling load per unit of circumference, for the general instability mode
N_{min}	minimum postbuckling load per unit of circumference for the general instability mode
N_x	applied axial load per unit of circumference
R	cylinder radius
t	cylinder wall thickness
$\bar{t}$	equivalent thickness of a stiffened cylinder having uniform material properties, for purposes of weight calculation
$\bar{\bar{t}}$	equivalent thickness of a stiffened cylinder having non-uniform material properties, for purposes of non-dimensionalization of weight. Equal to W_i/ρ_w
W_i	weight of cylinder per unit of surface area
Y	effective width correction factor, Eqs. (18), (32) and (33)
Z	non-dimensionalized centroidal distance of stiffener-cylinder wall combination; measured from midplane of cylinder wall
α	geometric constant, Eq. (58)
β	$m\pi R/L_1$, Eq. (49)
γ	geometric constant, Eq. (55)
ϵ	strain
η_p	geometric constant, Eq. (57)
η_s	geometric constant, Eq. (56)
μ_1	increase in effective cross-sectional area of the shell due to the stringers
μ_2	increase in effective cross-sectional area of the shell due to rings
ν_w, ν_x, ν_y	Poisson's ratio for cylinder wall, stringer and ring material, respectively

ρ_w, ρ_x, ρ_y material density for cylinder wall, stringers and rings, respectively

σ uniform axial compressive stress

ϕ empirical correction factor, Eq. (52)

X_1 change in extensional stiffness caused by the eccentricity of the stringers

X_2 change in extensional stiffness caused by the eccentricity of the rings

Subscripts

cr   critical

e   effective

s   stringer

r   ring

w   cylinder wall

x or 1   axial coordinate

y or 2   circumferential coordinate

cl   classical

See Figure A-1 for notations for stiffened cylinder dimensions.

2.0   LOCAL INSTABILITY EQUATIONS

The dimension d_x is usually small compared to the radius of the cylinder; therefore, curvature effects in the cylinder wall elements of this dimension may be neglected, and classical flat plate theory can be used to predict local instability in the cylinder wall:

$$(\sigma/E_w)_{cr} = \frac{4\pi^2}{12(1-\nu_w^2)} \ (\frac{t}{d_x})^2 \tag{1}$$

Local instability may occur in any of four elements in the J stiffener:

$$(\sigma/E_x)_{cr_{b_s}} = \frac{4\pi^2}{12(1-\nu_x^2)} \ (\frac{t_{1b}}{b_s})^2 \tag{2}$$

$$(\sigma/E_x)_{cr_{c_s}} = \frac{0.5\pi^2}{12(1-\nu_x^2)} \ (\frac{t_{1c}}{c_s})^2 \tag{3}$$

$$(\sigma/E_x)_{cr_{f_x}} = \frac{4\pi^2}{12(1-\nu_x^2)} \ (\frac{t_{1a}}{f_x})^2 \tag{4}$$

$$(\sigma/E_x)_{cr_{e_x}} = \frac{0.5\pi^2}{12(1-\nu_x^2)} \ (\frac{t_{1a}}{e_x})^2 \tag{5}$$

The attach-flange width a_x has been designated a restraint in a previous section; therefore, the elements f_x and e_x are not free to assume whatever widths required to yield local instability in all stringer elements simultaneously. Elements f_x and e_x must be treated independently as possible sources of the critical local instability stress in the stringer. Note that, as a result of these considerations, the dimension e_x must be specified by the designer. This situation is not common to the element c_s. The assumption can be made that local instability occurs simultaneously in elements b_s and c_s. Thus, solving Eqs. (2) and (3) simultaneously, we obtain the equality:

$$\frac{c_s}{t_{1c}} = \frac{1}{2\sqrt{2}} \frac{b_s}{t_{1b}} \tag{6}$$

If different materials are specified for the stringers and cylinder wall, the load carrying ability of the cylinder,

$$\frac{N_x}{R} = \sigma_w \cdot \frac{t}{R} + \sigma_x \cdot \frac{A_s}{d_x R} \tag{7}$$

may be expressed as

$$\frac{N_x}{R} = \epsilon_w E_w \cdot \frac{t}{R} + \epsilon_x E_x \cdot \frac{A_s}{d_x R} \tag{8}$$

The strains in the cylinder wall and stringers must be equal. Therefore, Eq. (8) becomes:

$$\frac{N_x}{R} = \epsilon_w E_w \left(\frac{t}{R} + \frac{E_x}{E_w} \frac{A_s}{d_x R} \right) \tag{9}$$

But, for local instability,

$$\epsilon_w = (\sigma/E_w)_{cr} \tag{10}$$

Substituting for ϵ_w in Eq. (9) and rearranging, the stringer spacing based on local instability requirements becomes:

$$\frac{d_x}{t} = \left\{ \frac{4\pi^2}{12(1-\nu_w^2)} \left(\frac{t}{R} + \frac{E_x}{E_w} \frac{A_s}{d_x R} \right) \left(\frac{N_x}{R E_w} \right)^{-1} \right\}^{1/2} \tag{11}$$

where

$$\frac{A_s}{d_x R} = \left(\frac{t}{d_x} \right) \left[\frac{a_x}{R} \cdot \frac{t_{1a}}{t_{1b}} \cdot \frac{t_{1b}}{t} + \frac{b_x}{R} \cdot \frac{t_{1b}}{t} + 2\frac{c_s}{t_{1c}} \left(\frac{t_{1c}}{t_{1b}} \cdot \frac{t_{1b}}{t} \right)^2 \left(\frac{R}{t} \right)^{-1} \right] \tag{12}$$

$$\frac{t_{1b}}{t} = \frac{t_{1b}}{R} \cdot \frac{R}{t} \tag{13}$$

$$\frac{b_s}{R} = \frac{b_x}{R} - \frac{t_{1b}/t}{R/t} \left[\frac{t_{1c}}{t_{1b}} + \frac{t_{1a}}{t_{1b}} \right] \tag{14}$$

$$\frac{b_s}{t_{1b}} = \frac{b_s}{R} \cdot \frac{R}{t} \cdot \frac{t}{t_{1b}} \tag{15}$$

Equation (11) is based on local instability taking place initially either in the cylinder wall, or in conjunction with local instability in one or more of the stringer elements. Should local instability in one of the stringer elements, Eqs. (2) through (5), precede local instability in the cylinder wall, then d_x/t is obtained from:

$$\frac{N_x}{RE_w} = (\sigma/E_x)_{cr} \left[\frac{t}{R} + \frac{E_x}{E_w} \cdot \frac{A_s}{d_x R} \right] \tag{16}$$

where $(\sigma/E_x)_{cr}$ is the strain corresponding to the lowest local instability stress in the stringer cross section.

3.0   GENERAL INSTABILITY EQUATIONS

3.1   The Classical Buckling Load

The method utilized here to predict general instability in axially-compressed, eccentrically-stiffened cylinders is the same as the method used in References A-1 and A-2. However, for the present analysis, the equations have been generalized to account for differences in materials in the cylinder wall, stringers and rings. The resulting equations, expressed non-dimensionally in terms of stiffnesses measured about the centroid of the stiffener-skin combination, follow:

$$\frac{N_{c1}}{RE_w} = \frac{F}{\beta^2 (R/t)^3 \, 12(1 - \nu_w^2)} \tag{17}$$

where:

$$\begin{aligned}
F \; = \; & \left[\frac{D_x}{D_f} + 3Z_x^2 (1 - \nu_w^2 + \mu_1) \right] \beta^4 + \left\{ \frac{D_y}{D_f} + 3Z_y^2 \left[Y(1 - \nu_w^2) \right. \right. \\
& \left. \left. + \mu_2 \right] \right\} \; n^4 + \left(\frac{2D_{33}}{D_f} - 1 + 2\nu_w \right) 2\beta^2 n^2 + 12(\frac{R}{t})^2 \left[X_1(-\beta^3 a_n) \right. \\
& \left. + X_2(-2n^2 - b_n n^3) + (1 + \mu_2)(1 + b_n n) + \nu_w \beta a_n \right] \tag{18}
\end{aligned}$$

$$a_n \; = \; \frac{D_{1n}}{D_{0n}} \tag{19}$$

$$b_n \; = \; \frac{D_{2n}}{D_{0n}} \tag{20}$$

$$\begin{aligned}
D_{0n} = \; & 0.5(1 - \nu_w)(1 + \mu_2)n^4 + \left[(1 + \mu_1)(1 + \mu_2) - \nu_w \right] \beta^2 n^2 \\
& + 0.5(1 + \mu_1)(1 - \nu_w)\beta^4 \tag{21}
\end{aligned}$$

$$\begin{aligned}
D_{1n} = \; & -0.5(1 + \nu_w)X_2\beta n^4 + (1 + \mu_2)\left[X_1\beta^3 + 0.5(1 - \nu_w)\beta \right] n^2 \\
& + 0.5 X_1(1 - \nu_w)\beta^5 - 0.5\nu_w(1 - \nu_w)\beta^3 \tag{22}
\end{aligned}$$

$$\begin{aligned}
D_{2n} = \; & 0.5(1 - \nu_w)X_2 n^5 + \left[(1 + \mu_1)X_2\beta^2 - 0.5(1 - \nu_w)(1 + \mu_2) \right] n^3 \\
& + \left\{ \left[0.5(1 + \nu_w)\nu_w - (1 + \mu_1)(1 + \mu_2) \right] \beta^2 - 0.5(1 + \nu_w)X_1\beta^4 \right\} n \tag{23}
\end{aligned}$$

and

$$\frac{D_x}{D_f} = 1 + 3(1 - \nu_w^2) Z_x^2 + \frac{E_x}{E_w} (1 - \nu_w^2) \left\{ 2K_2 \left[K_1^2 + 3(2K_3 - K_1 \right. \right.$$

$$\left. + 1 - Z_x)^2 \right] + K_4 \left[K_3^2 + 3(K_3 + 1 - Z_x)^2 \right]$$

$$\left. + K_6 \left[K_5^2 + 3(K_5 + 1 - Z_x)^2 \right] \right\} \tag{24}$$

$$Z_x = \frac{2K_2(2K_3 - K_1 + 1) + K_4(K_3 + 1) + K_6(K_5 + 1)}{2K_2 + K_4 + K_6 + \frac{E_w}{E_x}} \tag{25}$$

$$K_1 = \frac{t_{1c}}{t_{1b}} \cdot \frac{t_{1b}}{t} \tag{26}$$

$$K_2 = \frac{\frac{c_s}{t_{1c}} \cdot K_1^2}{\frac{d_x}{t}} \tag{27}$$

$$K_3 = \frac{b_x}{R} \cdot \frac{R}{t} \tag{28}$$

$$K_4 = \frac{K_3 \cdot \frac{t_{1b}}{t}}{\frac{d_x}{t}} \tag{29}$$

$$K_5 = \frac{t_{1a}}{t_{1b}} \cdot \frac{t_{1b}}{t} \tag{30}$$

$$K_6 = \frac{\frac{a_x}{R} \cdot \frac{R}{t} \cdot K_5}{\frac{d_x}{t}} \tag{31}$$

$$\frac{D_y}{D_f} = 1 + 3Y(1 - \nu_w^2) Z_y^2 + \frac{E_y}{E_w} (1 - \nu_w^2) \left\{ 2C_2 \left[C_1^2 + 3(2C_3 - C_1 \right. \right.$$

$$\left. + 1 - Z_y)^2 \right] + C_4 \left[C_3^2 + 3(C_3 + 1 - Z_y)^2 \right] + C_6 \left[C_5^2 + 3(C_5 \right.$$

$$\left. \left. + 1 - Z_y)^2 \right] \right\} \tag{32}$$

$$Z_y = \frac{2C_2(2C_3 - C_1 + 1) + C_4(C_3 + 1) + C_6(C_5 + 1)}{2C_2 + C_4 + C_6 + Y\dfrac{E_w}{E_y}} \tag{33}$$

$$C_1 = \frac{t_{2c}}{t_{2b}} \cdot \frac{t_{2b}}{t} \tag{34}$$

$$C_2 = \frac{\dfrac{c_s}{t_{2c}} \cdot C_1^2}{\dfrac{d_y}{t}} \tag{35}$$

$$C_3 = \frac{b_y}{R} \cdot \frac{R}{t} \tag{36}$$

$$C_4 = \frac{C_3 \cdot \dfrac{t_{2b}}{t}}{\dfrac{d_y}{t}} \tag{37}$$

$$C_5 = \frac{t_{2a}}{t_{2b}} \cdot \frac{t_{2b}}{t} \tag{38}$$

$$C_6 = \frac{\dfrac{a_y}{R} \cdot \dfrac{R}{t} \cdot C_5}{\dfrac{d_y}{t}} \tag{39}$$

$$\frac{2D_{33}}{D_f} = 2(1 - \nu_w) + 3 \left[\frac{E_x}{E_w} \cdot \frac{(1 - \nu_w^2)}{(1 + \nu_x)} \cdot \frac{J_x}{t^3} \right.$$

$$\left. + \frac{E_y}{E_w} \cdot \frac{(1 - \nu_w^2)}{(1 + \nu_y)} \cdot \frac{J_y}{t^3} \right] \tag{40}$$

$$\frac{J_x}{t^3} = \frac{1}{3} \left[2K_2 K_1^2 + K_4 \left(\frac{t_{1b}}{t}\right)^2 + K_6 K_5^2 \right] \tag{41}$$

$$\frac{J_y}{t^3} = \frac{1}{3} \left[2C_2 C_1^2 + C_4 \left(\frac{t_{2b}}{t}\right)^2 + C_6 C_5^2 \right] \tag{42}$$

$$\mu_1 = (1 - \nu_w^2) \frac{E_x}{E_w} (2K_2 + K_4 + K_6) \tag{43}$$

$$\mu_2 = (1 - \nu_w^2) \frac{E_y}{E_w} (2C_2 + C_4 + C_6) \tag{44}$$

$$X_1 = \mu_1 \frac{e_1}{R} \tag{45}$$

$$X_2 = \mu_2 \frac{e_2}{R} \tag{46}$$

$$\frac{e_1}{R} = \frac{0.5 \left[1 + \dfrac{2K_2(2K_3 - K_1) + K_3 K_4 + K_5 K_6}{2K_2 + K_4 + K_6} \right]}{R/t} \tag{47}$$

$$\frac{e_2}{R} = \frac{0.5 \left[1 + \dfrac{2C_2(2C_3 - C_1) + C_3 C_4 + C_5 C_6}{2C_2 + C_4 + C_6} \right]}{R/t} \tag{48}$$

$$\beta = \frac{m\pi R}{L_1} \tag{49}$$

The above equations represent the case of simply supported cylinder ends; that is, at the ends of the cylinder, the radial and circumferential displacements are zero, and the force and moment resultants in the axial direction are also zero.

The eccentricity of the stiffeners may be accounted for in the above equations by assuming a sign convention whereby the positive direction is radially inward. Thus, positive values of e_2/R, Eq. (48), and e_1/R, Eq. (47), represent internal rings and stringers, respectively, while negative values of these ratios represent external rings and stringers, respectively.

Equations (41) and (42) above for J_x/t^3 and J_y/t^3, respectively, are based on the assumption that the slenderness ratios for the individual elements comprising the rings and stringers are always greater than one. Note also that an effective width correction factor Y appears in Eqs. (18), (32) and (33). This factor is used to determine the effective cylinder wall acting with each ring in designs having widely spaced rings. It is assumed that the stringer spacing is sufficiently small to result in full effective cylinder wall acting with each stringer. The effective width correction factor Y may be obtained from Figure 4 of Reference A-4, or from a reproduction of this figure appearing with related discussion in Reference A-5. The reader is cautioned to observe differences in notation when obtaining Y from either of the references noted.

The preceding equations contain the quantities n, the number of circumferential waves, and m, the number of axial half-waves. For given values of the remaining quantities appearing in the equations, values of n and m must be found which minimize N_{c1}/RE.

3.2   The Critical Buckling Load

This load is defined as the load at which the stiffened cylinder buckles in the general instability mode. Following the methods presented in References A-1 and A-2, the critical buckling load is equal to the minimum postbuckling load plus a percentage of the difference between the classical buckling load and the minimum postbuckling load. (See Appendix B.) Expressed mathematically:

$$
\left(\frac{N_x}{R E_w}\right)_{cr} = \frac{N_{cl}}{R E_w} \left[\frac{N_{min}}{N_{cl}} + c\left(1 - \frac{N_{min}}{N_{cl}}\right) \right] \tag{50}
$$

The classical buckling load is seen to be attained when the factor c reaches its maximum value of unity; otherwise, the critical buckling load is less than the classical buckling load, unless $N_{min} = N_{cl}$.

It is easily shown that:

$$
c = (\phi - 0.12)/0.88 \tag{51}
$$

When the ratio of the experimental to classical buckling load is termed ϕ, and the ratio of the minimum postbuckling load to the classical buckling load (based on monocoque cylinders) is 0.12. In the present analysis, the following values of ϕ are used:

$$
\phi = 1.0 \text{ when } (R/t)_e \leq 33
$$

$$
\phi = 6.48 (R/t)_e^{-0.54} \text{ when } (R/t)_e > 33 \tag{52}
$$

where

$$
\left(\frac{R}{t}\right)_e = \frac{R}{t} \left[\frac{1}{2} \left(\frac{D_x}{D_f} + \frac{D_y}{D_f}\right) \frac{A_{11}}{A_f} \right]^{-0.5} \tag{53}
$$

$$\frac{A_{11}}{A_f} = \left[1 + \frac{E_x}{E_w} (2K_2 + K_4 + K_6) \right]^{-1} \tag{54}$$

and D_x/D_f and D_y/D_f are as previously defined. These expressions for ϕ are used at LMSC to predict buckling in long, axially compressed monocoque cylinders (L/R > 0.75). They are based on an analysis of the available experimental data for axially compressed, monocoque cylinders, where selected low test results obtained with poor quality specimens were weeded out. They represent the lower bound of the data considered. Their use is necessary here because sufficient test data to develop ϕ equations specifically for stiffened cylinders are not available. Considering those experimental data for stiffened cylinders which are available, Eq. (52) appears to yield conservative values of ϕ .

The ratio N_{min}/N_{cl} in Eq. (50) may be obtained from Reference A-6 in terms of the geometric factors γ , η_s, η_p and α . These factors are defined below. Note that the data of Reference A-6, although developed for orthotropic cylinders, are assumed to be applicable to cylinders with eccentric stiffeners as well.

$$\gamma = \frac{(D_x/D_f) \cdot (A_{11}/A_f)}{(D_y/D_f) \cdot (A_{22}/A_f)} \tag{55}$$

$$\eta_s = \frac{(A_{12}/A_f) + 0.5 (A_{33}/A_f)}{\left[(A_{11}/A_f) \cdot (A_{22}/A_f) \right]^{0.5}} \tag{56}$$

$$\eta_p = \frac{(D_{12}/D_f) + (2D_{33}/D_f)}{\left[(D_x/D_f) \cdot (D_y/D_f) \right]^{0.5}} \tag{57}$$

$$\alpha = \frac{(L_1/R)^2 \, (R/t)}{2\pi^2 m^2 \, (A_{22}/A_f)} \left[\frac{(A_{11}/A_f) \cdot 12(1 - \nu_w^2)}{(D_y/D_f)}\right]^{0.5} \tag{58}$$

where

$$\frac{D_{12}}{D_f} = + \nu_w \tag{59}$$

$$\frac{A_{12}}{A_f} = - \nu_w \, (\frac{A_{11}}{A_f}) \, (\frac{A_{22}}{A_f}) \tag{60}$$

$$\frac{A_{22}}{A_f} = \left[1 + \frac{E_y}{E_w} \, (2C_2 + C_4 + C_6)\right]^{-1} \tag{61}$$

$$\frac{A_{33}}{A_f} = 2(1 + \nu_w) \tag{62}$$

Definitions for the remaining quantities have been presented previously.

Reference A-6 evaluates the ratio N_{min}/N_{cl} for cylinders of both finite and infinite length. In order to classify a particular design with regard to length, set m in Eq. (58) equal to one and find N_{min}/N_{cl} from the minimum postbuckling data for short cylinders in Figure 7 of Reference A-6. Solve Eq. (50) for $(N_x/RE)_{cr}$ using N_{cl}/RE obtained from Eq. (17). Repeat these steps for a value of m slightly greater than one. If the first $(N_x/RE)_{cr}$ obtained is equal to or less than the second, the cylinder may be considered a finite length cylinder in the postbuckling range and the first $(N_x/RE)_{cr}$ represents the critical buckling load. Otherwise, the cylinder may be considered to be of infinite length in the postbuckling range, and N_{min}/N_{cl} should be obtained from either Figure 4 or 5 of Reference A-6. Equation (50) is again used to calculate $(N_x/RE)_{cr}$.

3.3   Panel Instability

The preceding general instability equations may be specialized to apply to panel instability by:(1) setting L_1 in Eqs. (49) and (58) equal to ring spacing, d_y, and (2) setting t_{2a}, t_{2b} and t_{2c} = 0, since the rings do not participate in this buckling mode.

3.4   Overall Instability

For the preceding general instability equations to apply to this type of instability, L_1 in Eqs. (49) and (58) is set equal to cylinder length L. It is assumed that the rings are equally spaced.

3.5   Cylinders With Stringers Only

If no rings are present in the cylinder, the preceding general instability equations apply when: (1) L_1 in Eqs. (49) and (58) is set equal to cylinder length, L, and (2) t_{2a}, t_{2b}, and t_{2c} = 0. Note that the case of cylinders, stiffened with rings only,is not included in the present analysis.

4.0   WEIGHT EQUATION

In previous structural optimization analyses (References A-1 and A-2), the same material has been used throughout the cylinder. This situation enables the notation $\bar{t}$ to be used to denote weight, where $\bar{t}$ represents thickness per unit of wall surface area of an isotropic cylinder which is equivalent to the stiffened cylinder with respect to weight only. It includes both rings and stringers for cylinders designed with both types of stiffeners. The notation $\bar{t}$, of course, represents unit volume, and unit weight can easily be obtained by multiplying unit volume by material density. However, the notation $\bar{t}$ is preferred, since it is easily non-dimensionalized.

In the present analysis, variations in materials may be specified for the cylinder wall, stringers and rings. Thus, weight is expressed:

$$\frac{W_i}{R} = \rho_w \frac{t}{R} + \frac{\rho_x}{\rho_w} \cdot \frac{A_s}{d_x R} + \frac{\rho_y}{\rho_w} \cdot \frac{A_r}{d_y R} \tag{63}$$

where $A_s/d_x R$ is defined by Eq. (12) and

$$\frac{A_r}{d_y R} = (\frac{d_y}{t})^{-1} \left[\frac{a_y}{R} \cdot \frac{t_{2a}}{t_{2b}} \cdot \frac{t_{2b}}{t} + \frac{b_y}{R} \cdot \frac{t_{2b}}{t} + 2 \frac{c_s}{t_{2c}} (\frac{t_{2c}}{t_{2b}} \cdot \frac{t_{2b}}{t})^2 (\frac{R}{t})^{-1} \right] \tag{64}$$

For cylinders stiffened with stringers only, the last quantity within the brackets of Eq. (63) is, of course, zero.

For purposes of comparing existing optimum cylinder design information utilizing the quantity $\bar{t}$ with similar information for cylinders with non-uniform material properties, it is desirable to non-dimensionalize Eq. (63). This can be easily accomplished by dividing the quantity W_i/R by ρ_w. The resulting quantity shall be termed $\bar{\bar{t}}$, in order to distinguish it from $\bar{t}$:

$$\bar{\bar{t}} = \frac{W_i/R}{\rho_w} \tag{65}$$

The combination of Eqs. (63) and (65) is noted to result in the general form of the usual equations for obtaining $\bar{t}$; that is, when $\rho_x = \rho_y = \rho_w$, the resulting $\bar{\bar{t}}$ is identical to $\bar{t}$ obtained for cylinders having the same material throughout.

5.0 MODIFICATIONS REQUIRED FOR ZEE OR CHANNEL STIFFENERS

As noted previously, zee or channel section stiffeners may be obtained by eliminating one of the elements of width c_s found in the J section stiffener (Figure A-1). This procedure has the singular effect of reducing the effectiveness of the stiffener. Note, however, that unlike J section

stiffeners, zee and channel section stiffeners may be formed from sheet, resulting in bend radii of varying magnitude between adjacent elements. The presence of these bend radii will not be considered here.

If the preceding equations are applied to zee or channel stiffened cylinders, the following equations require redefinition:

(1)   Eq. (12):

$$\frac{A_s}{d_x R} = \frac{t}{d_x} \left[\frac{a_x}{R} \cdot \frac{t_{1a}}{t_{1b}} \cdot \frac{t_{1b}}{t} + \frac{b_x}{R} \cdot \frac{t_{1b}}{t} + \frac{c_s}{t_{1c}} \left(\frac{t_{1c}}{t_{1b}} \cdot \frac{t_{1b}}{t} \right)^2 \left(\frac{R}{t} \right)^{-1} \right]$$ (66)

(2)   Eq. (27):

$$K_2 = \frac{0.5 \frac{c_s}{t_{1c}} \cdot K_1^2}{\frac{d_x}{t}}$$ (67)

(3)   Eq. (35):

$$C_2 = \frac{0.5 \frac{c_s}{t_{2c}} \cdot C_1^2}{\frac{d_y}{t}}$$ (68)

(4)   Eq. (64):

$$\frac{A_r}{d_y R} = \left(\frac{d_y}{t} \right)^{-1} \left[\frac{a_y}{R} \cdot \frac{t_{2a}}{t_{2b}} \cdot \frac{t_{2b}}{t} + \frac{b_y}{R} \cdot \frac{t_{2b}}{t} + \frac{c_s}{t_{2c}} \left(\frac{t_{2c}}{t_{2b}} \cdot \frac{t_{2b}}{t} \right)^2 \left(\frac{R}{t} \right)^{-1} \right]$$ (69)

Note that Eqs. (66) and (67) apply to stringers while Eqs. (68) and (69) apply to rings. Zee or channel section stiffeners, therefore, may be specified for either or both applications as desired.

6.0   OPTIMIZATION PROCEDURE

The optimization analysis proceeds in the following manner for cylinders stiffened with both stringers and rings:

(1)   Calculate N_x/RE_w, L/R from given data.

(2)   Affix values to restraints. Indicate type and location of stringers and rings relative to the cylinder wall. Select other options desired and assign numerical values.

(3)   Arbitrarily select a ring spacing-to-cylinder wall thickness ratio, d_y/t.

(4)   Set (t_{1b}/R) and b_x/R equal to some initial values, and calculate d_x/t based on local instability requirements. Check stresses in cylinder wall and stringers against maximum stresses permissible and adjust proportions as needed.

(5)   Find panel instability load and compare with applied load. Adjust b_x/R up or down as needed until equality in these two loads is found. If b_x/R reaches the maximum permitted, reset t_{1b}/R to a higher value and continue calculations. If b_x/R approaches zero, reset t_{1b}/R to a lower value if permissible and continue calculations. Insure stress does not exceed maximum stress.

(6)   Set (t_{2b}/R) and (b_y/R) equal to some initial values. Find overall instability load and compare with applied load. Adjust b_y/R and t_{2b}/R up or down in the same manner as described in step (5) with reference to b_x/R.

(7)   Calculate cylinder weight.

(8)   Repeat steps (4) - (7) with sufficient additional values of d_y/t to define the minimum weight cylinder proportions for the restraints imposed:

Note that the ratio R/t need not be considered a restraint; by repeating the above procedure for several R/t ratios, that ratio resulting in minimum cylinder weight may be determined.

As the optimization analysis progresses, two checks on d_x are made:

(I)   Check to see if $a_x > d_x$. If so, interference exists between adjacent stringer attach-flanges. Correct by reducing a_x, if possible, and/ or decreasing R/t.

(II)   Check to see if $2 \cdot c_s > d_x$ for "J" stringers or $c_s > d_x$ for "Z" (or channel) stringers. If so, interference exists between adjacent stringer outstanding flanges. This may be corrected by decreasing R/t and/or t_{1c}/t_{1b}.

REFERENCES FOR APPENDIX A

A-L.   Lockheed Missiles & Space Company, Evaluation of the Effects of Ring/Stringer Eccentricity upon the Structural Optimization of Axially Compressed Cylinders Stiffened with Rings and/or Stringers of Rectangular Cross-Section, by A. Bruce Burns, LMSC Report 6-65-65-11, Palo Alto, Calif., April 1965.

A-2.   Lockheed Missiles & Space Company, Structural Optimization of Axially Compressed Cylinders Stiffened with Corrugations and Rings, Including the Effects of Corrugation/Ring Eccentricity, by A. Bruce Burns, LMSC Report 6-65-65-12, Palo Alto, Calif., May 1965.

A-3.   Lockheed Missiles & Space Company, Structural Optimization of Foam-Core and Honeycomb-Core Sandwich Cylinders under Axial Compression, by A. Bruce Burns, LMSC Report 6-62-64-17, Palo Alto, Calif., December 1964.

A-4.   Bruno Thürlimann and Bruce G. Johnston, "Analysis and Tests of a Cylindrical Shell Roof Model," ASCE Transactions, Paper 2757, 1955, pp. 615-643.

A-5.   Lockheed Missiles & Space Company, Structural Optimization of Axially Compressed Cylinders Stiffened Externally with Rings and/or Stringers of Rectangular Cross Section, by A. Bruce Burns, LMSC Report 6-62-64-7, Palo Alto, Calif., May 1964.

A-6.   Lockheed Missiles & Space Company, Buckling of Orthotropic Cylinders under Axial Compression, by B. O. Almroth, LMSC Report 6-90-63-65, Palo Alto, Calif., June 1963.

A-7.   Lockheed Missiles & Space Company, Structural Optimization of Axially Compressed Cylinders Reinforced with Conventional, Flanged Stiffeners, by A. B. Burns, LMSC M-99-65-1, September 1965.

REFERENCES FOR APPENDIX A

A-1. Lockheed Missiles & Space Company, Evaluation of the Effects of Ring/Stringer Eccentricity upon the Structural Optimization of Axially Compressed Cylinders Stiffened with Rings and/or Stringers of Rectangular Cross-Section, by A. Bruce Burns, LMSC Report 6-65-65-11, Palo Alto, Calif., April 1965.

A-2. Lockheed Missiles & Space Company, Structural Optimization of Axially Compressed Cylinders Stiffened with Corrugations and Rings, Including the Effects of Corrugation/Ring Eccentricity, by A. Bruce Burns, LMSC Report 6-65-65-12, Palo Alto, Calif., May 1965.

A-3. Lockheed Missiles & Space Company, Structural Optimization of Foam-Core and Honeycomb-Core Sandwich Cylinders under Axial Compression, by A. Bruce Burns, LMSC Report 6-62-64-17, Palo Alto, Calif., December 1964.

A-4. Bruno Thürlimann and Bruce G. Johnston, "Analysis and Tests of a Cylindrical Shell Roof Model," ASCE Transactions, Paper 2757, 1955, pp. 615-643.

A-5. Lockheed Missiles & Space Company, Structural Optimization of Axially Compressed Cylinders Stiffened Externally with Rings and/or Stringers of Rectangular Cross Section, by A. Bruce Burns, LMSC Report 6-62-64-7, Palo Alto, Calif., May 1964.

A-6. Lockheed Missiles & Space Company, Buckling of Orthotropic Cylinders under Axial Compression, by B. O. Almroth, LMSC Report 6-90-63-65, Palo Alto, Calif., June 1963.

A-7. Lockheed Missiles & Space Company, Structural Optimization of Axially Compressed Cylinders Reinforced with Conventional, Flanged Stiffeners, by A. B. Burns, LMSC M-99-65-1, September 1965.

APPENDIX B

GENERAL INSTABILITY METHODS

APPENDIX B

GENERAL INSTABILITY METHODS

The classical buckling load is an upper bound for the critical load of an axially compressed cylindrical shell. For the monocoque cylinder, the classical buckling stress is expressed by the well-known equation $\sigma_{CR} = 0.6\ E \cdot t/R$, but test specimens generally fail at a stress which is only a fraction of this prediction. Classical theory solutions exist also for stiffened or orthotropic shells but in view of the behavior of the monocoque shell it is questionable whether these are applicable in practical analysis.

For ring-stringer stiffened cylinders it has commonly been assumed that in order to avoid buckling between rings (i.e., panel buckling) we can allow only the wide column load. The wide column load is based on the assumption that the individual axial fibers can buckle independently of one another. When the wide-column approach is used, the rings often are sized by use of the so-called Shanley approach, which attempts to make the general instability load equal to the panel buckling load. This is done by use of experience from available test results, which unfortunately are too sparse. However the wide column load is an extremely conservative estimate of the panel buckling load and the use of Shanley's approach tends to make the shell equally overdesigned with respect to general instability.

Considerable weight saving can be achieved by use of a more realistic but still conservative method of analysis. Such a method was suggested in a Lockheed report in June 1963* and will be referred to here as the Lockheed Method. For a vehicle such as RIFT the method saves about 10,000 pounds in comparison with a structure based on the wide column approach with Shanley rings.

---

*"Buckling of Orthotropic Cylinders under Axial Compression," by B. O. Almroth, Lockheed Report 6-90-63-65, June 1963.

This disparity clearly demonstrates that the quality of a structural optimization/design study depends primarily on the methods used to predict the critical loads of the shell. The Lockheed Method, although still conservative, is believed to be the best available method and has therefore been used in the computer programs. A short description of this method follows.

The classical buckling load can be found from the linear differential equations of equilibrium. By solution of the nonlinear equations we can also study the shell behavior in the postbuckling range. A load displacement curve in the postbuckling range is shown in Fig. B-1 and it can be seen that stable buckled equilibrium configurations exist at loads considerably below the classical buckling load. This makes the shell extremely sensitive to disturbances such as initial deviations from the perfect geometry, and explains why the classical theory, which is so useful for columns and flat plates, provides only an upper bound to the buckling load for thin shells.

In a study of postbuckling behavior we can determine the lowest load under which a buckled configuration can be maintained, and this load, of course, is a lower bound to the critical load of the shell. For the monocoque shell this lower bound is only one-tenth of the upper bound. All available test results do fall within these two bounds. Due to the fact that thicker cylinders are less sensitive to disturbances, test results tend towards the upper bound at low values of R/t and towards the lower bound for large R/t values. We notice that the designer does not use the lower bound as a limit for monocoque shells, but takes advantage of the reduced sensitivity for thicker shells.

Consequently if the designer uses the wide column load as a design limit for stiffened shells he is somewhat inconsistent, and the conservatism involved is augmented by the fact that such cylinders, due to the stiffening, generally are reasonably thick and also because the wide column load is not the greatest lower bound.

LOAD

N_{cl}

PREBUCKLING

POSTBUCKLING

END SHORTENING

———————— STABLE EQUILIBRIUM

— — — — UNSTABLE EQUILIBRIUM
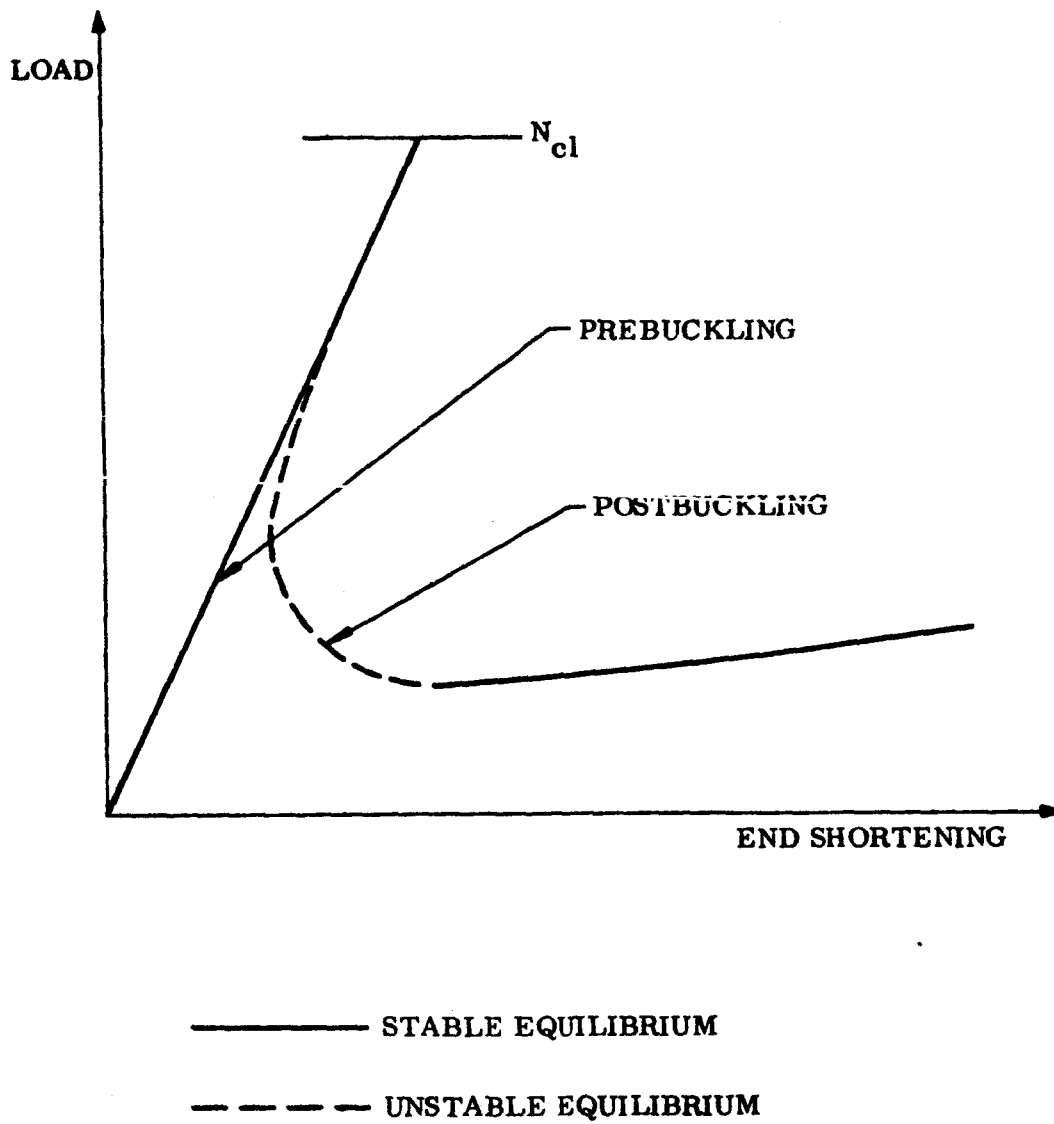
Fig. B-1 - Postbuckling Behavior of Axially Loaded Shell

A basically sound method of practical analysis was suggested by Peterson and Dow at Langley in 1959[*]. The wide column load was recognized as a lower bound to the buckling load. A reduction factor was applied to the difference between upper and lower bounds, i. e. , to the so-called "curvature effect." Due to lack of test data for stiffened shells, Peterson and Dow had to assume an expression for the effective radius-to-thickness ratio for stiffened shells and, in the establishment of the reduction factor, to take advantage of the wealth of test data for monocoque shells.

A lower bound analysis was presented in the before-mentioned Lockheed report. The trends of the results of that analysis are illustrated in Fig. B-2. The analysis is applicable to infinitely long shells. For such shells only the ring-stiffened cylinders deviate appreciably from the monoque in postbuckling behavior.

Figure B-2(a) shows the relation between load and end-shortening for such shells in the postbuckling range. The minimum point on the curve represents the lower bound. This bound is shown in relation to the upper bound in Fig. B-2(b). We notice that the two bounds approach one another with increasing ring stiffness. Also it has been shown, by Gerard[**], that ring-stiffened cylinders buckle at loads close to the classical buckling load.

Another type of shell for which there appears to be agreement between test and theory is short to moderately long stringer-stiffened cylinders. An accurate lower bound analysis for such shells appears to be virtually impossible, but an approximate and conservative estimate can easily be obtained. The only restraint imposed is that the axial half-wave length be not larger than the length of the shell. The behavior of such shells is illustrated in Fig. B-3. It may be seen from Fig. B-3(a) that, as the shell length decreases, the behavior becomes more like that of a flat plate. The upper and lower bounds are shown in Fig. B-3(b). We observe that, for fixed stringer stiffness, the bounds approach one another with decreasing shell length to a point where they actually coincide.

---

[*] "Compression Tests on Circular Cylinders Stiffened Longitudinally by Closely Spaced Z-Section Stringers," by J. P. Peterson and M. B. Dow, NASA Memo 2-12-59L, 1959.

[**] "Experiments on Axial Compressive General Instability of Monolithic Circumferentially Stiffened Circular Cylindrical Shells," New York University Tech. Report SM-62-5, May 1962.
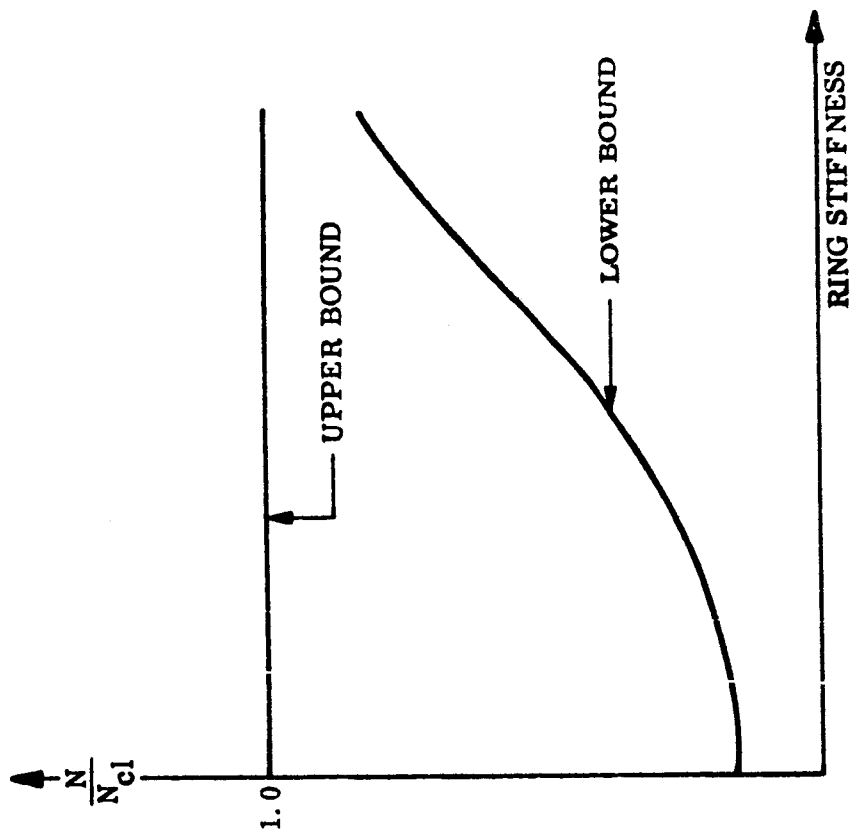
a) POSTBUCKLING EQUILIBRIUM
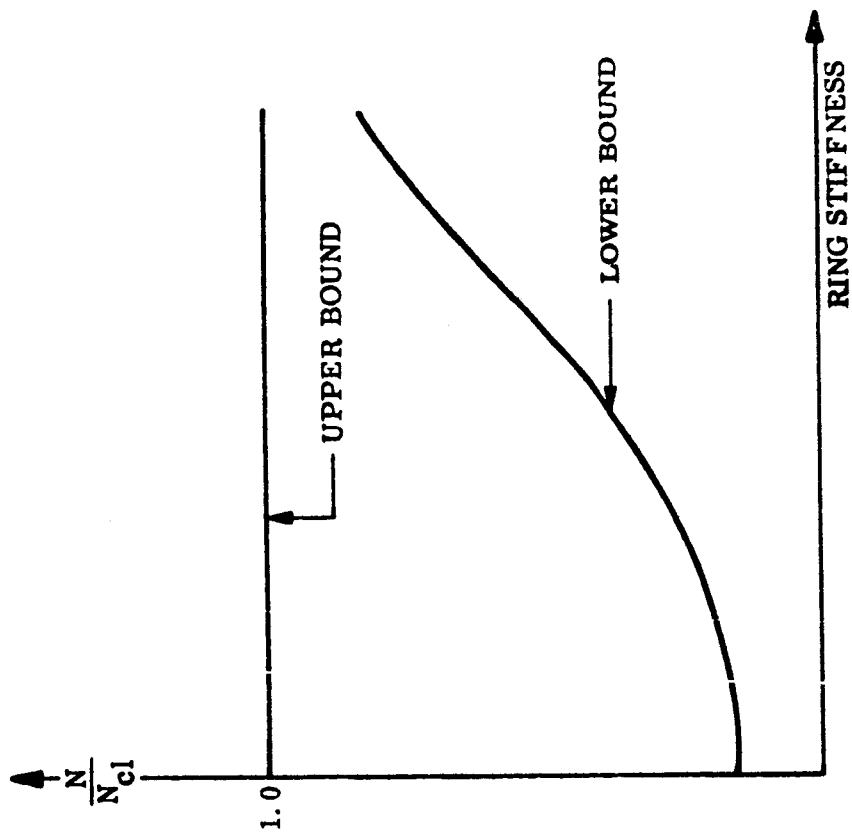
b) BUCKLING-LOAD BOUNDS

Fig. B-2 - Ring-Stiffened Cylinders
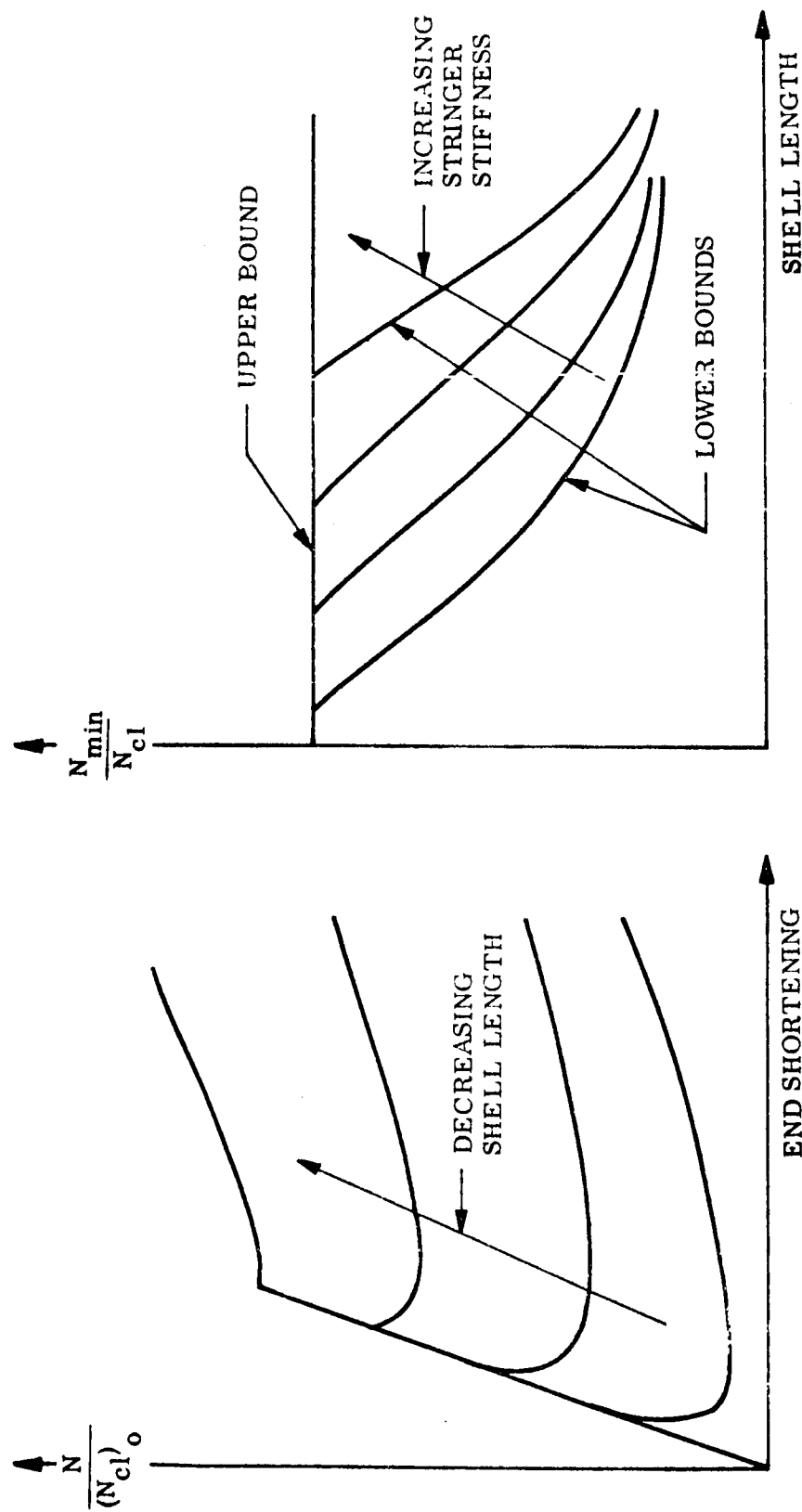
(a) POSTBUCKLING EQUILIBRIUM

(b) BUCKLING-LOAD BOUNDS

Notation

$(N_{CL})_o$	=	critical load of monocoque cylinder according to classical theory
N_{MIN}	=	minimum postbuckling load
N_{CL}	=	critical load according to classical theory

Fig. B-3 - Stringer-Stiffened Cylinders

For even shorter shells the classical buckling load should be applicable as a design limit. It must be emphasized that these curves represent a conservative estimate of the lower bound, and that if we were able to take the boundary conditions properly into account the curves would move to the right.

When a postbuckling analysis is available, the Peterson-Dow method can be improved in an obvious way. As a lower bound the minimum postbuckling load is substituted for the wide column load. The method will then be less conservative for many stringer-stiffened shells, as this lower bound usually is considerably above the wide column load; and moreover the usefulness of the method will not be restricted to this type of shell but can be applied also to determine ring sizes, and hence we can dispense with the Shanley method. The method of analysis is illustrated in Fig. B-4. As in the Peterson-Dow analysis, the reduction factor is applied to the difference between upper and lower bounds such that the reduced buckling load always will stay between these two bounds. The experience from tests of monocoque shells is used to establish the reduction factor.

Later work in the field at LMSC includes extension of the method discussed here to shells of sandwich construction[*]. This has been achieved through inclusion of effects of transverse shear deformations in the analyses of the upper and lower bounds to the critical load.

Other topics which have been studied are the effects of stiffener eccentricity and of edge restraint. In 1947, van der Neut's[**] theoretical analysis indicated that the critical load would change drastically if eccentricities of stiffeners with respect to the midsurface of the skin were considered. In recent tests at LMSC[***] and at Langley this surprisingly large effect of stiffener eccen-

---

[*]   "Buckling of Axially Compressed Sandwich Cylinders," by B. O. Almroth, Lockheed Report 6-62-64-9, July 1964.

[**]   "The General Instability of Stiffened Shells under Axial Compression," by A. van der Neut, Nationaal Luchtvaartlaboratorium Rept S 314 and Transactions, XIII, 1947.

[***] "Theoretical and Experimental Analysis of Orthotropic-Shell Theory," Lockheed Report LMSC-A701014 for Contract NAS8-9500, September 1964.

a) MONOCOQUE SHELLS

$\dfrac{N}{N_{cl}}$

END SHORTENING

$N_l = 0.1 \cdot N_{cl}$

N_u

N_{cr}

b) STIFFENED SHELLS

$\dfrac{N}{N_{cl}}$

END SHORTENING

$C = C(R/t) = \dfrac{N_{cr} - N_l}{N_u - N_l}$

N_u

N_{cr}

N_l
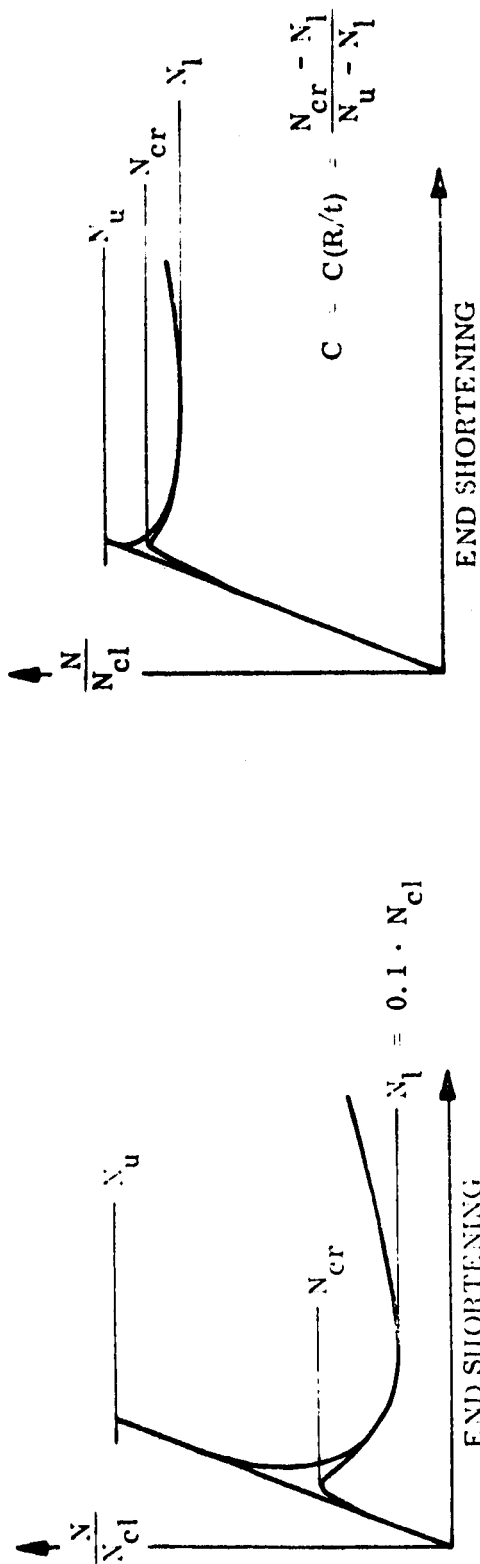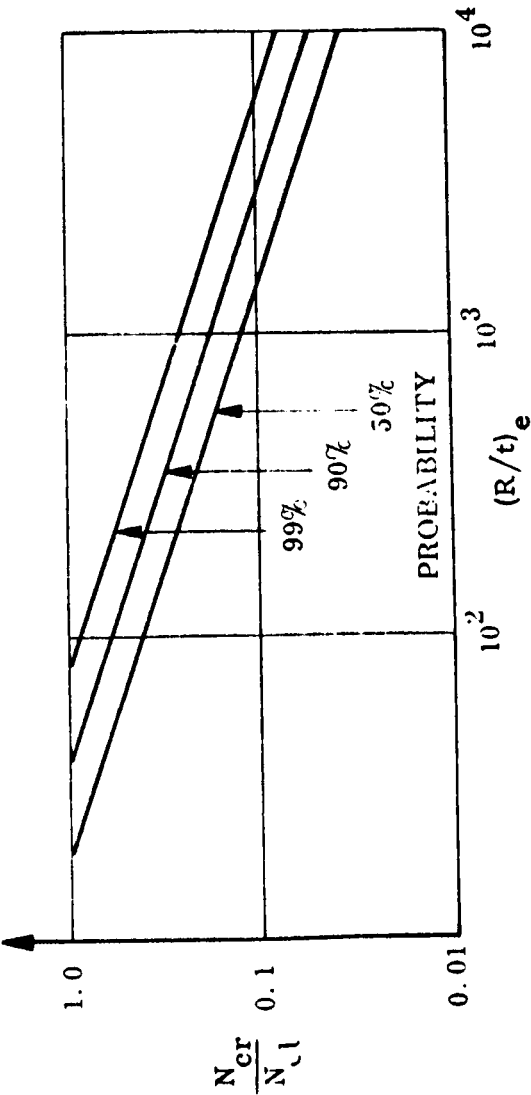
Notation

N	=	axial load per unit width
N_{cr}	=	critical load per unit width
N_u	=	upper bound to critical load
N_l	=	lower bound to critical load
N_{cl}	=	critical load according to classical theory
C	=	reduction factor
R	=	cylinder radius
t	=	skin thickness

c) BUCKLING OF MONOCOQUE SHELLS

$\dfrac{N_{cr}}{N_{cl}}$

1.0

0.1

0.01

10^2 10^3 10^4

$(R/t)_e$

PROBABILITY

99%

90%

50%

Fig. B-4 - Practical Method of Analysis

tricity was experimentally verified. Consequently it appears necessary to include this effect in stiffened shell analysis.

The effects of edge fixity are presently being investigated. The few numerical results so far obtained indicate that it may be necessary to modify the common assumption that the edge-fixity factor should be applied only to the wide column load part of the critical load.

It is readily admitted that the analysis method discussed here needs to be supported or eventually modified by an extensive experimental analysis. The experimental results now available, including those by Gerard for ring-stiffened cylinders, by Peterson and Dow for stringer-stiffened cylinders, by March and Kuenzi[*] for plywood cylinders, and by L. Katz, NASA/MSFC for ring-stringer stiffened cylinders (TM X 54-315) are in reasonable agreement with predictions but do not adequately cover the parameter ranges.

Of course, it would be more satisfactory if a purely theoretical method could be derived, which could be verified by very few experimental results. It should be kept in mind, however, that for the simple special case of a monocoque cylinder, the buckling problem is still largely unsolved, in spite of the fact that a tremendous effort has been devoted to it — with contributions from several outstanding investigators such as von Karman, Koiter, Donnell, and Hoff. A complete understanding of this problem will eventually be attained and the way will be opened for further progress in the field of stiffened shell analysis. However, as more than 20 years have gone by since von Karman's "breakthrough," it seems unrealistic to expect such a development very soon. Hence practical methods of analysis have been developed in the interim which are adaptable to state-of-the-art improvements.

---

[*] "Buckling of Cylinders of Sandwich Construction in Axial Compression," by H. W. March and E. W. Kuenzi, FPL Report 1830, December 1957.

APPENDIX C

COST-PRODUCIBILITY STUDY

APPENDIX C

COST-PRODUCIBILITY STUDY*

New techniques for creating large light-weight space vehicles with high structural integrity, and the technology needed to use these materials efficiently with high reliability, must be developed. The feasibility of using beryllium-aluminum alloys (Be-38% Aℓ) and unalloyed beryllium to meet these requirements is considered from a cost and manufacturing standpoint in this study.

INTRODUCTION

This cost effectiveness and design/manufacturing feasiblity evaluation was made on optimized configurations of light-weight materials for Saturn-type vehicles. The cost effectiveness comparison of several design approaches, using various combinations of aluminum, unalloyed and alloyed beryllium is covered. Also, this study endeavors to bring out the development requirements needed for design and manufacturing.

ASSUMPTIONS

The configurations used for cost analysis conform closely to the minimum-weight designs from the structural optimization phase. The cost effectiveness portion of the study ran concurrent with the weight-saving design studies, requiring preliminary estimates of some configurations.

The cost parameters are based on a detail design program originating 30 months downstream, allowing for an orderly development in both manufacturing costs and raw material cost. In both cases, sponsored development programs are required to approach the cost figures used.

All cost analyses are comparative because many fixed costs items such as overhead, planning, design, orderwriting, liaison, storage, etc., were not considered. These costs would be about equal in all cases.

Joining methods used, in general, were rivets. Considerable weight saving would be available in the beryllium-aluminum alloy configurations by spot-bonding stringers to the basic skin. Even in the short (36 inch) interstages considered, about five pounds (5%) of the structural weight could be reduced by spot welding.

The material prices were based on estimates by the Beryllium Corporation, Hazelton, Pennsylvania subject to a yearly market of 10,000 pounds and a funded development program leading the material procurement by 12 to 24 months.

---

*Based on a Lockheed report (LMSC 65-212) by G. R. Clemens, Dept. 55-53, October 1965.

The configuration parameters were:

Diameter	260 inches
Length	36 inches
End Rings	None
Intermediate Rings	One Maximum

SUMMARY OF RESULTS

Table I summarizes the results of each configuration, based on ten units total to be manufactured. The costs shown may seem low, but this is due to the simplified comparison method chosen and described earlier.

Of particular interest is the $13,000 figure for both the integrally milled aluminum (Configuration I) as well as the aluminum skin stiffened with aluminum stringers and rings of conventionally flanged Z sections (Configuration VI). With the exception of the corrugated core aluminum ($4,680) all the other cost figures fall in a close band between $40,000 and $51,000.

INTEGRALLY STIFFENED SKIN, CONFIGURATION I

This configuration of integrally stiffened skin is machined from one inch 2219 aluminum plate stock. The circumference is divided into eight skins which are assembled by welding, representing present "state-of-the-art."

The skins are machined by numerical control equipment. Plate stock is held down on machine tool by vacuum chuck. Raw stock size is 1" x 37" x 104".

This design configuration with a circumferential ring cutting through the transverse stiffeners in the middle of the panel makes more costly machining than if stiffeners were machined through and the ring added to the opposite side. However, the cost of the raw stock will double and no cost advantage will be realized.

TRAPEZOIDAL CORE, CONFIGURATION II

This configuration is made from 7075 aluminum sheet stock. The trapezoidal core section may be formed with a forming roll (roll cylinders resembling gear teeth) or a form die. Formed sections may be spot welded or riveted to face sheets. Face sheets with core sections attached should

be overlapped .70 inch at splice joints and riveted. This method is within present "state-of-the-art."

The following material is required:

1.　8 face sheets .040" x 36" x 96" 7075 Aℓ

　　1 face sheet　.040" x 36" x 54" 7075 Aℓ

2.　17 (formed trapezoidal core sheets) .018 x 36 x 96　7075 Aℓ

　　1 (formed trapezoidal core sheet)　.018 x 36 x 11.5　7075 Aℓ

There are 428 formed trapezoidal sections.

Alloyed Beryllium (Be-38% Aℓ) and Unalloyed Beryllium

The fabrication of parts and assemblies from unalloyed Beryllium or Be-38% Aℓ requires some special considerations. Beryllium rolled sheet, or plate, physical and mechanical properties are not compatible with normal "state-of-the-art" fabrication methods. The Beryllium rolled product is anisotropic; i.e., it has preferred crystal orientation and mechanical properties. The best properties are in the plane of the material, generally the longitudinal direction; the short transverse properties are the poorest.

Be-38% Aℓ is essentially isotropic in the sheet form, showing slight anisotropy at -320°F. This is brought out in elongation test specimens when tested at room temperature. Be-38% Aℓ specimens showed 50% of their reduction in area occurred in the thickness direction; whereas in unalloyed Beryllium specimens, no thinning occured in the thickness direction.

Shapes

The technology of extruding Be-38% Aℓ shapes other than bar and tube has not been fully developed. A limited amount of development work has been done with beryllium extrusions. LMSC had three Beryllium shapes under development at Nuclear Metals; however, only short sections were produced. A production capability for miscellaneous types of shapes has not been developed. Therefore, if either alloyed or unalloyed Beryllium shapes of the type used in this study are to be made by the extrusion process on a production basis, a development program must be initiated.

There are other methods for producing shapes. One method is forming sheet metal. The "Z" section could be made this way. Another method joins strip stock together by welding or diffusion bonding. Manufacturing shapes by using strip stock and diffusion bonding is feasible but would require considerable development.

Manufacturing shapes from strip stock welded together is a method that should be considered. It should be noted, however, that the weldability of alloyed (Be-38% Aℓ) beryllium shows considerably more promise than

unalloyed beryllium. While this method of welding strip stock to make shapes is still in the research stage, the tube industry has been making millions of feet of tubing yearly by this process in other metals. This tube making technology need only be altered to accept different shapes and different weldable materials. When this is accomplished, the result may be a less costly, closer tolerance shape than is possible by the extrusion method. Also, shapes that cannot be formed may be produced by this method.

Forming

Beryllium is usually formed by the creep method at temperatures from 1200° to 1400°F. Due to the low short transverse ductility, the un-alloyed beryllium configuration used in this study would probably have to be creep formed; making it necessary to have special heating and forming equipment for face sheets as well as rings and stringers. Alloyed beryl-lium face sheet may be formed at room temperature on simple roll equip-ment.

Both alloyed and unalloyed beryllium stringers and rings, when made by forming from sheets, must be hot-creep formed. Alloyed beryllium (Be-38% Aℓ) is formed at a lower temperature than unalloyed beryllium. Form-ing of beryllium to a 6T radius is "state-of-the-art". Development in form-ing methods are needed in order to obtain 2T bends consistently in both alloyed and unalloyed material. Bends as low as 2T have been made in the laboratory in both materials.

Drilling

Drilling holes in rolled unalloyed beryllium sheet for bolt or rivet installations presents a serious problem. The anisotropic structure of this material makes it susceptible to spalling, cracking, and delamination. Ex-perience has established that beryllium must be processed carefully during and after forming and machining operations. Proper control of forming and hole producing operations limits the surface damage in the area to .001 to .003 inch deep. Then, to keep these minute surface cracks and delamina-tions from propagating into large cracks, it is necessary to stress relieve fabricated beryllium parts. The stress relieving is then followed by a chem-etching operation which removes the surface damage. The importance of overcoming this problem is apparent when one realizes that there are some 21,752 holes for fasteners in the short 36-inch structure under con-sideration.

Lockheed has developed equipment and processes for production manufacturing of a beryllium interstage on the Agena upper-stage booster. These are skins and doors that may be taken to a sensitive drilling machine, a electrical discharge hole producing machine or other specialized equip-ment. When drilling beryllium on the sensitive drilling machine, specially developed burr-type drill bits and tornetic controls are used. Each type of equipment has been developed so that satisfactory parts may be repeatedly reproduced. However, on large assemblies it may not be practical to produce final attachment holes with fixed equipment. This means that special portable

equipment that could be taken to the work would have to be developed. Stress relieving and chem-etching problems would require solution.

Manufacturing problems are much less severe when alloyed beryllium (Be-38% Aℓ) structures are considered. Alloyed beryllium components can be drilled and fastened using aluminum technology. Thus, the distinct advantage alloyed beryllium has over unalloyed beryllium is that large contours may be formed at room temperature and parts may be drilled without any subsequent processing and with "state-of-the art" methods.

TABLE I

COST SUMMARY

Configuration	Description	Stringers	Rings	Cost Each (lots of 10) dollars
I	Rectangular rings and stringers, integrally milled 2219 Aluminum, t_{wall} = .030	0.808 high .054 thick, spaced 1.30	One only, 0.77 high 0.246 thick	13,231
IIA	Single-face sheet, trapezoidal core 7075 Aluminum, t_{wall} = 0.040	θ = 80 deg, 0.85 high t_c = 0.0185	No ring	4,680
IIB	Single-face sheet, trapezoidal core, Be-38 Aℓ Alloy, t_{wall} = .030	θ = 74 deg. 0.68 high t_c = .012	No ring	51,100
IIIA	Conventional flanged stringers & rings, Aluminum skin, t = .025 Be-38 Aℓ stringers	Be-38 Aℓ "J" stringer t_{1b} = 0.025 height b_x = .74, spacing = 1.43	No ring	41,235
IIIB	Conventional flanged stringers & rings Aluminum skin, t = .025 Be-38 Aℓ stringers	Be-38Aℓ "J" stringers t_{1b} = .025 height b_x = .74, spacing = 1.43	Be-38 Aℓ "J" ring t_{2_b} = .025 height b_x = 1.14	43,601
IV	Conventional flanged stringers & rings Aluminum skin, t = .030 Be-38 Aℓ stringers	Be-38 Aℓ "Z" stringers t_{1b} = .025 height b_x = .82 spacing = 1.51	Be-38 Aℓ "Z" ring $t2_b$ = .025 height b_x = 1.14	40,336

TABLE I

COST SUMMARY (Continued)

Configuration	Description	Stringers	Rings	Cost Each (lots of 10) dollars
V A	Conventional flanged Be-38 Aℓ Alloy stringers & rings Be-38 Aℓ skin t = .020	"Z" Be-Aℓ t = .020 height = .75 spacing = 1.6	"Z" Be-Aℓ t = .020 height = 1.02	44,800
V B	Conventional flanged Be-38 Aℓ Alloy stringers & rings Be-38 Aℓ skin t = .025	"Z" Be-Aℓ t = .025 height = .75 spacing = 1.6	"Z" Be-Aℓ t = .025 height = 1.02	46,450
V C	Conventional flanged Be-38 Aℓ Alloy stringers & rings Be-38 Aℓ skin t = .030	"Z" Be-Aℓ t = .030 height = .75 spacing = 1.6	"Z" Be-Aℓ t = .030 height = 1.02	48,300
VI	Aluminum skin. t = .030 Conventional flanged Alum stringers & rings	"Z" Alum t = .025 height = 1.0 spacing = 1.35	"Z" Alum t = .040 height = 1.6	13,200
VII	Be skin t = .020 Conventional flanged Be stringers and rings	Be "Z" t = .015 height = .78 spacing = 1.31	Be "Z" t = .015 height = 1.5	52,140

ALUMINUM INTEGRALLY STIFFENED SKIN
CONFIGURATION I
2219 ALUMINUM

Lot Run Units	Cost of One Unit					
	Material	Handling	Tooling	Mfg. Setup & Run	Total	
1	3,500	400	15,150	8,340	27,390	
10	3,500	200	1,515	8,016	13,231	
50	3,500	175	303	7,987	11,965	
100	3,500	170	151	7,900	11,721	

TRAPEZOIDAL CORE
CONFIGURATION II A
ALUMINUM

Lot Run Units	Cost of One Unit				
	Material	Handling	Tooling	Mfg. Setup & Run	Total
1	250	300	14,200	3250	18,000
10	250	120	1,420	2890	4,680
50	250	104	234	2858	3,456
100	250	102	142	2854	3,348

Be-38% Aℓ - TRAPEZOIDAL CORE & FACE SKINS
CONFIGURATION II B

Lot Run Units		Cost of One Unit				
		Material	Handling	Tooling	Mfg. Setup & Run	Total
1	Skins 66.5 lb x 200 Core 54.2 lb x 257 Ring 1.77 lb x 280	13,300 13,930 495 27,725	2,322	16,200	21,960	68,207
10		27,725	522	1,620	21,240	51,107
50		27,725	362	324	21,176	49,587
100		27,725	342	162	21,168	49,397

J STIFFENERS
CONFIGURATION III A
ALUMINUM SKIN, Be-38% Al STIFFENERS

Lot Run		Cost of One Unit				
Units		Material	Handling	Tooling	Mfg. Setup & Run	Total
1	Al Skin Be-38% Al 75.2 lb x 225 No Ring	815 16,920 ‾‾‾‾‾‾ 17,735	50 1,500 600 ‾‾‾‾‾ 2,150	19,000	21,160	60,045
10		17,735	800	1,900	20,800	41,235
50		17,735	680	380	20,768	39,563
100		17,735	665	190	20,080	38,670

J STIFFENERS
CONFIGURATION III B
ALUMINUM SKIN, Be-38% Al RINGS AND STRINGERS

Lot Run	Cost of One Unit				
Units	Material	Handling	Tooling	Mfg. Setup & Run	Total
1	Al Skin 816 (Be-38% Al) 75.2 lb x 225 16,920 Ring 495 ——— 18,231	2,680	23,300	22,880	67,091
10	18,231	880	2,330	22,160	43,601
50	18,231	720	466	22,096	41,513
100	18,231	700	233	22,088	41,252

Z STIFFENERS
CONFIGURATION IV
ALUMINUM SKIN, Be-38% Al RINGS AND STRINGERS

Lot Run (Units)	Cost of One Unit				
	Material	Handling	Tooling	Mfg. Setup & Run	Total
1	Al Skin 995 Be-38% Al Str. 79.2 lb x 225 17,820 Be-38% Al Ring 3.37 lb x 225 758 19,573	2,613	17,000	18,970	58,156
10	19,573	813	1,700	18,250	40,336
50	19,573	653	340	18,186	38,752
100	19,573	633	170	18,178	38,554

Be-38% Aℓ/Z STIFFENERS-AND SKIN
CONFIGURATION V A
.020 INCH THICKNESS

Be-38% Aℓ Stringers and Skin
.020 Inch Thickness

Lot Run Units	Cost of One Unit				
	Material	Handling	Tooling	Mfg. Setup & Run	Total
1	Face Sheet 44.4 lb 11,966 Stringers 46.2 lb 12,374 Ring 2.47 lb 635 —— 24,975	2,583	17,000	18,070	62,628
10	24,975	783	1,700	17,350	44,808
50	24,975	623	340	17,286	43,224
100	24,975	603	170	17,278	43,026

Be-38% Aℓ/Z STIFFENERS-AND SKIN
CONFIGURATION V B
.025 INCH THICKNESS

Lot Run		Cost of One Unit				
Units		Material	Handling	Tooling	Mfg. Setup & Run	Total
1	Face Sheet 56.6 lb x 225	12,510				
	Stringers 59.6 lb x 225	13,410				
	Ring 3.1 lb x 225	698				
		26,618	2,583	17,000	18,070	64,271
10		26,618	783	1,700	17,350	46,451
50		26,618	623	340	17,286	44,867
100		26,618	603	170	17,278	44,669

Be-38% Aℓ/Z STIFFENERS AND SKIN
CONFIGURATION V C
.030 INCH THICKNESS

Lot Run	Material		Handling	Tooling	Mfg. Setup & Run	Total
		Cost of One Unit				
Units						
1	Face Skin 66.6 lb x 200	13,320				
	Stringers 71.5 lb x 200	14,400				
	Ring 3.65 lb x 200	730				
		28,450	2,583	17,000	18,070	66,103
10		28,450	783	1,700	17,350	48,283
50		28,450	623	340	17,286	46,699
100		28,450	603	170	17,278	46,501

7075 ALUMINUM SKINS AND Z STIFFENERS
CONFIGURATION VI

Lot Run		Cost of One Unit				
Units		Material	Handling	Tooling	Mfg. Setup & Run	Total
1	Skin Stringers Ring	995 7,260 272 8,527	677	14,400	3,360	26,964
10		8,527	600	1,440	2,640	13,207
50		8,527	550	288	2,576	11,941
100		8,527	500	144	2,568	11,739

UNALLOYED BERYLLIUM SKIN AND Z STIFFENERS
CONFIGURATION VII

Lot Run			Cost of One Unit					
Units			Material	Handling	Tooling	Mfg. Setup & Run	Total
1	Skin 39.8 lb x 340		13,520				
	Stringers 40.0 lb x 340		13,600				
	Ring 1.6 lb x 340		544				
			27,665	2,696	17,000	32,680	80,441
10			27,665	896	1,700	21,880	52,141
50			27,665	736	340	20,920	49,661
100			27,665	716	170	20,800	49,351

APPENDIX D

A MECHANICAL PROPERTY EVALUATION OF
Be-38% Aℓ ALLOY FROM -320° TO 800° F

APPENDIX D

A MECHANICAL PROPERTY EVALUATION OF
Be-38% Al ALLOY FROM -320° TO 800° F*

By: R. W. Fenn, Jr., D. D. Crooks, G. H. Watts,
and A. S. Neiman, Lockheed Palo-Alto Research
Laboratories

SUMMARY

Detailed studies were made on six heats of commercially produced Be-38% Al (by wt.) alloy in the annealed temper to determine the level and reproducibility of the mechanical properties, microstructural features, and general metallurgical quality of the material. Young's Modulus, tensile, compressive, shear, bearing, and bend properties were determined at temperatures between -320° and 800°F. Tensile properties at 75°F were found to be unaffected by exposure at temperatures up to 800°F for times up to 1000 hr. Sheet properties were consistently isotropic, while the extrusion properties displayed some anisotropy.

Reproducibility of properties from heat to heat was investigated by statistical analysis; variations were found to be equal to or less than those reported for several commercial alloys in current use in aerospace vehicles.

The substantial decrease in strength in the 400°F temperature region, normally associated with aluminum alloys, was not observed for the Be-38% Al alloy. Over 50% of the room temperature tensile properties was retained at 800°F.

INTRODUCTION

In April 1964, Lockheed Missiles & Space Company (LMSC) disclosed work (1) on the beryllium-aluminum system designed to develop an alloy for aerospace applications. Although beryllium is theoretically very efficient for compressively loaded structures, certain undesirable characteristics — i. e., brittleness, low bend ductility, sensitivity to surface damage and defects, chemical etching requirements following working, poor weldability and high manufacturing costs – have retarded its acceptance. Alloying beryllium with aluminum alleviates or eliminates these undesirable characteristics while retaining the desirable ones – i. e., high Young's modulus ($\sim$29 x 10^6 psi) and low density (0.075 lb/in.^{3}) for the Be-38% Al composition. Bend ductilities at room temperature are four to five times that of unalloyed beryllium; sensitivity to surface damage is reduced, comparable to other conventionally used metals; no chemical etching is required following machining operations; weldability is good; and reduced manufacturing costs result from excellent machinability, punching and shearing characteristics, forming at low temperatures commonly used for magnesium alloys, and elimination of the chemical etching and controlled-torque-drilling requirements.

Most of the published data (1-7) refer to developmental rather than commercial alloys. Fenn et al. have described mechanical and physical properties; shop and service characteristics; a structural efficiency study and calculated effects of various types of radiation (1, 2); mechanical properties at elevated temperatures (3); and elevated-temperature data, stress-strain curves, and fatigue and strain rate data primarily on developmental material (4). Short reviews of the previous referenced articles have also been published (5, 6). The work of Santschi and Marz (7) presents information on extrusion and welding of the commercial composition, Be-38% al alloy.

RESULTS AND DISCUSSION

Summaries of the mechanical properties of annealed extrusions and sheet at temperatures between -320 and 800°F are given in Tables 1 and 2, respectively. The designations used for the properties are: E = Young's Modulus, F_{tu} = tensile strength, F_{ty} = tensile yield strength, F_{cy} = compressive yield strength, $F_{0.7 \text{ sec yield}}$ = 0.7 compression secant yield strength, S_u = ultimate shear strength, F_{bru} = ultimate bearing strength, F_{bry} = bearing yield strength, e = elongation, R. A. = reduction in area, L = longitudinal and T = transverse. Longitudinal and transverse refer to the major dimension of the test specimen to the direction of maximum working. Although they have meaning for the extrusions, the designations are somewhat arbitrary for the sheet, which is essentially isotropic.

Young's modulus data averages for each heat are shown graphically as a function of temperature in Figure 1. Tensile properties versus temperature

for extrusions and sheet material are shown in Figures 2 and 3. Compression stress-strain curves for extrusions are presented in Figures 4 and 5 for the longitudinal and transverse directions, respectively. Compression stress-strain curves for sheet, which are the same for the longitudinal and transverse directions, are plotted in Figure 6.

Shear strength properties of extrusions and sheet at 75°, 400°, and 800° F are summarized in Tables I and II, respectively, and plotted for the sheet in Figure 8. The explanation of shear planes and direction is shown schematically in Figure 7 and is similar to that used by Kaufman and Davis (8). In this figure's coordinate system, the yz plane is a transverse plane with the z direction being short transverse and the y direction being long transverse. The xz plane is a longitudinal plane with the x direction, the longitudinal direction and the z direction the short transverse direction. Shear tests were made at 75, 400 and 800°F.

Bearing yield strengths and ultimate strengths are summarized for extrusions and sheet in Tables I and II, respectively, and plotted for sheet in Figure 9.

Elevated-Temperature Exposure Effects

The effect of elevated-temperature exposure on Be-38% Aℓ alloys was evaluated by exposing duplicate longitudinal extrusion specimens and duplicate longitudinal and transverse sheet specimens to 400° to 800° F for 10, 100 and 1000 hr and comparing the 75°F tensile results to those of unexposed control specimens. Results of those tests are shown in Tables III and IV. Although certain differences exist between the "zero-exposure" control specimens and the 10-hr exposure points, in no case is there significant variation from 10 through 1000 hr. Therefore, the apparent variations (i. e., heat 21-31 T. Y. S. , heat 21-35 T. S.) are attributed to statistical scatter in the control specimen data, and it is concluded that the exposures given do not affect the 75°F tensile properties. Figure 10 shows a typical set of 75°F tensile data subsequent to exposure in 800°F air.

Bend Evaluations

Bend angle results obtained at -320, 75, and 600°F are shown for extrusions and sheet in Tables I and II, respectively. The designations, longitudinal and transverse, refer to the specimen axis. The bend axis is at 90 deg to the designated specimen direction.

Of the three temperatures utilized, -320°, 75°, and 600^OF, the longitudinal extrusion specimens showed a maximum average bend angle of 38 deg at 75°F, the transverse extrusion specimens a maximum average bend angle of 14 deg at -320°F, and the sheet a maximum average bend angle of 39 to 44 deg at 75°F.

These values are 4 to 5 times those obtained with unalloyed beryllium. Although it might appear, from these limited tests, that 75°F is the optimum temperature for bending, other studies currently underway indicate two temperature regions of greater formability; 300 to 500°F and 1000 to 1100°F. Current work is also revealing a significant increase in formability with increased strain rate at approximately 500°F.

The bend angles at 75°F may at first appear to be rather low. However, the fact that 5/8-in. and 1-in. radius cylinders were roll formed at 75°F from 0.050-in. sheet (4) shows that the Be-38% al alloy is not brittle. Such an operation has not been possible at 75°F with unalloyed beryllium. Futhermore, no shattering at failure, as commonly observed in unalloyed beryllium, has ever been noted with Be-Al alloys. Additionally, under certain circumstances, the Be-38% Al alloy appears to retard and arrest the propagation of cracks.

Bend angle, which provides a measure of the short transverse ductility, is considered a better criterion for evaluating the serviceability of a material than uniaxial elongation. For example, in bolted lap-joint tests, as-rolled Be-38% Al with an elongation of 4.9% resulted in a net tensile strength of 51 ksi. This is about 40% higher than the 36 to 38 ksi obtained with unalloyed beryllium sheet with much higher elongation, 15%, despite the fact that the beryllium had a tensile strength (74 ksi) about 11% higher than the Be-38% Al (67 ksi).* Lap joints, whether bolted, riveted, brazed or welded, require some bending to develop maximum strengths. In this case, bend angles (Be-38% Al alloy with 21 deg* and unalloyed beryllium with 8 to 10 deg) would have given a better prediction of the material performance. The yield strengths of both metals were about the same, i.e., Be-38% Al = 56 ksi* and Be = 54 ksi.

STATISTICAL CONSIDERATIONS

A statistical analysis was made to determine the reproducibility of tensile strength and tensile yield strength. Assuming that exposure to temperatures of 400 and 800°F had no effect on the 75°F tensile properties, all 75°F tensile test results (including those on defective specimens) were used to calculate** estimate of the universe standard deviations for: (1) each heat of metal, (2) three heats of extrusions, and (3) three heats of sheet as shown on the following page.

---

*As-rolled sheet.
**Calculated using equation:

$$s = \sqrt{\frac{\sum_{i=1}^{n} x_i^2 - \left(\sum_{i=1}^{n} x_i\right)^2 / n}{n - 1}}$$

These data show very low standard deviation values for the tensile yield strength of extrusions, ie. , 0.8 and 1.14 ksi in the longitudinal and transverse directions respectively. In the sheet, heat 21-30 and 20-34 also had very low T.Y.S. standard deviations, 0.5 to 0.8 ksi. Heat 21-31, which contained deep grinding scratches and pits at the bottom of the scratches from heavy etching, has a standard deviation of ~2.0 ksi, contributing strongly to the three heat standard deviation of 2.4 ksi. Elimination of the data for the defective sheet (2C in heat 21-31), which would automatically occur using standard quality control acceptance procedures, lowers the three heat standard deviation to 1.96 ksi. However, either of these values is acceptable and compares favorably with other commonly used aircraft quality alloys, as shown in the following tabulation of standard deviations.

STANDARD DEVIATIONS

Material	Longitudinal			Transverse		
	Tests	T.Y.S. (ksi)	T.S. (ksi)	Tests	T.Y.S. (ksi)	T.S. (ksi)
Extrusions						
Be-38% Al-O	45	0.81	2.49	6-9	1.14	1.85
Sheet						
Be-38% Al-O	46	2.40	2.70	50	2.00	2.09
Ti 8-1-1[a] (single anneal)	52	4.55	4.70	55	5.16	4.6
17-7 PH[b] (stainless steel)	44	3.54	3.65	63	7.18	5.9
6061-T6(Al)[c]	1648	~4 (estimated from handbook data)				
AZ31B-O(Mg)[c]	1630	~2.7 (estimated from handbook data)				
Block						
Be Block[d]	61	4.2[e]	2.6	130		3.8
	177	2.93[f]	3.5	294		3.83

(a) Item 63-14 (29), Agenda for the 29th Meeting of Mil Handbook V Working Group, Apr 1965
(b) Item 64-4 (29), Agenda for the 29th Meeting of Mil Handbook V Working Group, Apr 1965
(c) Ref. (9)
(d) Attachment 62-8 (27) to Minutes of 27th Meeting of Mil Handbook V Working Group, Apr 1964
(e) Based on 471 tests, both longitudinal and transverse
(f) Based on 190 tests, both longitudinal and transverse

| Heat No. | T.Y.S. (ksi) | | | | T.S. (ksi) | | | |
| | Longitudinal | | Transverse | | Longitudinal | | Transverse | |
	Avg.	s	Avg.	s	Avg.	s	Avg.	s
Extrusions								
21-33	$44.93^{15(a)}$	0.849	42.12^3	0.778	57.17^{15}	0.999	46.05^3	0.128
21-32	45.01^{15}	0.541	42.17^3	0.925	57.62^{15}	1.474	$46.05^{2(b)}$	0.354
21-35	44.17^{15}	0.772	43.13^3	1.666	52.97^{15}	1.481	$50.7^{1(b)}$	—
3 Heats	44.70^{45}	0.809	42.47^9	1.142	55.92^{45}	2.488	46.82^6	1.854
Sheet								
21-30	35.30^{16}	0.775	35.71^{18}	0.812	50.30^{16}	1.077	51.19^{18}	1.465
21-31	37.78^{17}	1.944	37.40^{17}	2.092	49.00^{15}	3.100	49.22^{17}	1.483
21-34	39.40^{15}	0.542	39.35^{15}	0.619	53.39^{15}	0.410	53.09^{15}	1.275
3 Heats	37.44^{46}	2.40	37.38^{50}	2.00	50.88^{46}	2.702	51.09^{50}	2.088
Excluding defective sheet #2C from heat 21-31								
21-31	38.65^{12}	0.786	38.02^{14}	1.742	50.18^{12}	1.391	49.49^{14}	1.510
3 Heats	37.66^{43}	1.965	37.56^{47}	1.913	51.34^{43}	1.946	51.29^{47}	1.995

(a) Exponents equal number of tests.
(b) Specimens run at different strain rate omitted.

Beryllium - 38% Aluminum
Standard Deviations

SUMMARY AND CONCLUSIONS

The reproducibility of mechanical properties from heat to heat of annealed Be-38% Al extrusions and sheet, as judged by the standard deviation of tensile yield strength, is excellent. The standard deviation for T.Y.S. is significantly less than some commonly used aircraft quality alloys, e.g., AZ31B-O, 6061-T6, Be, Ti 8-1-1, and 17-7 PH stainless steel.

From -320 to 800°F, the sheet is essentially isotropic with respect to both strength and ductility, while the extrusions show varying degrees of anisotropy depending upon direction, temperature, and the property measured.

Both the sheet and extrusions show significant increases in strength (~9 to 29%) upon decreasing the temperature from 75 to -320°F. At 800°F, the alloys retain ~30 to 59% of their room temperature strength.

Be-Al alloy does not exhibit the poor short transverse ductility of un-alloyed Be sheet. The isotropic nature of ductility in Be-Al sheet allows 100% more bendability than in unalloyed Be at 75°F. The lower, but adequate, uniaxial tensile elongations exhibited by Be-Al (as compared to unalloyed Be) are not in this case an indication, as is bendability, of the biaxial ductility so necessary for reliable structural service. The bendability of Be-Al at -320°F is also better than the room-temperature bendability of unalloyed beryllium. This fact, coupled with the significant strength increases at -320°F, makes Be-38% Al alloys a candidate material for cryogenic service.

Prolonged exposure for times up to 1000 hr in 400 and 800°F air showed no apparent effect on the room temperature tensile properties of the annealed sheet or extrusions.

ACKNOWLEDGMENTS

REFERENCES

1. R. W. Fenn, Jr., R. A. Glass, R. A. Needham, and M. A. Steinberg, Beryllium-Aluminum Alloys, Proc. AIAA Fifth Annual Structures and Materials Conference, Palm Springs, Calif., April 1964, p. 92

2. R. W. Fenn, Jr., R. A. Glass, R. A. Needham, and M. A. Steinberg, J. Spacecraft and Rockets, Vol. 2, No. 1, Jan-Feb 1965, p. 87

3. R. W. Fenn, Jr., D. D. Crooks, and R. C. Pasternak, New Ductile Beryllium-Aluminum Wrought Alloys, Newer Sturctural Materials for Aerospace Vehicles, ASTM Special Technical Publication 379, June 1964, p. 3

4. R. W. Fenn, Jr., D. D. Crooks, W. C. Coons, and E. E. Underwood, Properties and Behavior of Beryllium-Aluminum Alloys, International Conference on Beryllium Metallurgy and Technology, AIME, Philadelphia, October 1964

5. R. W. Fenn, Jr., D. D. Crooks, and E. E. Underwood, Beryllium-Aluminum Alloys - Promising New Structural Metals, Materials in Design Engineering, September 1964, p. 103

6. R. W. Fenn, Jr., and D. D. Crooks, Ductile Beryllium-Aluminum Alloys—Broaden Potential Uses, Space/Aeronautics, October 1964, p. 73

7. W. H. Santchi and W. G. Marz, Manufacturing and Properties of Beryllium-Aluminum Composite Materials, International Conference on Beryllium Metallurgy and Technology, AIME, Philadelphia, Pa., October 1964

8. J. G. Kaufman and R. E. Davies, Effects of Test Method and Specimen Orientation on Shear Strengths of Aluminum Alloys, ASTM Annual Meeting, Chicago, Ill., June 1964

9. Metals Handbook Vol. I, 8th Edition, American Society for Metals, Novelty, Ohio, 1961

Table I

SUMMARY OF MECHANICAL PROPERTIES FOR 3e-38% Al EXTRUSIONS

(Annealed temper, 3/16-in. x 2-1/2-in. bar; Strain rate: 0.005/min to yield, 0.08/min to failure)

Mechanical Properties	Dir	-320°F 21-33	-320°F 21-32	-320°F 21-35	-320°F 3 Heat Avg.	75°F 21-33	75°F 21-32	75°F 21-35	75°F 3 Heat Avg.	400°F 21-33	400°F 21-32	400°F 21-35	400°F 3 Heat Avg.	800°F 21-33	800°F 21-32	800°F 21-35	800°F 3 Heat Avg.
E (10⁶ psi)	L					29.9[16(a)]	27.7[3]	27.4[3]	28.3	31.0[2]	–	–	31.0	16.1[3]	14.1[3]	15.8[4]	15.3
	T					–	–	–	–	–	–	–	–	–	–	–	–
Ftu (ksi)	L	68.8[3]	68.6[3]	72.5[3]	70.0	57.0[3]	58.1[3]	54.4[3]	56.5	41.9[3]	43.4[3]	46.2[3]	43.8	28.9[3]	29.4[3]	30.8[3]	29.7
	T	57.3[3]	58.3[3]	63.2[3]	59.6	46.0[3]	46.1[3]	46.8[3]	46.3	38.8[3]	39.0[3]	41.5[3]	39.8	25.8[3]	25.4[3]	27.4[3]	26.2
Fty (ksi)	L	50.4[3]	50.3[3]	53.1[3]	51.3	44.5[3]	44.9[3]	44.2[3]	44.5	37.8[3]	38.1[3]	39.8[3]	38.6	24.5[3]	24.7[3]	26.0[3]	25.1
	T	42.1[3]	47.1[3]	49.6[3]	46.3	42.1[3]	42.2[3]	43.1[3]	42.5	38.2[3]	37.5[3]	39.1[3]	38.3	24.1[3]	24.2[3]	26.7[3]	25.0
Fcy (ksi)	L					41.8[3]	39.4[3]	43.8[3]	41.7	36.2[3]	34.2[3]	35.6[2]	35.3	13.7[3]	14.9[3]	15.4[3]	14.7
	T					41.3[3]	39.6[3]	43.5[3]	41.5	35.6[3]	36.2[3]	36.4[3]	36.1	11.9[3]	12.0[3]	11.7[3]	11.9
F0.7 sec yield (ksi)	L					33.2[3]	33.7[3]	36.8[3]	34.6	34.6[2]	29.8[2]	33.8[2]	32.9	11.5[2]	12.8[2]	12.6[2]	12.3
	T					30.8[3]	23.9[3]	31.9[3]	23.9	32.9[2]	33.0	32.9	32.9	10.4[2]	10.7[2]	10.0[2]	10.4
Fsu (ksi)	yz-z(c)					35.4[3]	35.8[3]	39.2[3]	36.8	26.0[2]	26.1[2]	27.1[2]	26.4	12.7[2]	12.2[2]	13.4[2]	12.8
	yz-y					39.5[3]	39.2[3]	43.6[3]	40.8	29.1[3]	28.2[2]	29.7[2]	29.0	13.9[2]	13.7[2]	14.8[2]	14.1
	xz-z					27.3[3]	24.3[3]	28.1[3]	26.6	21.8[2]	22.2[2]	24.0[2]	22.7	11.8[2]	12.0[2]	12.0[2]	11.9
	xz-x					29.6[3]	28.8[3]	29.0[3]	29.1	23.0[2]	23.6[2]	25.2[2]	23.9	12.5[2]	12.7[2]	13.4[2]	12.9
Fbru (ksi) e/D = 2 (3/16-in. pin)	L					89.6[3]	91.2[3]	93.5[3]	91.5	69.9[2]	70.0[2]	76.6[2]	72.2	36.2[4]	34.6[2]	36.9[4]	35.9
	T					87.1[3]	90.8[3]	99.7[3]	92.5	70.0[2]	72.5[2]	69.2[2]	70.6	30.2[2]	32.6[2]	34.2[4]	32.3
Fbry (ksi) e/D = 2	L					80.1[2]	79.3[3]	78.5[3]	79.9	64.9[2]	64.0[2]	68.6[2]	65.8	31.2[2]	32.2[2]	33.6[2]	32.3
	T					74.0[3]	75.8[3]	86.4[3]	78.7	58.8[2]	61.9[2]	69.2[2]	63.3	28.6[2]	30.5[2]	31.8[2]	30.3
Bend Angle (deg)(b)	L	30[2]	31[2]	31[2]	31	36[2]	42[2]	35[2]	38	22[2]	20[2]	27[2]	23				
	T	15[2]	12[2]	14[2]	14	9[2]	8.5[2]	8.5[2]	9	7[2]	6[2]	7[2]	7				
e (%)	L	2.2[3]	2.7[3]	2.8[3]	2.6	7.6[3]	7.3[3]	5.1[3]	6.7	7.2[3]	8.6[3]	9.2[3]	8.3	4.2[3]	4.1[3]	3.7[3]	4.0
	T	1.9[3]	2.0[3]	2.4[3]	2.1	2.5[3]	1.2[3]	0.7[3]	1.5	2.5[3]	2.5[3]	2.1[3]	2.4	1.9[3]	1.7[3]	1.9[3]	1.8
R.A. (%)	L	2.5[3]	2.8[3]	2.8[3]	2.8	7.4[3]	6.8[3]	5.4[3]	6.5	9.0[3]	10.2[3]	11.2[3]	10.1	9.0[3]	8.8[3]	10.1[3]	9.3
	T	1.3[3]	1.2[3]	1.5[3]	1.5	2.0[3]	3.5[3]	2.6[3]	2.7	3.0[3]	2.9[3]	2.8[3]	2.9	3.3[3]	2.0[3]	3.2[3]	2.8

Note: Bend Angle values under 400°F are annotated "600°F" in the original.

(a) Exponents = number of tests
(b) Nominal thickness 0.054 in.

(c) Shear plane:
xz = longitudinal
yz = transverse

Shear direction:
x = longitudinal
y = long transverse
z = short transverse

Table II

SUMMARY OF MECHANICAL PROPERTIES FOR Be-38% Al SHEET
(Annealed temper, 0.060-in. thick; Strain rate: ~0.005/min to yield, ~0.08 to failure)

Property	Dir	-320°F 21-30	-320°F 21-31	-320°F 21-34	-320°F 3 Heat Avg	75°F 21-30	75°F 21-31	75°F 21-34	75°F 3 Heat Avg	400°F 21-30	400°F 21-31	400°F 21-34	400°F 3 Heat Avg	800°F 21-30	800°F 21-31	800°F 21-34	800°F 3 Heat Avg
E (10⁶ psi)	L					28.2[6]	29.2[7]	29.9[3]	29.1	30.4[3]	29.6[3]		30.0	16.5[3]	16.6[3]	17.5[3]	16.9
	T					29.4[6]	28.5[6]	29.4[3]	29.1	28.6[3]	31.6[3]	40.4[3]	30.1	18.0[3]	16.5[3]	17.0[3]	17.2
F_{tu} (ksi)	L	60.1[3]	56.5[3]	63.6[3]	60.1	51.3[3]	45.9[4]	54.0[3]	50.4	38.8[3]	37.8[3]	41.6[3]	35.0	23.2[3]	24.0[3]	25.7[3]	24.3
	T	58.6[3]	52.9[3]	64.8[3]	58.3	51.9[5]	48.4[4]	52.5[3]	50.9	39.5[3]	38.1[3]	32.5[3]	35.7	23.3[3]	23.4[3]	25.5[3]	24.1
F_{ty} (ksi)	L	41.0[3]	40.4[3]	43.9[3]	41.8	36.2[5]	34.9[4]	38.6[3]	36.6	30.7[3]	29.4[3]	33.1[3]	30.9	19.7[3]	20.8[3]	22.5[3]	21.0
	T	43.0[3]	40.0[3]	46.3[3]	43.1	35.4[5]	34.6[4]	38.3[3]	36.1	30.7[3]	30.0[3]	29.8[2]	31.3	20.1[3]	20.1[3]	21.9[3]	20.7
F_{cy} (ksi)	L					34.0[3]	32.1[3]	36.6[3]	34.2	27.6[2]	25.6[2]	30.8[2]	27.7	14.3[2]	13.2[2]	14.6[2]	14.0
	T					33.4[2]	32.9[3]	36.6[3]	34.3	27.2[2]	27.2[2]	25.7[2]	28.4	14.5[2]	13.5[2]	15.1[2]	14.4
$F_{0.7\ sec\ yield}$ (ksi)	L					22.9[3]	22.3[3]	25.7[3]	23.6	24.1[2]	21.8[2]	26.8[2]	23.9	11.4[2]	11.0[2]	13.2[2]	11.9
	T					24.5[3]	22.4[3]	28.4[3]	25.1	22.4[2]	23.6[2]		24.3	12.6[2]	11.2[2]	13.2[2]	12.3
F_{su} (ksi)	yz-z (c)					27.7[2]	25.7[2]	28.1[2]	27.2	21.2[2]	21.0[2]	22.4[2]	21.5	10.1[2]	10.7[2]	11.5[2]	10.8
	yz-y					25.8[2]	27.2[2]	28.0[2]	27.0	21.4[2]	20.6[2]	22.8[2]	21.6	10.4[2]	10.4[2]	11.3[2]	10.7
	xz-z																
	xz-x																
F_{bru} (ksi) e/D = 2	L					94.8[2]	93.6[3]	100.9[3]	96.4	65.3[2]	65.1[2]	73.3[2]	67.9	32.5[2]	33.7[2]	38.2[2]	34.8
3/16-in. pin	L					94.8[3]	95.2[3]	97.0[3]	95.7	63.6[2]	64.8[2]	72.2[2]	66.9	30.8[2]	30.3[2]	33.9[2]	31.8
F_{bry} (ksi) e/D = 2	L					62.0[2]	63.5[3]	72.8[3]	66.1	54.1[2]	53.2[2]	59.2[2]	55.5	27.5[2]	29.5[2]	32.9[2]	29.7
	T					66.0[3]	68.6[3]	74.0[3]	69.5	52.8[2]	54.0[2]	58.0[2]	54.9	28.8[2]	29.4[2]	32.4[2]	30.2
Bend Angle (deg) (b)	L	32[2]	29[2]	22[2]	28	48[2]	45[2]	38[2]	44	38[2]	22[2]	24[2]	25				
	T	31[2]	32[2]	33[2]	32	46[2]	37[2]	34[2]	39	38[2]	24[2]	24[2]	29				
e (%)	L	2.3[3]	2.3[3]	2.5[3]	2.4	10.8[3]	6.2[4]	7.4[3]	8.1	9.4[3]	11.8[3]	10.5[3]	10.6	5.3[3]	3.9[3]	5.2[3]	5.0
	T	2.0[3]	3.8[3]	2.7[3]	2.8	9.6[5]	7.1[4]	7.8[3]	8.2	12.0[3]	11.8[3]	11.9[3]	11.9	7.4[3]	4.4[3]	4.8[3]	5.5
R.A. (%)	L	2.5[3]	2.2[3]	2.4[3]	2.4	8.4[3]	6.2[4]	7.4[3]	7.3	13.1[3]	16.5[3]	10.7[3]	13.4	12.1[3]	9.0[3]	11.2[3]	10.9
	T	3.2[3]	2.6[3]	2.5	2.8	10.4[5]	7.2[4]	8.2[3]	8.6	15.9[3]	15.9[3]	12.1[3]	14.6	13.8[3]	10.8[3]	9.1[3]	11.2

Note: "600° F" indicated in the 800°F column group for the lower-temperature (bearing/bend/elongation) rows.

(a) Exponents = number of tests
(b) Nominal thickness 0.054 in.

(c) Shear plane:
  xz = longitudinal
  yz = transverse

Shear direction:
  x = longitudinal
  y = long transverse
  z = short transverse

Table III

EFFECT OF 400°F AND 800°F EXPOSURE ON THE 75°F TENSILE PROPERTIES OF Be-38% Al EXTRUSIONS
(Annealed; Strain rate: ~0.005/min to 1% strain; ~0.08/min beyond 1% strain)

Heat No.	Expo-sure Time (hr)	400°F AIR EXPOSURE Longitudinal					800°F AIR EXPOSURE Longitudinal				
		Spec-men No.	T.Y.S. (ksi)	T.S. (ksi)	Elong (%)[b]	R.A. (%)	Spec-men No.	T.Y.S. (ksi)	T.S. (ksi)	Elong (%)[b]	R.A. (%)
21-33	0[a]	4A, 5B	44.5^3	57.0^3	7.6^3	7.4^3	4A	44.5^3	57.0^3	7.6^3	7.4^3
	10	5A-12	45.8	58.6	8.0	8.8	5A-18	45.6	58.2	7.4	7.0
	10	5A-13	45.5	57.5	7.5	8.4	5A-19	45.6	56.9	6.6	8.7
		Avg.	45.7	58.1	7.8	8.6		45.6	57.6	7.0	7.9
	100	5A-14	45.5	57.2	7.6	8.6	5A-20	45.3	58.0	7.8	8.3
	100	5A-15	44.4	56.1	7.4	8.4	5A-21	44.2	56.7	6.9	7.7
		Avg.	45.0	56.7	7.5	8.5		44.8	57.4	7.4	8.0
	1000	5A-16	45.0	57.2	8.5	8.3	5A-22	42.8	55.3	7.6	9.4
	1000	5A-17	45.8	56.6	6.0og	5.0	5A-23	44.9	58.8	10.1	9.7
		Avg.	45.4	56.9	7.3	6.6		43.9	57.1	8.9	9.6
21-32	0[a]	2A, 8	44.9^3	58.1^3	7.3^3	6.8^3	2A, 8	44.9^3	58.1^3	7.3^3	6.8^3
	10	2A-1	44.8	57.8	7.8	7.2	2A-7	45.7	59.5	9.0	8.8
	10	2A-2	44.9	57.0	7.2og	7.4	2A-8	45.9	58.9	8.3	7.5
		Avg.	44.8	57.4	7.5	7.3		45.8	59.2	8.7	8.2
	100	2A-3	44.7	56.9	8.2	8.0	2A-9	45.3	58.8	7.9og	6.8
	100	2A-4	44.3	53.7	4.1og	6.1	2A-13	45.9	59.2	8.0	7.8
		Avg.	44.5	55.3	6.2	7.0		45.6	59.0	8.0	7.3
	1000	2A-5	44.6	56.4	8.3	8.4	2A-14	44.5	57.6	8.3	10.7
	1000	2A-6	44.9	56.6	6.9	7.9	2A-15	44.6	57.5	7.2	7.6
		Avg.	44.8	56.5	7.6	8.2		44.6	57.6	7.8	9.2
21-35	0[a]	307	44.2^3	54.4^3	5.1^3	5.4^3	307	44.2^3	54.4^3	5.1^3	5.4^3
	10	307-1	42.8	50.7	4.1	3.8	307-7	44.7	54.4	5.9	4.6
	10	307-2	43.4	51.1	4.8	4.3	307-8	45.0	54.4	4.6	3.7
		Avg.	43.1	50.9	4.4	4.0		44.9	54.4	5.3	4.2
	100	307-3	43.0	51.3	5.3og	4.5	307-9	44.4	53.2	5.2	5.1
	100	307-4	43.4	52.1	5.7og	3.7	307-10	45.5	54.9	5.2	5.9
		Avg.	43.2	51.7	5.5	4.1		45.0	54.0	5.2	5.5
	1000	307-5	45.0	51.8	4.2	3.8	307-11	44.1	52.3	4.9	6.9
	1000	307-6	44.8	52.0	4.8og	3.1	307-12	44.1	53.3	5.1	6.4
		Avg.	44.9	51.9	4.5	3.4		44.1	52.8	5.0	6.6

(a) See tensile data for details on control tests
(b) 1-in. gage length
(c) og = failed outside gage length

Table IV

EFFECT OF 400°F AND 800°F EXPOSURE ON THE 75°F TENSILE PROPERTIES OF Be-38% Al SHEET
(Annealed; strain rate: ~0.005/min to 1% strain; ~0.08/min beyond 1% strain)

Heat No.	Exposure Time (hr)	400°F AIR EXPOSURE Longitudinal Speci-men No.	T.Y.S. (ksi)	T.S. (ksi)	Elong. (%)(b)	R.A. (%)	Transverse Speci-men No.	T.Y.S. (ksi)	T.S. (ksi)	Elong. (%)(b)	R.A. (%)	800°F AIR EXPOSURE Longitudinal Speci-men No.	T.Y.S. (ksi)	T.S. (ksi)	Elong. (%)(b)	R.A. (%)	Transverse Speci-men No.	T.Y.S. (ksi)	T.S. (ksi)	Elong. (%)(b)	R.A. (%)
21-30	0[a]	3B	36.2[c]	51.3[3]	10.3[3]	8.4[3]	3B	35.4[5]	51.9[5]	9.6[5]	10.1[5]	3B	36.2[3]	51.3[3]	10.8[3]	8.4[3]	3I	35.4[5]	51.9[5]	9.6[5]	10.1[5]
	10	3D-1	34.7	48.9	9.5	12.3	3D-16	36.5	52.5	10.1	12.4	3D-2	34.6	50.0	7.8	9.4	3I-19	34.6	50.7	10.8	14.9
	10	3D-4	36.4	50.5	6.9	6.9	3D-23	36.1	52.0	9.7	9.6	3D-3	34.7	51.0	10.0	10.8	3I-20	36.6	46.7	11.0	10.8
	Avg.		35.6	49.7	8.2	9.6		36.3	52.2	9.9	11.0		34.6	50.5	8.9	10.1		35.6	48.7	10.9	12.8
	100	3D-5	35.5	50.0	9.3	10.8	3D-21	36.5	51.6	10.2	10.5	3D-9	34.9	51.4	11.2[d]	12.7	3I-17	35.4	50.0	6.6	7.3
	100	3D-6	34.2	50.0	10.2	13.4	3D-22	36.8	51.6	12.8	13.2	3D-10	35.3	51.2	9.0[g]	7.8	3I-18	35.0	51.3	8.6	9.1
	Avg.		34.9	50.0	9.8	12.1		36.7	51.7	11.5	11.8		35.1	51.3	10.1	10.2		35.2	50.6	7.6	8.2
	1000	3D-7	34.6	49.7	9.6	10.0	3D-41	36.4	51.4	10.2	7.1	3D-11A	35.0	51.2	8.4	8.7	3I-24	35.7	51.0	9.2	9.0
	1000	3D-8	35.5	48.3	7.7	9.9	3D-42	36.1	49.5	7.9	10.0	3D-11B	34.6	50.0	8.9	10.4	3I-25	35.1	52.9	13.2	14.4
	Avg.		35.0	49.0	8.7	10.0		36.2	50.5	9.1	8.6		34.8	50.6	8.6	9.6		35.4	52.0	10.7	11.7
21-31	0[a]	2C 2B	34.3[3] 36.8	44.3[3] 50.7	5.2[3] 9.1	5.3[3] 9.2	2C 2B	34.5[3] 34.8	48.0[3] 49.4	6.4[3] 9.2	6.9[3] 7.9	2C 2B	34.3[3] 36.8	44.3[3] 50.7	5.2[3] 9.1	5.3[3] 9.2	2C 2E	34.3[3] 34.8	48.0[3] 49.4	6.4[3] 9.2	6.9[3] 7.9
	10	2B-5	38.9	50.0	7.3	10.5	2B-17	38.1	50.0	6.7	8.4	2B-1	39.3	51.0	6.9	11.5	2E-13	39.7	52.6	8.5	8.9
	10	2B-6	39.3	50.6	7.6	9.2	2B-18	38.8	50.1	7.8	10.1	2B-2	39.1	51.0	5.7	7.9	2E-14	39.4	52.3	8.6	10.6
	Avg.		39.1	50.3	7.5	9.9		38.4	50.0	7.2	9.2		39.2	50.5	6.3	9.7		39.6	52.5	8.6	9.8
	100	2B-7	38.8	47.0	4.5	5.0	2B-19	37.3	47.2	3.8	7.6	2B-3	39.6	51.4	7.9	9.4	2B-15	38.5	51.3	7.0	7.0
	100	2B-8	38.1	47.8	5.9	9.3	2B-20	38.0	47.3	5.9	5.9	2B-4	39.2	50.6	7.0	10.8	2B-16	38.0	52.1	9.1	11.0
	Avg.		38.5	47.4	5.2	6.6		37.7	47.3	5.9	6.8		39.4	51.0	7.4	10.1		38.2	51.7	8.0	9.0
	1000	2B-25	38.0	51.4	9.6	10.4	2B-11	39.5	48.5	5.5	8.7	2B-21	38.1	50.4	7.4	12.2	2B-9	38.0	53.1	9.7	10.1
	1000	2B-24	38.2	(e)	(e)	(e)	2B-12	38.2	48.7	5.9	8.2	2B-22	38.6	51.2	7.9	9.2	2B-10	39.0	52.2	9.0	9.8
	Avg.		38.2	51.4	9.6	10.4		38.8	48.6	5.7	8.4		38.4	50.8	7.6	10.7		38.5	52.6	9.4	10.0
21-34	0[a]	300A	38.6[3]	54.0[3]	7.4[3]	7.4[3]	300A	38.3[3]	52.5[3]	7.8[3]	9.2[3]	300A	38.6[3]	54.0[3]	7.4[3]	7.4[3]	300A	38.3[3]	52.5[3]	7.3[3]	8.3[3]
	10	300A-1	40.4	53.4	8.0	7.8	300A-21	39.2	52.3	7.0	6.3	300A-2	39.3	53.7	7.4	9.3	300A-17	38.5	53.4	9.0	9.1
	10	300A-6	39.6	53.2	7.9	9.1	300A-22	39.0	51.4	5.7	5.6	300A-5	39.7	54.8	9.2	8.3	300A-18	38.8	51.9	6.9	6.2
	Avg.		40.0	53.3	8.0	8.0		39.1	51.9	6.4	5.9		39.5	54.2	8.3	8.8		38.6	52.6	7.4	7.2
	100	300A-7	39.2	49.7	5.1	5.4	300A-23	38.9	51.2	6.1	7.3	300A-3	40.0	53.6	6.6	6.9	300A-19	39.7	53.5	7.9	8.9
	100	300A-8	39.0	52.7	3.1	8.7	300A-24	38.2	51.0	6.0	6.1	300A-4	39.6	55.3	9.7	8.0	300A-20	39.3	46.4	3.5	4.5
	Avg.		39.1	51.2	6.6	7.0		38.6	51.1	6.0	6.8		39.8	54.4	8.2	7.4		39.5	50.0	5.7	6.4
	1000	300A-11	39.4	52.2	7.2	5.8	300A-27	39.4	52.8	8.2	9.3	300A-9	39.7	53.4	7.3	7.3	300A-25	39.7	52.0	7.0	5.9
	1000	300A-12	39.6	53.2	9.2	7.1	300A-28	39.1	51.8	7.5	9.1	300A-10	39.7	53.7	7.9	8.0	300A-26	38.7	50.7	5.6	6.7
	Avg.		39.5	52.7	7.7	6.4		38.7	52.3	7.9	8.7		39.7	53.6	7.8	7.6		38.7	51.4	6.3	6.3

(a) See tensile data tables for details
(b) 1-in. gage length
(c) Exponents = number of tests
(d) log = failed outside gage length
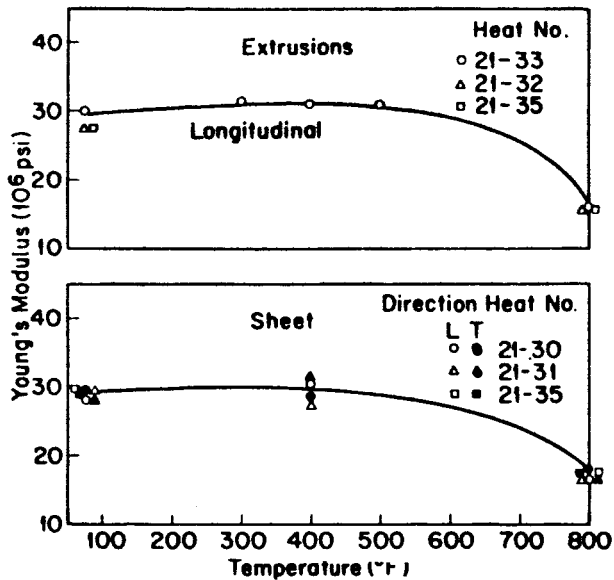(e) Defect - dross inclusion

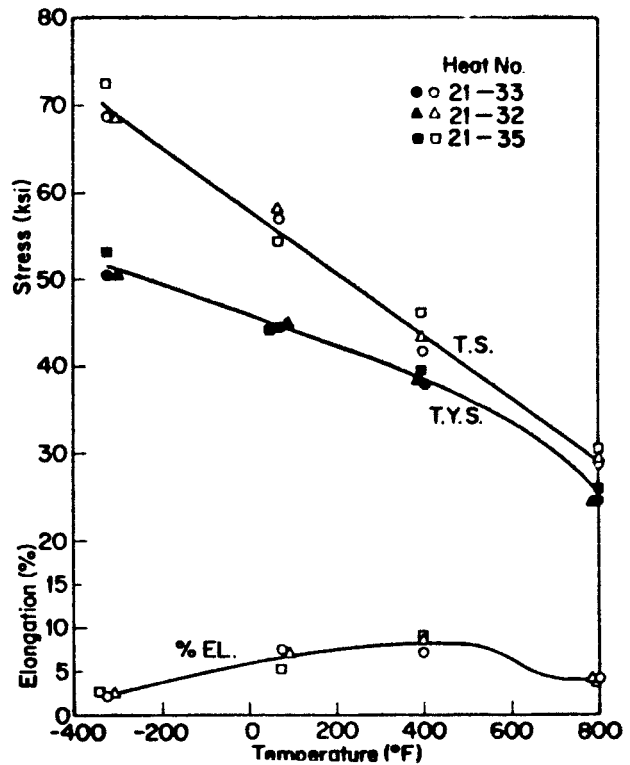Fig. 1 Young's Modulus of Annealed Be-38% Al Alloy

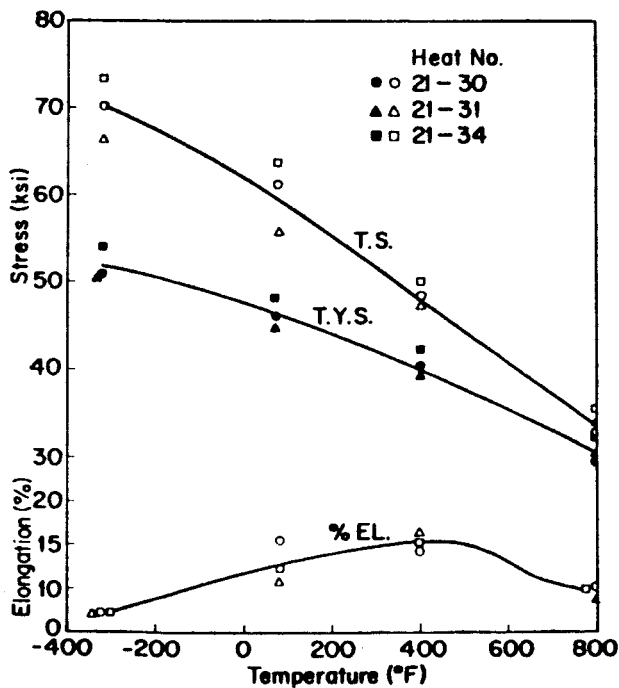Fig. 2 Longitudinal Tensile Proper-ties of Annealed Be-38% Al Extrusions

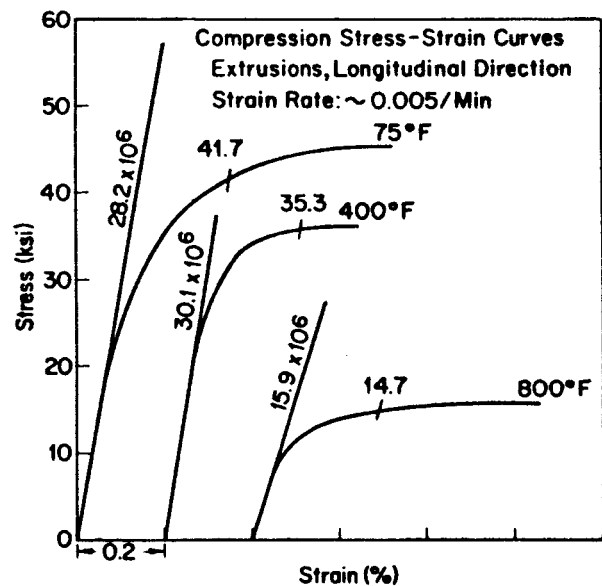Fig. 3 Longitudinal Tensile Pro-perties of Annealed Be-38% Al Sheet

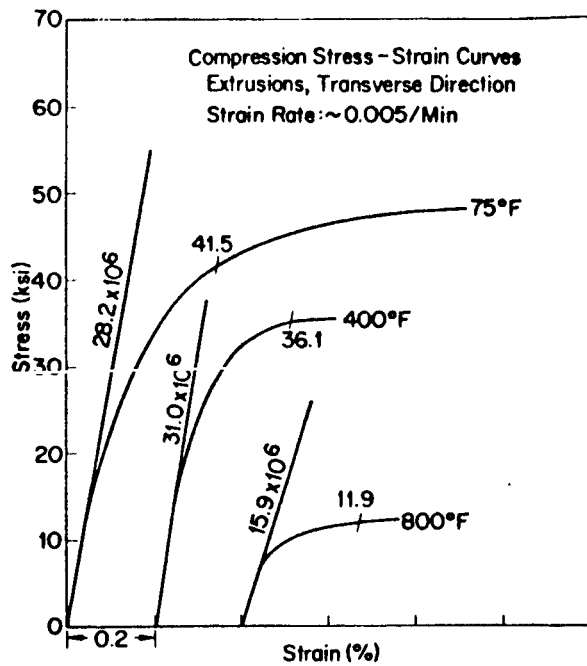Fig. 4 Longitudinal Compression Stress-Strain Curves for An-nealed B3-38% Al Extrusions

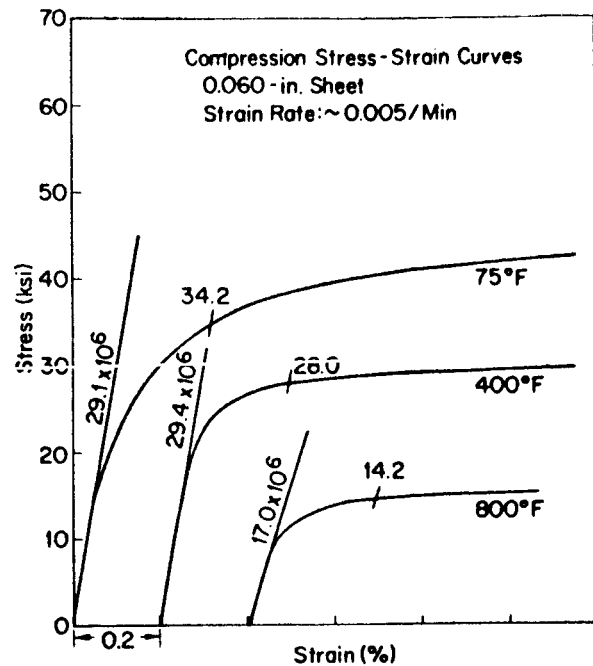Fig. 5 Transverse Compression Stress-Strain Curves for Annealed Be-38% Al Extrusions

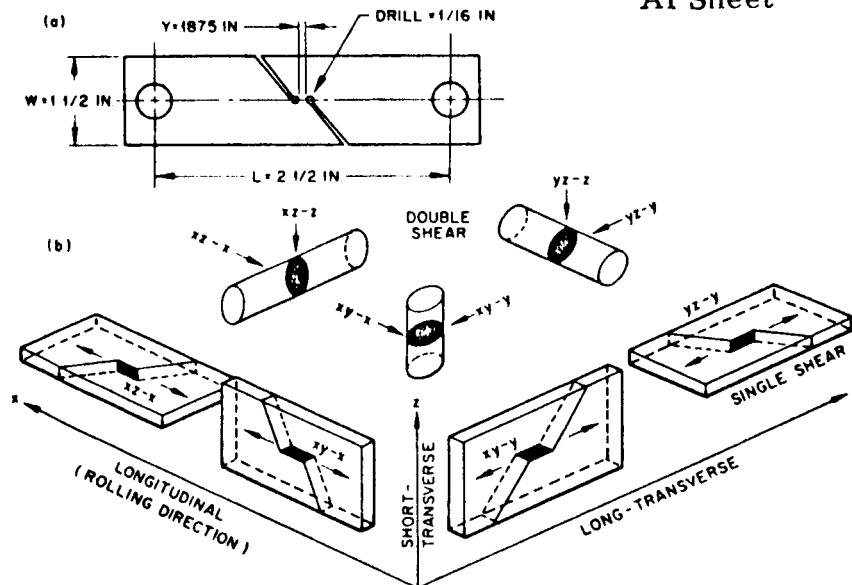Fig. 6 Longitudinal and Transverse Compression Stress-Strain Curves for Annealed Be-38% Al Sheet

Fig. 7 Shear Test Specimens and Orientations
(a) Sheet-Shear Test Specimen
(b) Schematic Drawing Showing Types of Shear Tests. Shear Planes and Directions (After Kaufman and Davies Reference 8
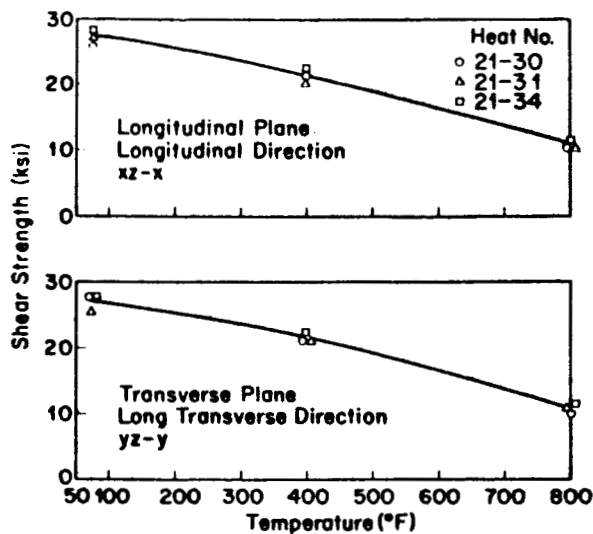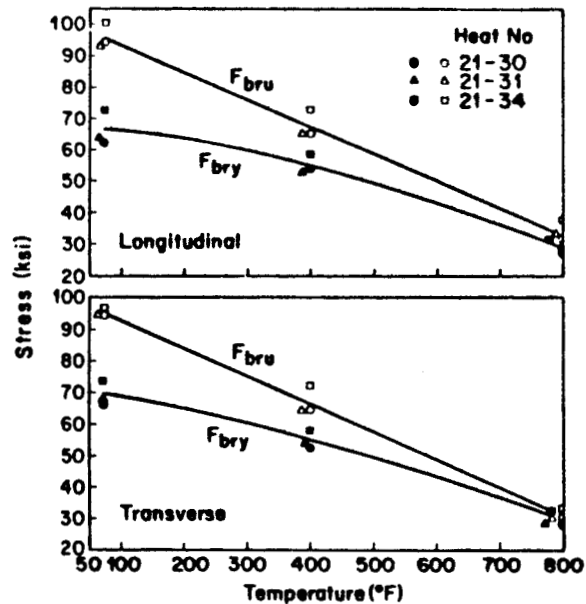
Fig. 8 Shear Strength of Annealed
Be-38% Al Sheet

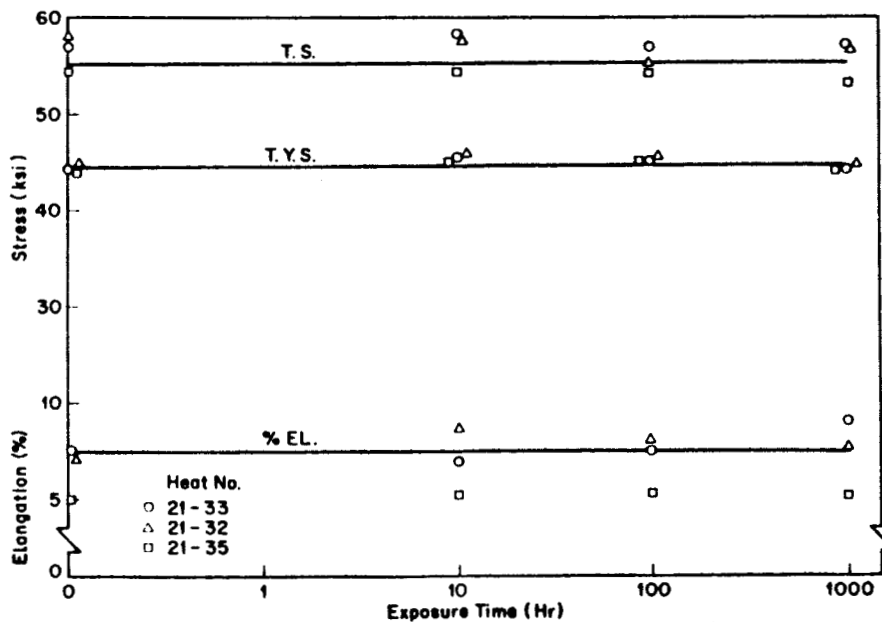Fig. 9 Bearing Strength Properties
of Annealed Be-38% Al Sheet

Fig. 10 Longitudinal 75°F Tensile Properties of Annealed Be-38% Al
Extrustions as a Function of Exposure time at 800°F